High-Frequency Cyclotron Resonance in an Electron-Phonon Gas*

H. SCHER† AND T. HOLSTEIN‡
Department of Physics, University of Pittsburgh, Pittsburgh, Pennsylvania
(Received 26 January 1966)

The surface impedance of an isotropic electron-phonon gas in the presence of a static magnetic field and high-frequency electromagnetic wave ($\omega \sim \omega_D$, the Debye frequency) has been calculated. The calculation is based on a recently derived quantal transport equation, by one of the authors, which is modified to include the effects of the external magnetic field. The resultant expression for the (wave-vector- and frequency-dependent) bulk conductivity $\sigma(q,\omega)$ incorporates effects due to electron-phonon interaction (EPI). The bulk conductivity is related to the surface impedance by the standard expression for the extreme anomalous limit. The EPI effects are manifested in the surface impedance by (a) a frequency-dependent effective cyclotron mass, and (b) frequency-dependent damping (attenuation of the higher subharmonics) associated with frequency-dependent collision processes.

INTRODUCTION

A GENERAL quantal treatment of transport phenomena in a model electron-phonon system has been developed by one of the authors.[1] The model description of the system is based on the Fröhlich Hamiltonian. In particular, the transport theory developed is valid for all frequencies of an impressed electromagnetic field. The basic aim of the present paper is to extend some aspects of the treatment by considering the presence of a magnetic field and applying the results to an investigation of the electron-phonon interaction (EPI) effects on the transport phenomenon of cyclotron resonance[2] in metals.

No attempt will be made to develop the general quantal transport equations in the magnetic field case. This will be shown, under the conditions of cyclotron resonance, to be unnecessary.

Briefly, the conditions under which one usually observes cyclotron resonance (Azbel'-Kaner effect) in metals are as follows: (1) One is in the extreme anomalous skin-effect region $l \gg \delta$, where $l \equiv v_F \tau$ (v_F = Fermi velocity and τ = lifetime of an electron) and δ is the skin-depth penetration of the electromagnetic field. (2) The magnetic field should be closely parallel to the surface of the metal. (3) $\omega\tau \gg 1$; ω is the frequency of the electromagnetic field.

Under these conditions one can have the following picture: There are electrons which do not collide with the surface and which return to the skin layer after each revolution, the layer playing the same role as the gap in a cyclotron. If synchronism occurs and ω is equal to or an integral multiple of the cyclotron frequency, $\omega_c = eH/mc$, the electrons are successively accelerated $l/2\pi R_c$ times, producing a "cyclotron resonance" ($R_c \equiv v_F/\omega_c$). The $\omega\tau \gg 1$ ensures many revolutions before a collision.

It is the fact that one is in the extreme anomalous skin-effect region that enables one to proceed without the general quantal transport equations in the magnetic field case. The results will be correct to first order in δ/l.

Before discussing what kind of information one can glean about the electron-phonon system in a high-frequency cyclotron resonance experiment, a few general facts about such a system will first be reviewed.

As is well known, electron-phonon interactions result in both renormalization and lifetime effects on an electron. These inductive and resistive aspects of EPI are connected by the Kronig-Kramers relations and both are fully described by the complex electron self-energy part.

Low-frequency ($\omega \ll \omega_D$, the Debye frequency) cyclotron resonance,[3] de Haas–van Alphen (dHvA),[4] and low-temperature specific-heat[5] experiments on the alkali metals all give about the same effective mass m^* for each metal. This effective mass is about 20–30% higher than the band-theory calculation.[6] It is evident that correlation effects due to EPI and Coulomb[7] interactions modify the electron-excitation spectrum. Optical experiments ($\omega \gg \omega_D$) give values of the optical mass[8] m_{op} in agreement with the bare-band mass.

From the theoretical point of view, Nakajima and

* This work was supported by the U. S. Air Force Office of Scientific Research Grant No. AF 196-63.

† Present address: Bell Telephone Laboratories, Murray Hill, New Jersey.

‡ Present address: University of California, Los Angeles, California.

[1] T. Holstein, Ann. Phys. (N.Y.) **29**, 410 (1964). This paper will be referred to as H and any part of this paper will be prefaced by H, i.e., H. Eq. (2.4). A more complete discussion of some basic theoretical points concerning transport phenomena in an electron-phonon gas is to be found in this paper. A set of transport equations agreeing with the ones in H in the limit of low frequency has been developed by R. E. Prange and L. P. Kadanoff, Phys. Rev. **134**, A566 (1964).

[2] The Azbel'-Kaner effect. M. Ia. Azbel' and E. A. Kaner, Zh. Eksperim. i Teor. Fiz. **32**, 896 (1956) [English transl.: Soviet Phys.—JETP **5**, 730 (1957)].

[3] C. C. Grimes and A. F. Kip, Phys. Rev. **132**, 1991 (1963).

[4] D. Shoenberg and P. J. Stiles, Proc. Roy. Soc. (London) **A281**, 62 (1964).

[5] D. L. Martin, Phys. Rev. **124**, 438 (1961); Proc. Roy. Soc. (London) **A263**, 378 (1961); and Phys. Rev. **139**, A150 (1965); W. H. Lien and N. F. Phillips, in *Proceedings of the Seventh International Conference on Low-Temperature Physics* (University of Toronto Press, Toronto, 1960), p. 675. See footnote 27, p. 2535, of Ref. 6.

[6] F. S. Ham, Phys. Rev. **128**, 82 (1962); **128**, 2524 (1962).

[7] Coulomb effects are believed to be small; see T. M. Rice, Ann. Phys. (N. Y.) **31**, 100 (1965), especially Table I, p. 107.

[8] M. H. Cohen, Phil. Mag. **3**, 762 (1958).

Watabe[9] have calculated the electron self-energy in a low-frequency approximation and have shown that the cyclotron mass, as modified by EPI, is essentially the same as the thermal mass. For very high frequencies, $\omega \gg \omega_D$, it is shown in H. Sec. V.B, that the mass in the conductivity is m_{op} independent of EPI effects.

Thus, the electron mass is frequency-dependent and one can anticipate dispersion effects in the conductivity for frequencies in the neighborhood of the Debye frequency, $\omega \sim \omega_D$. The collision rate due to EPI will also be frequency-dependent. A simple physical picture explains the frequency dependence of the collision rate. When the system is energized by an external electromagnetic field, electron-hole pairs are created. The pairs then undergo real collisions with phonons. The greater the separation of the pairs and therefore the greater the distance from the Fermi level the more phonon modes they sample (up to the order of the Debye cutoff); hence, increasing the relaxation rate, even in an ideal metal at the absolute zero of temperature. The functional form of the frequency dependence is determined by the integral of the effective electron-phonon coupling function times the phonon density of states.

The relative contributions of EPI and Coulomb (Fermi liquid effects) to m^* is not completely clear. The above discussed energy dependence of the real and imaginary parts of the electron self-energy, in the Debye frequency region, is, however, unique to EPI. It is therefore of considerable physical interest to determine experimentally measurable effects of the energy dependence of the electron self-energy in the transitional region $\omega \sim \omega_D$.

Cyclotron resonance at $\omega \sim \omega_D$ is well suited for the study of these effects[10] for three basic reasons: (1) The magnetic field introduces a discreteness into the electron-energy spectrum. For fields such that $\omega_c \lesssim \omega_D$, the electromagnetic field can induce transitions between discrete states (near the Fermi level) with energy differences of the order of the Debye energy. Such states differ significantly in their interaction with phonons; and the resonant absorption from the electromagnetic field is a sensitive function of the energy shifts, due to EPI, of these discrete states. (2) Under the cyclotron-resonance conditions outlined above it can be seen that a select group of electrons make the dominant contribution to the current. It is those electrons which do not collide with the surface and move parallel to the surface in the skin layer. The details of boundary scattering in the solution of the quasiclassical transport equation[2] are, therefore, not important. (3) The magnetic fields to be used in the proposed experiment are available at present.

A few numerical estimates should be made to clarify the last point. In the alkali metals the energy bands are nearly spherical (for potassium[3,4] to within less than 1.0% and for cesium[11] to within less than 5.0%). Since the present calculation assumes spherical bands, the discussion will center on these metals. The Debye frequencies of K and Cs are 1.18×10^{13} sec^{-1} and 5.5×10^{12} sec^{-1}, respectively, corresponding to fields of 6.7×10^5 G and 3.12×10^5 G. These are large magnetic fields; however, in cyclotron resonance one can use subharmonics of the electromagnetic frequency (ten or more can usually be observed[3]). For Cs the second subharmonic of $\omega \sim \omega_D$ can be obtained with the presently available magnetic fields.

One can expect the EPI effects in cyclotron resonance to be: (1) A frequency-dependent resonance-line shift. (2) A frequency-dependent collision rate resulting in increased attenuation of the signal at higher frequencies. Both are due to the characteristic energy dependence of the EPI contribution to the electron self-energy part.

Central to the theoretical analysis of EPI in normal metals is the existence of the small parameter c_s/v_F (c_s = the velocity of sound). This fact coupled to the assumption of slow momentum variation of the electron self-energy, which can be justified self-consistently (H. Sec. II), permits a classification of EPI effects and a solution of the problem.[12] In Sec. II the electron self-energy in the presence of a magnetic field is calculated and the main result is to establish the slow-momentum dependence. The oscillatory part of the self-energy is calculated in Appendix I for a completeness of the discussion; the oscillatory part is not used in the conductivity. In Sec. III the conductivity is calculated in the lowest order skeleton diagram. In both of these sections use is made of the "temperature" diagram technique, as presented in Luttinger and Ward.[13] The application of this technique to the calculation of the velocity-correlation function is established in H. Appendix II and the relation between this function and the conductivity, due originally to Kubo,[14] is reviewed in H. Appendix I. Section IV is concerned with the calculation of the surface impedance and a presentation of numerical results.

I. BASIC PRELIMINARIES

As stated in the Introduction, the present aim is to extend some aspects of the theory of transport phenomena in an electron-phonon gas[1] to include the presence of a magnetic field. Therefore, some basic preliminaries, as they differ in the magnetic-field case, will now be discussed.

[9] S. Nakajima and M. Watabe, Progr. Theoret. Phys. (Kyoto) **29**, 341 (1963); **30**, 772 (1963). The two papers will be referred to as Refs. 9(1) and 9(2), respectively.

[10] Another experiment suggested by M. Fowler and R. E. Prange, Physics **6**, 315 (1965), is the field and temperature dependence of the amplitude of high-field dHvA oscillations.

[11] K. Okumura and I. M. Templeton (preliminary dHvA experimental result).

[12] The pioneer effort in the solution of this problem is in A. Migdal, Zh. Eksperim. i Teor. Fiz. **34**, 1438 (1958) [English transl.: Soviet Phys.—JETP **7**, 996 (1958)]. See footnote 23 of H.

[13] J. M. Luttinger and J. C. Ward, Phys. Rev. **118**, 1417 (1960). To be referred to as LW.

[14] R. Kubo, J. Phys. Soc. Japan **12**, 570 (1957).

The Fröhlich Hamiltonian to describe the electromagnetic field-free electron-phonon system is

$$H=\sum_t \epsilon_t a_t^\dagger a_t+\sum_Q \hbar\omega_Q{}^{(0)} b_Q^\dagger b_Q + \sum_{t,t',Q} V_{t't}{}^{(0)}(Q) a_{t'}^\dagger a_t (b_Q+b_{-Q}^\dagger). \quad (1.1)$$

The first term of (1.1) is the Hamiltonian of a system of independent Bloch electrons in a static magnetic field. $a_t^\dagger$, a_t are the usual fermion creation and annihilation operators for the single-particle states of quantum number t and of energy ϵ_t. The magnetic field is chosen to be in the z direction and described by a vector potential in the Landau gauge,

$$A_{0,y}=H_0 x; \quad (1.2)$$

the subscript zero is used to distinguish this vector potential from that of the electromagnetic field. Also, as stated in the Introduction, the present calculation is restricted to the consideration of spherical energy bands. The single-particle states can therefore be taken in the Landau representation with a set of quantum numbers

$$t\equiv\{n,k_y,k_z\}, \quad (1.3a)$$

and an energy

$$\epsilon_t=(n+\tfrac{1}{2})\hbar\omega_c+\hbar^2k_z^2/2m. \quad (1.3b)$$

The mass m is the bare-band mass and n is the Landau quantum number.

The spin variables of the electrons are suppressed, as all the interactions being considered conserve individual spin. An account of this degree of freedom is taken, by the insertion of a factor of 2, in the final expression for the conductivity.

The second term of (1.1) is the Hamiltonian for a system of noninteracting phonons; $\omega_Q{}^{(0)}$ is the frequency for the lattice vibration mode of wave vector $\mathbf{Q}$[15] and $b_Q^\dagger$, b_Q are the boson creation and annihilation operators for this mode. The remaining term in (1.1) represents the electron-phonon interaction, typically describing transitions of an electron from state t to t' with the annihilation of a phonon of wave vector $\mathbf{Q}$, or the creation of one of $-\mathbf{Q}$. The matrix element for both transitions is denoted by $V_{t't}{}^{(0)}(Q)\equiv\langle t'|V^{(0)}(Q)|t\rangle$. The matrix element of $V^{(0)}(Q)$ in a plane-wave (or Bloch) basis is often approximated by[16]

$$V_{\mathbf{p}+\mathbf{Q},\mathbf{p}}{}^{(0)}\equiv\langle\mathbf{p}+\mathbf{Q}|V^{(0)}(Q)|\mathbf{p}\rangle = iC|Q|(\hbar/2NM\omega_Q{}^{(0)})^{1/2}, \quad (1.4)$$

where M is the atomic mass, N the number of atoms in the sample, and C is the phenomenological Sommerfeld-Wilson interaction constant.

The right-hand side of (1.4) shall be denoted by $V_Q{}^{(0)}$; using this expression the matrix element in the Landau representation can be written as

$$V_{t't}{}^{(0)}(Q)=V_Q{}^{(0)}\sum_{\mathbf{p}}\langle n'k_y'k_z'|\mathbf{p}+\mathbf{Q}\rangle\langle\mathbf{p}|nk_yk_z\rangle, \quad (1.5)$$

where

$$\langle\mathbf{p}|nk_yk_z\rangle=L^{1/2}\left(\frac{2\pi}{\Omega^{1/3}}\right)^{1/2}\delta_{k_yp_y}\delta_{k_zp_z} \times\exp\left[-\frac{ihp_xk_y}{m\omega_c}\right]\Phi_n(Lp_x), \quad (1.6)$$

$$\Phi_n(p)=\frac{H_n(p)e^{-p^2/2}}{(n!2^n\sqrt{\pi})^{1/2}} \quad (1.7)$$

is the harmonic-oscillator wave function, $L=(\hbar c/eH)^{1/2}$ is the magnetic length, and Ω is the volume of the system. After summing over p_y, p_z and converting the p_x sum into an integral, (1.5) can be written as[17]

$$V_{t't}{}^{(0)}(Q)=V_Q{}^{(0)}\delta_{k_y',k_y+Q_y}\delta_{k_z',k_z+Q_z} \times\exp\left\{\frac{ih}{m\omega_c}(Q_xk_y+\tfrac{1}{2}Q_xQ_y)\right\}e^{i(n-n')\varphi}\mathcal{G}_{nn'}\left(\frac{\hbar Q_\perp{}^2}{2m\omega_c}\right), \quad (1.8)$$

where, for $n\geq n'$,

$$\mathcal{G}_{nn'}(x)=\left[\frac{n'!}{n!}\right]^{1/2}e^{-x/2}x^{(n-n')/2}L_{n'}{}^{n-n'}(x), \quad (1.9)$$

$Q_x+iQ_y=Q_\perp e^{i\varphi}$, and $L_n{}^m(x)$ is the associated Laguerre polynomial.

The superscript (0) on the phonon frequencies and the interaction matrix element, designates the fact that they are "unrenormalized." A discussion of phonon renormalization in the magnetic field case is referred to Appendix III; the results of this appendix will be included in the next section.

As in H, the starting point of the treatment is the relationship between the (wave-vector- and frequency-dependent) conductivity tensor[18] and the thermodynamic velocity-correlation function of the system. This relationship reads[19]

$$\sigma_{xy}(\mathbf{q},\omega)=-(ne^2/im\omega)\delta_{xy}+(e^2/im\Omega)\mathfrak{F}_{xy}(\omega+is), \quad (1.10)$$

[15] $\mathbf{Q}$ will be understood to also incorporate the polarization indices of the vibration mode.

[16] A. H. Wilson, *Theory of Metals* (Cambridge University Press, Cambridge, 1953), 2nd ed., p. 257. The electrons interacting with the EPI of (1.4) do not couple to transverse phonons. When umklapp processes are included the transverse modes can couple to the electrons, as $\hbar(\mathbf{p}-\mathbf{p}')$, the electron momentum transfer, need not be parallel to $\hbar\mathbf{Q}$ [cf. J. M. Ziman, *Electrons and Phonons* (Oxford University Press, New York, 1960), Chap. V]. Some mention of transverse modes will be included in Sec. IV.

[17] Bateman Manuscript Project, *Integral Transforms* edited by A. Erdélyi (McGraw-Hill Book Company, Inc., New York, 1954), Vol. II, p. 292, formula 30. Note: $He_m(\sqrt{2}x)=H_m(x)/(2^m)^{1/2}$. For an interesting application of $\mathcal{G}_{nn'}$ in another physical context see P. Carruthers and M. M. Nieto, Am. J. Phys. 33, 537 (1965), Sec. V.

[18] In the case of cyclotron resonance, the conductivity tensor is not directly accessible to experimental measurement. However, as shown in Sec. IV [cf. Eq. (4.7)], it is related in a rather simple way to the experimentally observable surface impedance of the sample.

[19] For a derivation of Eq. (1.10), see H. Appendix I. or J. M. Luttinger and P. Nozieres, Phys. Rev. 127, 1431 (1962), Appendix A.

where n is the density of conduction electrons, $\mathbf{q}$, ω are the wave vector and frequency of an arbitrary space-time component of the electromagnetic field, Ω is the volume of the system, and $\mathfrak{F}(\omega+is)$ (with s an infinitesimally small positive quantity) is the analytical continuation (regular throughout the complex plane, with the exception of a branch cut on the real axis) of the function

$$\mathfrak{F}_{xy}(\omega_r)\equiv-\frac{1}{\beta}\int_0^\beta du_2\int_0^\beta du_1\, e^{\hbar\omega_r(u_2-u_1)}F_{xy}(u_2,u_1), \quad (1.11)$$

where $F_{xy}(u_2,u_1)$, the thermodynamic velocity-correlation function, is given by

$$F_{xy}(u_2,u_1)=(1/Z_G)\,\mathrm{Tr}\{Te^{-\beta(H-\mu N)}e^{u_2H}v_x(-\mathbf{q})\times e^{-u_2H}e^{u_1H}v_y(\mathbf{q})e^{-u_1H}\}. \quad (1.12)$$

In (1.12) $\omega_r\equiv 2\pi ir/\beta$ (with r integral), Z_G is the grand partition function, $\beta\equiv 1/\kappa T$, T is Dyson's time-ordering operator, and[20]

$$\mathbf{v}(\mathbf{q})=\sum_{t't}\langle t'|\,\mathbf{v}_q\,|t\rangle a_{t'}^\dagger a_t, \quad (1.13)$$

where

$$\langle t'|\,\mathbf{v}_q\,|t\rangle\equiv\int\Psi_{t'}^*(\mathbf{r})\frac{1}{2m}\left\{e^{i\mathbf{q}\cdot\mathbf{r}}\left[\frac{\hbar}{i}\mathrm{grad}_r-\frac{e}{c}\mathbf{A}(\mathbf{r})\right]+\left[\frac{\hbar}{i}\mathrm{grad}_r-\frac{e}{c}\mathbf{A}(\mathbf{r})\right]e^{i\mathbf{q}\cdot\mathbf{r}}\right\}\Psi_t(\mathbf{r})d^3r, \quad (1.14)$$

with

$$\Psi_t(\mathbf{r})\equiv\Psi_{nk_yk_z}(\mathbf{r})=\frac{1}{\Omega^{1/3}L^{1/2}}\Phi_n\left(\frac{x-\hbar k_y/m\omega_c}{L}\right)\times\exp\{i(k_yy+k_zz)\}. \quad (1.15)$$

As will be seen more explicitly in Sec. IV, the geometry appropriate to the typical cyclotron-resonance experiment is such that the electromagnetic field propagates along, say, the x axis, perpendicular to the magnetic field (i.e., the z axis) whereas the electric polarization is chosen along the third perpendicular direction, i.e., the y axis. It then follows that only the y component of (1.14) is needed. Employing the same manipulations as for the EPI matrix element, one has

$$\langle t'|\,v_{q,y}\,|t\rangle=\delta_{k_yk_y'}\delta_{k_zk_z'}\omega_c\times\exp\{ihq_xk_y/m\omega_c\}i\frac{\partial}{\partial q_x}\mathcal{G}_{nn'}(hq_x^2/2m\omega_c). \quad (1.16)$$

The evaluation of $\mathfrak{F}_{xy}(\omega+is)$ by thermodynamic many-body perturbation theory is carried out in close analogy with the nonmagnetic case. In particular, the rules given at the end of H. Sec. I are, for the most part, immediately applicable. The only changes which are required are those associated with the replacement of plane waves by the Landau states, $\Psi_{nk_yk_z}(\mathbf{r})$ [given by (1.15)], as the fundamental one-electron representation. Thus, in particular, for a fermion line labeled by n, k_y, k_z, ζ_l, one introduces a factor

$$S_l^{(0)}(\zeta_l)\equiv S_{nk_yk_z}^{(0)}(\zeta_l)=(\zeta_l-\epsilon_{nk_z})^{-1}, \quad (1.17)$$

where

$$\zeta_l=\mu+(2l+1)\pi i/\beta, \quad (1.18)$$

and where ϵ_{nk_z} is given by (1.3b). Moreover, for each EPI vertex, one introduces the matrix element $V_{t't}^{(0)}(Q)\equiv V_{n'k_y'k_z',nk_yk_z}^{(0)}$, given by (1.8) and (1.9), in place of the usual EPI matrix element, $V_{k',k+Q}^{(0)}\delta_{k',k+Q}$, appropriate to the nonmagnetic case (where, cf. H. 1.3, $\mathbf{k}'$ and $\mathbf{k}$ are three-dimensional wave vectors). Finally, for each external field (EF) vertex,[21] one introduces the matrix element $\langle t'|\,v_{\pm q,y}\,|t\rangle$, given explicitly by (1.16), in place of the vector $v_{(k+k')/2}\delta_{k',k\pm q}$, appearing in H. p. 418, rules (E) and (F).

Added note: In both the EPI and EF matrix elements [cf. (1.8) and (1.16)], the exact expression (1.9) for $\mathcal{G}_{nn'}$ has limited use in detailed calculations. Titeica[22] generated a differential equation for $\mathcal{G}_{nn'}$, and solved the equation with the WKB method. The WKB solution for $\mathcal{G}_{nn'}$, which is valid for large quantum numbers n, n', is

$$\mathcal{G}_{nn'}\left(\frac{\alpha^2}{2}\right)=\left[\frac{2}{\pi}\right]^{1/2}\frac{\cos\left\{\int_{\alpha_0}^{\alpha}[(n+n'+1)-(n-n')^2/\alpha'^2-\alpha'^2/4]^{1/2}d\alpha'-\pi/4\right\}}{(\sqrt{\alpha})[(n+n'+1)-(n-n')^2/\alpha^2-\alpha^2/4]^{1/4}}, \quad (1.19)$$

where α_0 is the lower root of the expression in the square bracket. The approximate expression for $\mathcal{G}_{nn'}$ in (1.19) will be used throughout the present paper. It will be seen in this section and Sec. III that significant values for the first term $(n+n'+1)$ in the square bracket of (1.20) are $\sim E_F/\hbar\omega_c\gg 1$. When $\alpha^2=\hbar Q_t^2/m\omega_c$ as in the EPI matrix element: $\alpha^2\sim\hbar Q_m^2/m\omega_c\sim E_F/\hbar\omega_c$, where Q_m is the Debye maximum wave vector [$Q_m=(2/z_e)^{1/3}k_F$, z_e=number of valence electrons per atom], and $n-n'$, the change in n due to phonon scattering, can vary up to v_FQ_m/ω_c. When $\alpha^2=\hbar q_x^2/m\omega_c$ as in the EF matrix

[20] Equations (1.13) and (1.14) constitute the analog of H. (1.18) [incidentally the right-hand side of H. (1.8) should read "$\mathbf{v}^*(-q)$"].

[21] An nth-order diagram for $\mathfrak{F}$ has $n-2$ EPI vertices (scattering of an electron by absorption or emission of a phonon) and two EF vertices (absorption/emission of momentum from/to the external electromagnetic field by an electron). See H. p. 417.

[22] S. Titeica, Ann. Phys. (Leipzig) **22**, 128 (1935). In Titeica's paper an expression for $|\mathcal{G}_{nn'}|^2$ can be found in Eq. (12) on p. 139. The cosine factor in Eq. (1.19) of the present paper is chosen to agree with the correct asymptotic formula for the Laguerre polynomial in terms of Bessel functions [see L. Slater, *Confluent Hypergeometric Functions* (Cambridge University Press, Cambridge, 1960), Secs. 5.5 and 4.4.3]. In both the EPI and EF cases, a $1/4\alpha^2$ term has initially been dropped from the square bracket expression in (1.19) (see text immediately below).

element $\alpha^2\sim(q_x/k_F)^2E_F/\hbar\omega_c\ll n+n'+1$, and $n-n'$, the change in n due to the electromagnetic field can vary up to $v_Fq_x/\omega_c=R_c/\delta\gg1$. In both cases, therefore, $(n-n')^2/\alpha^2$ can vary up to $E_F/\hbar\omega_c$. In the EPI case all the expressions in the square bracket in (1.19) are comparable and all must be retained. In using (1.19) for the EPI matrix element, integrations will be restricted to non-negative values of the square bracket.

In the EF case, the $\alpha^2/4$ term can be neglected as compared to $n+n'+1$. The resulting expression, after performing the α' integration, can be seen to be the asymptotic form for $J_\nu(z)$, the Bessel function of order ν, when[23] $\nu<z$. Thus, for the EF case

$$\mathcal{J}_{nn'}(\hbar q_x^2/2m\omega_c)\cong J_{n-n'}([(n+n'+1)\hbar q_x^2/m\omega_c]^{1/2}). \quad (1.20)$$

II. SELF-ENERGY PARTS

It is important to note that, with the changes in the basic rules described towards the end of the previous section, only the y and z components of the single-particle wave vector are conserved at each EPI vertex. Under these circumstances, it is not *a priori* guaranteed that the exact electron (phonon) propagator—obtained as described, e.g., in H. Sec. II by summing over all possible insertions of electron (phonon) self-energy parts into an electron (phonon) line—is diagonal in the single-particle quantum numbers, n, k_y, k_z (Q_x,Q_y,Q_z).[24] However, as shown in Appendix IV, although the Hamiltonian of the system is not invariant with respect to pure translations,[25] it does exhibit an invariance with respect to translation, followed by an appropriate gauge transformation [cf. Eqs. (AIV.6) and (AIV.10) of Appendix IV]. With the use of this symmetry property, it is shown in Appendix IV that (a) the exact phonon propagator is diagonal[26] in $\mathbf{Q}$ (as in the nonmagnetic case), and (b) with the added assumption of invariance of the total Hamiltonian with respect to rotations about an axis parallel to the magnetic field—this property holds for the special case of the spherical model, treated in this paper—the electron propagator is also diagonal in the relevant single-particle quantum numbers (n, k_y, and k_z).

From these results, it follows immediately that the electron and phonon self-energy parts, given generally by[27]

$$G(\zeta_l)=[S^{(0)}(\zeta_l)]^{-1}-[S(\zeta_l)]^{-1}, \quad (2.1)$$

and

$$P(\xi_m)=[D^{(0)}(\xi_m)]^{-1}-[D(\xi_m)]^{-1} \quad (2.2)$$

are also diagonal in (n,k_y,k_z) and (Q_x,Q_y,Q_z), respectively. Thus,

$$\langle t'|S(\zeta_l)|t\rangle=\frac{\delta_{tt'}}{\zeta_l-\epsilon_t-G_t(\zeta_l)}, \quad (2.3)$$

$$\langle\mathbf{Q}'|D(\xi_m)|\mathbf{Q}\rangle=\delta_{Q'Q}\frac{2\hbar\omega_Q{}^{(0)}}{\hbar^2\omega_Q{}^{(0)2}-\xi_m{}^2-2\hbar\omega_Q{}^{(0)}P_Q(\xi_m)}, \quad (2.4)$$

where $G_t(\zeta_l)$ and $P_Q(\xi_m)$ are the diagonal components of electron and phonon self-energy parts—i.e., diagonal in their respective single-particle quantum numbers.

The dominant contribution to the phonon self-energy part is evaluated in Appendix III. Apart from a negligibly small oscillatory part, the results are identical to those in H. Appendix III. As in that work, it is convenient to express these results in terms of a renormalization recipe. This recipe reads: (1) Replace $\hbar\omega_Q{}^{(0)}$ by $\hbar\omega_Q$;

$$(\hbar\omega_Q)^2=(\hbar\omega_Q{}^{(0)})^2-2\hbar\omega_Q{}^{(0)}P_Q(0)+\Delta_Q{}^2,$$

where[28]

$$\Delta_Q=\lim_{\xi\to0}\frac{\hbar\omega_Q{}^{(0)}}{\xi}\mathrm{Im}P_Q(\xi+i0)$$

$$=\hbar\omega_Q\pi\sum_k|V_{k+Q,k}|^2\delta(\epsilon_k-\mu)\delta(\epsilon_k-\epsilon_{k+Q}). \quad (2.5)$$

(ϵ_k=Bloch energy of an electron of wave vector k in the absence of the magnetic field.) (2) Replace $V_Q{}^{(0)}$ by V_Q;

$$V_Q=V_Q{}^{(0)}(\omega_Q{}^{(0)}/\omega_Q)^{1/2}=iC|Q|(\hbar/2NM\omega_Q)^{1/2}. \quad (2.6)$$

[This replacement has already been inserted into (2.5).] (3) The exact phonon propagator associated with a phonon line is

$$D_Q(\xi_m)=\int_0^\infty\frac{2\xi'\rho_Q(\xi')d\xi'}{\xi'^2-\xi_m{}^2}, \quad (2.7)$$

where the spectral density function is equal to

$$\rho_Q(\xi)=\frac{\Delta_Q}{\pi}\left[\frac{1}{(\hbar\omega_Q{}^2-\xi)^2+\Delta_Q{}^2}-\frac{1}{(\hbar\omega_Q+\xi)^2+\Delta_Q{}^2}\right]. \quad (2.8)$$

[23] G. N. Watson, *A Treatise in the Theory of Bessel Functions* (Cambridge University Press, New York, 1945), 2nd ed., Eq. (1) on p. 234.

[24] As discussed in H. Sec. II, when exact propagators are used in the place of free propagators, the only $\mathfrak{F}_{xy}(\omega_r)$ diagrams which are to be summed are *skeleton* diagrams, i.e., diagrams which are devoid of self-energy parts. An electron (phonon) self-energy part is any component of a diagram which does not contain EF vertices and which can be separated from the remainder of the diagram by cutting two fermion (phonon) lines. As in H., one deals only with proper electron (phonon) self-energy parts—diagrammatic entities which cannot be further subdivided by the severing of a single electron (phonon) line.

[25] Such invariance, when present (as in the nonmagnetic case) leads directly to the diagonality of electron and phonon propagators in the single-particle quantum numbers, k_x, k_y, k_z and Q_x, Q_y, Q_z, respectively.

[26] It should be mentioned in passing that a similar property, the diagonality of the conductivity tensor σ_{xy} in the external wave-vector $\mathbf{q}$—which is also not *a priori* obvious in the absence of pure translational invariance—is established in Appendix IV.

[27] These equations constitute matrix generalizations of H. (2.2a) and H. (2.2b). In particular, in the representation of the single-particle quantum numbers $[S^{(0)}(\zeta_l)]^{-1}$ and $[D^{(0)}(\xi_m)]^{-1}$ symbolize the diagonal matrices $(\zeta_l-\epsilon_t)\delta_{t't}$ and $[\hbar^2\omega_Q{}^{(0)2}-\xi_m]\delta_{Q'Q}/2\hbar\omega_Q{}^{(0)}$, respectively. Similarly, $[S(\zeta_l)]^{-1}$ and $[D(\xi_m)]^{-1}$ represent matrices whose elements are $\delta_{t't}/S_{nk_yk_z}(\zeta_l)$ and $\delta_{Q'Q}/D_Q(\xi_m)$, respectively.

[28] ω_Q is understood to be the observed phonon frequency. An explicit expression for $P_Q(0)$ will not be needed in this paper.

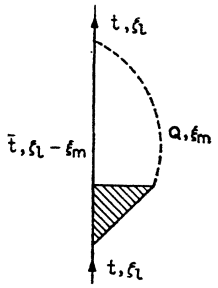

FIG. 1. General diagram for proper electron self-energy part.

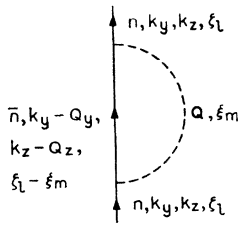

FIG. 2. Lowest order skeleton diagram for the proper electron self-energy part.

It is shown on H. p. 510 that to within a good approximation

$$\rho_Q(\xi)\cong\delta(\hbar\omega_Q-\xi)\,, \tag{2.9}$$

and therefore

$$D_Q(\xi_m)=\frac{2\hbar\omega_Q}{(\hbar\omega_Q)^2-\xi_m{}^2}=\sum_{\pm}\frac{1}{\hbar\omega_Q\pm\xi_m}\,, \tag{2.10}$$

characteristic of a free boson propagator. It is a simple matter to generalize final expressions when (2.10) is used. Replace $\hbar\omega_Q$ by a variable phonon energy ξ, multiply by the exact $\rho_Q(\xi)$, (2.8), and integrate ξ (from zero to infinity).[29]

The most general diagram for the electron proper self-energy matrix element, $G_l(\zeta_l)$, is shown in Fig. 1. The shaded triangle in Fig. 1 represents the full EPI vertex part. Migdal's theorem[12] states that to within zeroth order in c_s/v_F the full EPI vertex part can be replaced by the elementary EPI vertex, $V_{\bar{\imath},\imath}(\mathbf{Q})$. This result is established in the magnetic case, modulo oscillatory parts, in Appendix III. It will, thus, suffice to now calculate the contribution to the electron proper self-energy part, by the lowest order skeleton diagram shown in Fig. 2.

The contribution of this diagram is

$$G_{nk_z}(\zeta_l)=\frac{1}{\beta}\sum_{\bar{n},\mathbf{Q},\xi_m,\pm}\frac{|V_{i\imath}(\mathbf{Q})|^2}{[\zeta_l-\xi_m-\epsilon_{\bar{\imath}}-G_{\bar{n},k_z-Q_z}(\zeta_l-\xi_m)][\hbar\omega_Q\pm\xi_m]}\,. \tag{2.11}$$

Although $G_{nk_z}(\zeta_l)$ is defined at isolated points in the complex plane, the analytical continuation[30] $\zeta\to\mathcal{E}\pm i0$ to the real ζ axis will be of ultimate physical interest. The notation $\pm i0$ is used to take cognizance of the discontinuity[31] of the self-energy on the real axis; specifically,

$$G_{nk_z}(\mathcal{E}\pm i0)=M_{nk_z}(\mathcal{E})\mp i\Gamma_{nk_z}(\mathcal{E})\,, \tag{2.12}$$

where $M_{nk_z}(\mathcal{E})$ and $\Gamma_{nk_z}(\mathcal{E})$ are real and $\Gamma_{nk_z}(\mathcal{E})\geq 0$. The self-energy is regular everywhere in the cut complex plane.

In transforming the sum over ξ_m in (2.11) into an integral over a suitable contour in the complex ξ plane, the ξ plane must be cut along the discontinuity of $G_{\bar{n},k_z-Q_z}$, i.e., $\mathrm{Im}(\xi-\zeta_l)=0$. With the introduction of the function $[1-e^{\mp\beta\xi}]^{-1}$, which has simple poles at $\xi=\xi_m$ with residues $\pm\beta^{-1}$, the self-energy (2.11) can be written as

$$G_{nk_z}(\zeta_l)=\frac{1}{2\pi i}\sum_{\bar{n},\mathbf{Q},\pm}\mp\int_{\Gamma_0}\frac{|V_{i\imath}(\mathbf{Q})|^2\{[1-e^{\mp\beta\xi}]^{-1}+N_Q\}d\xi}{[\zeta_l-\xi_m-\epsilon_{\bar{\imath}}-G_{\bar{n},k_z-Q_z}(\zeta_l-\xi)][\hbar\omega_Q\pm\xi]}\,, \tag{2.13}$$

where $N_Q\equiv[e^{\beta\hbar\omega_Q}-1]^{-1}$ is the contribution from the poles of the phonon propagator and the contour Γ_0 goes from $-\infty$ to $+\infty$ just below the line $\mathrm{Im}(\xi-\zeta_l)=0$ and from $+\infty$ to $-\infty$ just above. To regain the original sum over ξ_m, the contour Γ_0 need just be transformed into a contour encircling the poles of $[1-e^{\mp\beta\xi}]^{-1}$. Now $\xi=\zeta_l-x\pm i0$ is substituted for the integrations above and below the line $\mathrm{Im}(\xi-\zeta_l)=0$ and use is made of $e^{\pm\beta\zeta_l}=-e^{\pm\beta\mu}$, to rewrite (2.13) as

$$G_{nk_z}(\zeta_l)=\frac{1}{2\pi i}\sum_{\bar{n},\mathbf{Q},\pm}\int_{-\infty}^{\infty}\frac{dx\,|V_{i\imath}(\mathbf{Q})|^2 f^{(\mp)}(x)}{(\zeta_l-x\pm\hbar\omega_Q)}\left[\frac{1}{x-\epsilon_{\bar{\imath}}-G_{\bar{n},k_z-Q_z}(x-i0)}-\frac{1}{x-\epsilon_{\bar{\imath}}-G_{\bar{n},k_z-Q_z}(x+i0)}\right], \tag{2.14}$$

where $f^{(\mp)}(x)\equiv[1+e^{\pm\beta(x-\mu)}]^{-1}$, the Fermi occupancy (vacancy) function. The term N_Q has been dropped from the integrand of (2.14) in accordance with the conditions of this paper,

$$\kappa T\ll\hbar\omega_c\sim\hbar\omega\sim\kappa\Theta\,. \tag{2.15}$$

[29] The effect of the corrections to (2.9) on the electron self-energy is discussed on H. pp. 435–436.

[30] For a discussion of the uniqueness of the analytical continuation from isolated points in the complex plane, see N. D. Mermin and G. Baym, J. Math. Phys. 2, 236 (1961).

[31] J. M. Luttinger, Phys. Rev. 121, 942 (1961).

The algebraic sum of the two expressions in the square bracket of (2.14) has the familiar form of a Lorentzian resonance function of width $\sim\Gamma_{\bar{n},k_z-Q_z}(x)$, centered at $x-\epsilon_l-M_{\bar{n},k_z-Q_z}(x)=0$. A considerable simplification to the problem can be achieved by replacing this resonance function by a delta function, $\delta(x-\epsilon_l-M_{\bar{n},k_z-Q_z}(x))$, plus higher corrections. In order to use such an approximation in a subsequent integration, the rest of the integrand must be slowly varying over the width of the resonance, $\Gamma_{\bar{n},k_z-Q_z}(x)$. For the conditions stated in (2.15), it is readily seen that $f^{(\mp)}(x)$ varies by an order of itself in an interval $|x-\mu|\ll\kappa\Theta$. Now $\Gamma_{\bar{n},k_z-Q_z}(x)$ will be shown to be a measure of the EPI coupling and for the case of interest here, that of strong coupling, $\Gamma(\mu+\kappa\Theta)\sim\kappa\Theta$. The function $f^{(\mp)}(x)$ cannot, therefore, be considered as [cf. (2.29)] slowly varying over an interval of the order of a typical value of $\Gamma(x)$.

To justify the delta-function approximation, attention is now focused on the $\bar{n}$, $\mathbf{Q}$ sums. Inspection[32] of Eq. (1.20) shows that when $\alpha^2=\hbar Q_\perp^2/m\omega_c$, a change $\Delta Q_\perp\sim\pi\omega_c/(\hbar Q_\perp/m)\sim\pi\omega_c/v_F$ causes a complete oscillation of the cosine phase factor. Since $\hbar\omega_c\sim\Gamma(\mu+\kappa\Theta)$ [from (2.15)], the phase factor in (1.20) cannot be considered as slowly varying over an interval of Q associated with the width of the resonance, i.e., $\Delta Q\sim\Gamma(x)/\hbar v_F$. The EPI matrix element in (2.14) however, enters as an absolute square and using $\cos^2(\theta-\pi/4)=\frac{1}{2}+\frac{1}{2}\sin 2\theta$, the oscillating part can be separated out. The oscillating part of the EPI matrix element can be shown to contribute to order $\hbar\omega_c/E_F$ ($\ll 1$) by calculations similar to those carried out in Appendix I. The $\bar{n}$ sum itself will give rise to oscillatory terms which cannot be considered as slowly varying over an interval of the order of $\Delta\bar{n}\sim\Gamma/\hbar\omega_c$. All the oscillatory terms are due to the essentially new feature of the present problem, that of the discreteness of the electron energy levels. The oscillatory part of the $\bar{n}$ sum is most conveniently treated by the use of the Poisson sum rule.[33] With the method of the Poisson sum rule the expression (2.14) for the self-energy can now be written

$$G_{nk_z}(\zeta_l)=\frac{1}{2\pi i}\sum_{\mathbf{Q},\pm}\sum_{l=-\infty}^{\infty}(-)^l\int_0^\infty d\eta\int_{-\infty}^{\infty}\frac{dx\,|V_Q|^2e^{2\pi il\eta}f^{(\mp)}(x)}{\pi[(n+\frac{1}{2}+\eta)(\hbar Q_\perp^2/m\omega_c)-(n+\frac{1}{2}-\eta)^2-(\hbar Q_\perp^2/2m\omega_c)^2]^{1/2}(\zeta_l-x\pm\hbar\omega_c)}$$
$$\times\left[\frac{1}{x-\eta\hbar\omega_c-(\hbar^2/2m)(k_z-Q_z)^2-G_{\eta-\frac{1}{2},k_z-Q_z}(x-i0)}-\frac{1}{x-\eta\hbar\omega_c-(\hbar^2/2m)(k_z-Q_z)^2-G_{\eta-\frac{1}{2},k_z-Q_z}(x+i0)}\right], \tag{2.16}$$

where $\bar{n}+\frac{1}{2}$ has been replaced by η and the oscillatory part of the EPI matrix element is neglected for the reasons discussed above. The oscillatory part of the self-energy, the $l\neq 0$ terms, will be treated in detail in Appendix I. A treatment analogous to that of the zero-magnetic field case in H. will now be considered for the $l=0$ term. It can be seen that for $l=0$ the terms in the integrand manifest small changes relative to their typical values ($Q\sim Q_m$, $\epsilon_l\sim E_F$) for intervals corresponding to $\Delta\eta\sim\Gamma/\hbar\omega_c$ and $\Delta Q\sim\Gamma/\hbar v_F$. In particular, for a term that is not included in the discussion in H. Appendix III

$$F_n(\eta,Q_\perp)\equiv[(n+\tfrac{1}{2}+\eta)\hbar Q_\perp^2/m\omega_c-(n+\tfrac{1}{2}-\eta)^2-(\hbar Q_\perp^2/2m\omega_c)^2]^{-1/2} \tag{2.17}$$

one has

$$\Delta\eta\left(\frac{\partial\ln F_n(\eta,Q_\perp)}{\partial\eta}\right)\sim\frac{\Gamma}{E_F}\ll 1, \tag{2.18}$$

for $\Delta\eta\sim\Gamma/\hbar\omega_c$, $n+\frac{1}{2}\sim E_F/\hbar\omega_c$, $Q_\perp\sim Q_m$. The self-energy parts in the square bracket in (2.16) will be assumed to have a weak dependence on η, Q_z. This weak dependence will be justified *a posteriori*. The delta-function approximation can now be used and one has

$$G_{nk_z}(\zeta_l)=\sum_{\mathbf{Q},\pm}\int_0^\infty d\eta\int_{-\infty}^{\infty}\frac{dx\;|V_Q|^2f^{(\mp)}(x)\delta(x-\eta\hbar\omega_c-(\hbar^2/2m)(k_z-Q_z)^2)}{\pi[(n+\frac{1}{2}+\eta)(\hbar Q_\perp^2/m\omega_c)-(n+\frac{1}{2}-\eta)^2-(\hbar Q_\perp^2/2m\omega_c)^2]^{1/2}(\zeta_l-x\pm\hbar\omega_Q)}. \tag{2.19}$$

The $M_{\eta-\frac{1}{2},k_z-Q_z}(x)$ term has been dropped from the argument of the delta-function as it will be shown that $M(x)\ll E_F$ [cf. (2.31)]. Including $M(x)$ would actually be inconsistent with the delta-function approximation. The higher order corrections to this approximation will be discussed in more detail in the next section (cf. footnote 39).

The x integration is now carried out, and after making the continuation $\zeta_l\to\mathcal{E}-i0$, the imaginary part of (2.19), $\Gamma_{nk_z}(\mathcal{E})$, is considered,

$$\Gamma_{nk_z}(\mathcal{E})=\pi\sum_{\mathbf{Q},\pm}\int\frac{d\eta\;|V_Q|^2f^{(\mp)}(\mathcal{E}\pm\hbar\omega_Q)\delta(\mathcal{E}\pm\hbar\omega_Q-\eta\hbar\omega_c-(\hbar^2/2m)(k_z-Q_z)^2)}{\pi[(n+\frac{1}{2}+\eta)(\hbar Q_\perp^2/m\omega_c)-(n+\frac{1}{2}-\eta)^2-(\hbar Q_\perp^2/2m\omega_c)^2]^{1/2}}. \tag{2.20}$$

[32] The integral in the cosine factor of (1.20) contributes a term

$$\tfrac{1}{2}[(n+n'+1)\alpha^2-(n-n')^2-\alpha^4/4]^{1/2}.$$

[33] P. M. Morse and H. Feshbach, *Methods of Theoretical Physics* (McGraw-Hill Book Company, Inc., New York, 1953), Part I, p. 466.

The η integration is performed and the $\mathbf{Q}$ sum is converted into an integral with the result

$$\Gamma_{nk_z}(\mathcal{E})=\frac{\Omega}{4\pi^2}\sum_{\pm}\int_0^{Q_m} dQ\, Q^2|V_Q|^2 f^{(\mp)}(\mathcal{E}\pm\hbar\omega_Q)\int_\alpha^\beta d\mu\,[-a\mu^2+b\mu+c]^{-1/2}, \tag{2.21}$$

where μ is the cosine of the polar angle of $\mathbf{Q}$. In the integral over μ in (2.21), the limits α, β are such as to keep the radicand nonnegative, and

$$a=\left(\frac{\hbar^2Q}{m}\right)^2\frac{2m\epsilon_t}{\hbar^2}, \tag{2.22}$$

$$b=\frac{\hbar Qk_z}{m}\left[\frac{\hbar^2Q^2}{m}+\epsilon_t-\mathcal{E}\right], \tag{2.23}$$

$$c=(\epsilon_t+\mathcal{E})\frac{\hbar^2Q^2}{m}-\frac{\hbar^2k_z^2}{m}\frac{\hbar Q^2}{m}-\left(\frac{\hbar^2Q^2}{2m}\right)^2-(\epsilon_t-\mathcal{E})^2. \tag{2.24}$$

As before, $\epsilon_t=(n+\frac{1}{2})\hbar\omega_c+\hbar^2k_z^2/2m$. The conditions of primary interest in the present calculation are: $\epsilon_t\sim E_F$. If $c\geq 0$, then $\mu=0$ is included in the range $\alpha\leq\mu\leq\beta$ and the μ integration is simply performed yielding

$$\frac{\pi}{\sqrt{a}}=\pi\left[\left(\frac{\hbar^2Q}{m}\right)^2\frac{2m\epsilon_t}{\hbar^2}\right]^{-1/2}. \tag{2.25}$$

For sufficiently large k_z and/or Q, then $c<0$ and the μ integral is separated into two integrals, one integrated over positive values of μ and the other over negative values of μ. One or the other integral separately contributes the value in (2.25) according to the algebraic sign of k_z. The geometric picture of the limitations on the Q integrals will be included in Appendix I. Finally, one has

$$\Gamma_{nk_z}(\mathcal{E})=\frac{\Omega}{4\pi^2}\sum_{\pm}\pi\int_0^{Q_m}\frac{|V_Q|^2mQ\,dQ\,f^{(\mp)}(\mathcal{E}\pm\hbar\omega_Q)}{\hbar^2[(2m/\hbar^2)(n+\frac{1}{2})\hbar\omega_c+k_z^2]^{1/2}}, \tag{2.26}$$

which is the zero-magnetic-field result, except k has been replaced by $[2m/\hbar^2(n+\frac{1}{2})\hbar\omega_c+k_z^2]^{1/2}$. The assumption of slow variation in n, k_z can now be justified *a posteriori*, i.e.,

$$\Delta n\frac{\partial\ln\Gamma_{nk_z}(\mathcal{E})}{\partial n}\simeq\frac{\hbar\omega_c}{\epsilon_t}\Delta n\ll 1 \tag{2.27}$$

for $\Delta n\sim\Gamma/\hbar\omega_c$ and $\epsilon_t\sim E_F$.

Similar results obtain for $M_{nk_z}(\mathcal{E})$, i.e., $M_{nk_z}(\mathcal{E})$ is the zero-magnetic-field result with k replaced by $[(2m/\hbar^2)(n+\frac{1}{2})\hbar\omega_c+k_z^2]^{1/2}$. In particular the slow variation of $M(\mathcal{E})$ with n, k_z as is the case for $\Gamma(\mathcal{E})$. With the use of (2.6) for V_Q and the Debye spectrum $\omega_Q=c_s|Q|$, the final results for the real and imaginary parts of the self-energy are [cf. H. Eqs. (2.31), (2.33), and (2.41)]:

$$\Gamma_{nk_z}(\mathcal{E})=\frac{k_F}{[(2m/\hbar^2)(n+\frac{1}{2})\hbar\omega_c+k_z^2]^{1/2}}\frac{\pi}{8}\left(\frac{z_e}{2}\right)^{1/3}\frac{C^2}{Mc_s^2E_F}\kappa\Theta\left(\frac{|\mathcal{E}-\mu|}{\kappa\Theta}\right)^3 \tag{2.28}$$

for $|\mathcal{E}-\mu|\leq\kappa\Theta$,

$$\Gamma_{nk_z}(\mathcal{E})=\frac{k_F}{[(2m/\hbar^2)(n+\frac{1}{2})\hbar\omega_c+k_z^2]^{1/2}}\frac{\pi}{8}\left(\frac{z_e}{2}\right)^{1/3}\frac{C^2}{Mc_s^2E_F}\kappa\Theta, \tag{2.29}$$

for $|\mathcal{E}-\mu|>\kappa\Theta$, and

$$M_{nk_z}(\mathcal{E})=\frac{1}{8}\frac{k_F}{[(2m/\hbar^2)(n+\frac{1}{2})\hbar\omega_c+k_z^2]^{1/2}}\left(\frac{z_e}{2}\right)^{1/3}\frac{C^2}{Mc_s^2E_F}\kappa\Theta$$
$$\times\left\{\ln\left[\frac{1+(\mu-\mathcal{E})/\kappa\Theta}{1-(\mu-\mathcal{E})/\kappa\Theta}\right]-\left(\frac{\mu-\mathcal{E}}{\kappa\Theta}\right)^3\ln\left(\frac{\mu-\mathcal{E}}{\kappa\Theta}\right)^2+\left(\frac{\mu-\mathcal{E}}{\kappa\Theta}\right)^3\ln\left[1-\left(\frac{\mu-\mathcal{E}}{\kappa\Theta}\right)^2\right]\right\}. \tag{2.30}$$

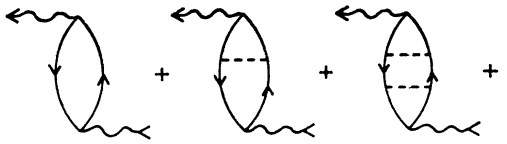

FIG. 3. Ladder diagram contributions to the velocity-correlation function.

In Sec. IV the values of the EPI coupling constant $C^2/Mc_s^2E_F$ will be discussed, but it suffices to say now that for the alkali metals it is of order unity. For $C^2/Mc_s^2E_F\sim 1$, it can be seen from (2.27) and (2.28) that $M(\mu+\kappa\Theta)\sim\Gamma(\mu+\kappa\Theta)\sim\kappa\Theta$ and therefore

$$M(\mu+\kappa\Theta)/E_F\sim\Gamma(\mu+\kappa\Theta)/E_F\ll 1\,, \qquad (2.31)$$

a condition that has already been anticipated in (2.19).

The energy $\mathcal{E}$ variation of $M(\mathcal{E})$ and $\Gamma(\mathcal{E})$ is not of the slowly varying type. In fact, the variation in $\mathcal{E}$ of $M(\mathcal{E})$ and $\Gamma(\mathcal{E})$ is such that these quantities change by an order of themselves in the range $|\mathcal{E}-\mu|\lesssim\kappa\Theta$ (cf. Fig. 7). This rapid energy variation over the range $|\mathcal{E}-\mu|\lesssim\kappa\Theta$ is unique to the EPI contribution to the electron self-energy. The main concern of this paper is to exhibit effects of this energy variation on typical transport coefficients, in particular, the bulk conductivity and the surface resistance.

III. BULK CONDUCTIVITY

In this section, the contributions of the principal skeleton diagrams of $\mathfrak{F}_{yy}(\omega+i0)$—and hence, by virtue of (1.10), to the conductivity tensor $\sigma_{yy}(q,\omega)$—will be evaluated.

In the zero magnetic field case this analysis is given in H. Secs. III, IV, and H. Appendices IV, V. The so-called "ladder" diagrams (illustrated in Fig. 3) were shown to be *the* diagrams contributing to zeroth order in the small parameter $\hbar/\tau E_F\sim c_s/v_F$ (where τ is the lifetime of an electron with an energy measured from the Fermi level of the Debye energy and c_s is the velocity of sound).

The complete summation of the ladder diagrams depicted in Fig. 3 is equivalent to solving a quantal transport equation for a suitably defined "electron-distribution function" (H. Sec. III, p. 451, 452). To account for deviations from equilibrium of the phonon

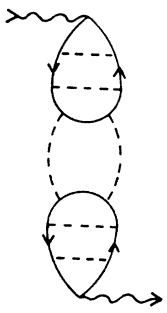

FIG. 4. Phonon-drag contributions to the velocity correlation function.

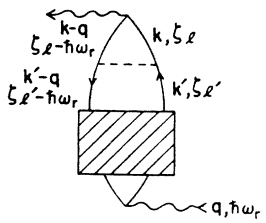

FIG. 5. Typical ladder diagram. Shaded box represents an arbitrary number of phonon lines.

system the above ladder diagrams must be appended by a class of "multiladder" diagrams, in which the external wave vector q and frequency ω are "carried" by phonon lines as well as electron lines. A generic type of the new class of diagrams is shown in Fig. 4.

The summation of both types of ladder diagrams is equivalent to solving two coupled transport equations for both the electron and phonon "distribution function" (H. Sec. IV, p. 465, 466). For the conditions of interest in this paper, namely, $T=0$, and $\omega\sim\omega_D\sim\Gamma(\mu+\hbar\omega)/\hbar$, these extra "phonon-drag" contributions are small in the ratio c_s/v_F to the straightforward ladder diagrams of Fig. 3 (H. Sec. IV, pp. 467, 468). No further discussion of phonon-drag effects (i.e., the multiladder diagrams) will be necessary.

Before getting into detailed calculations, it is desirable to discuss qualitatively the contribution of the nth "rung" ladder diagrams relative to the basic "zero-rung" contribution (first diagram of Fig. 3).

In the zero-magnetic-field case the structure of the ladder diagrams and the facts of momentum (single-particle variables) and "energy" conservation at every vertex[34] necessitates their inclusion to all orders of EPI vertices. With each addition of a phonon "rung," two EPI vertices (a factor of $|V_{kk'}|^2$) and a propagator pair appear (see the typical ladder diagram in Fig. 5).

The propagator pairs between rungs are such that the difference between their momentum (k) variables and the "energy" (ζ_l) variables are maintained to be q, $\hbar\omega_r$, respectively. After the analytical continuations $\zeta_l\to\mathcal{E}\pm i0$, $\omega_r\to\omega+i0$, and under the conditions

$$q\ll k_F\,, \qquad (3.1)$$

$$\hbar\omega\ll E_F\,, \qquad (3.2)$$

it is readily seen that the denominators of two such propagators become simultaneously small in the neighborhood of $\epsilon_k=\mathcal{E}$. Because of the "overlapping resonances" of the propagator pair their contribution is $1/\hbar\omega$, $1/\hbar\mathbf{v}_k\cdot\mathbf{q}$ or $1/\Gamma_k(\mathcal{E})$, whichever is the smallest (H. Sec. III, p. 445). Assuming the smallest is of the order $1/\Gamma_k(\mathcal{E})$, then the total factor due to the extra rung is of the order $|V_{kk'}|^2/\Gamma_k(\mathcal{E})$; this is independent of the EPI coupling constant [from an inspection of

[34] It may be recalled that the conservation of single-particle variables at every vertex is no longer completely true in the magnetic field case; i.e., n, the Landau quantum number, is not conserved. This has as its consequence the neglect of higher order ladder diagrams in the cyclotron resonance calculation; see the following text.

Eq. (2.26)]. The sum over all ladder diagrams is thus, imperative, for a proper evaluation of $\mathfrak{F}(\omega_r)$.

However, even in the zero-magnetic-field case under the conditions of the anomalous skin effect, $\hbar v_F q \gg \Gamma_{k_F}(\mu+\kappa\Theta)$ or [using $\Gamma_{k_F}(\mu+\kappa\Theta)\sim\hbar/\tau$ and $q\sim 1/\delta$] $l\gg\delta$, the contribution of the propagator pair is now $1/\hbar v_F q$ and the additional factor due to a phonon rung is $\sim\Gamma_{k_F}(\mu+\kappa\Theta)/\hbar v_F q \ll 1$. Moreover, even in the lowest order diagram (no rungs) the self-energy parts in the propagators can be neglected as compared to $\hbar\mathbf{v}_k\cdot\mathbf{q}$. It is, therefore, concluded that EPI effects are of negligible significance in the extreme anomalous skin-effect regime [see H. p. 454, footnote 68 and Ref. 9(1)].

In the present case[35] $(n-n')\hbar\omega_c$ ($n-n'=$integer and is the difference of the Landau quantum numbers of the propagator pair) takes the place of $\hbar\mathbf{v}_k\cdot\mathbf{q}$. As will be shown in this section the effective range of $(n-n')$ is $v_F q/\omega_c$.

In the lowest order skeleton diagram, ω (or ω_c) can be so adjusted that $\omega-(n-n')\omega_c\simeq 0$. The self-energy parts in the propagator denominators are not negligible for such values of ω,ω_c. In other words, one has the possibility for resonance, i.e., the domination of a single term in the discrete summation over the range of $n-n'$. If, now, the resonant condition, $\omega-(n-n')\omega_c\simeq 0$ were capable of being maintained at one and the same ω,ω_c for all the propagator pairs of nth-rung ladder diagrams, it would be necessary to consider such diagrams. Actually, however, it turns out that the quantity, $n-n'$, of any propagator pair may differ from its "predecessor" by as much as $v_F q/\omega_c$. Thus, the above-postulated resonance condition will not be maintained in higher order ladder diagrams.

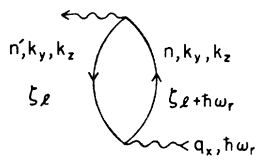

FIG. 6. The lowest order skeleton diagram for the velocity-correlation function in the magnetic field case.

The quantitative justification for the neglect of higher order ladder diagrams is carried out in Appendix II. An argument, to this end, based on the quasiclassical transport equation[36] can be found on p. 734 of Ref. 2.

Consider now the contribution to the velocity correlation function represented by the lowest order skeleton diagram of Fig. 5 (shown in detail in Fig. 6). It is recalled, that the magnetic field is chosen to lie along the z axis and the electromagnetic field is chosen to propagate along the x axis. As stated earlier, the polarization of the electromagnetic field is chosen so that the electric vector $\mathbf{E}$ is along the y axis, so that it suffices to calculate $\sigma_{yy}(\mathbf{q},\omega)$ (also cf. Sec. IV). Using the rules outlined in Sec. II and H. p. 418, one has

$$\mathfrak{F}_{yy}(\omega_r)=-\frac{1}{\beta}\sum_{\substack{n,n',k_z,k_y\\ \zeta_l}}\frac{|\langle t'|v_{q,y}|t\rangle|^2}{[\zeta_l-\epsilon_{k_z}{}^{n'}-G_{n'k_z}(\zeta_l)][\zeta_l+\hbar\omega_r-\epsilon_{k_z}{}^{n}-G_{nk_z}(\zeta_l+\hbar\omega_r)]}, \tag{3.3}$$

where

$$\epsilon_{k_z}{}^{n}\equiv(n+\tfrac{1}{2})\hbar\omega_c+\hbar^2k_z{}^2/2m.$$

The sum over ζ_l is converted into an integral over a suitable contour in the ζ plane. The procedure is similar to that used with the self-energy part in Sec. II. The ζ plane is cut along the lines of discontinuity of the self-energy parts in (3.3), the lines $\mathrm{Im}\zeta=0$ and $\mathrm{Im}(\zeta+\hbar\omega_r)=0$. The substitutions $\zeta=\mathcal{E}\pm i0$ and $\zeta=\mathcal{E}-\hbar\omega_r\pm i0$ are used for the parts of the contour above and below the lines $\mathrm{Im}\zeta=0$ and $\mathrm{Im}(\zeta+\hbar\omega_r)=0$, respectively. The resultant expression is

$$\mathfrak{F}_{yy}(\omega_r)=-\frac{1}{2\pi i}\sum_{\substack{n,n'\\ k_z,k_y}}\int_{-\infty}^{\infty}\frac{d\mathcal{E}\,f^{(-)}(\mathcal{E})|\langle t'|v_{q,y}|t\rangle|^2}{[\mathcal{E}+\hbar\omega_r-\epsilon_{k_z}{}^{n}-G_{nk_z}(\mathcal{E}+\hbar\omega_r)]}\left\{\frac{1}{\mathcal{E}-\epsilon_{k_z}{}^{n'}-G_{n'k_z}(\mathcal{E}-i0)}-\frac{1}{\mathcal{E}-\epsilon_{k_z}{}^{n'}-G_{n'k_z}(\mathcal{E}+i0)}\right\}$$

$$-\frac{1}{2\pi i}\sum_{\substack{n,n'\\ k_y,k_z}}\int_{-\infty}^{\infty}\frac{d\mathcal{E}'\,f^{(-)}(\mathcal{E}')|\langle t'|v_{q,y}|t\rangle|^2}{[\mathcal{E}'-\hbar\omega_r-\epsilon_{k_z}{}^{n'}-G_{n'k_z}(\mathcal{E}'-\hbar\omega_r)]}\left\{\frac{1}{\mathcal{E}'-\epsilon_{k_z}{}^{n}-G_{nk_z}(\mathcal{E}'-i0)}-\frac{1}{\mathcal{E}'-\epsilon_{k_z}{}^{n}-G_{nk_z}(\mathcal{E}'+i0)}\right\}. \tag{3.4}$$

The continuation $\omega_r\to\omega+i0$ can now be made, as the integrands in (3.4) are regular[37] functions of a complex frequency $\tilde{\omega}$ ($\mathrm{Re}\tilde{\omega}=\omega$) in the $\tilde{\omega}$ plane cut along $\mathrm{Im}\tilde{\omega}=0$. With a change in the variable of integration $\mathcal{E}'=\mathcal{E}+\hbar\omega$

[35] It will be assumed that the central significance of ladder diagrams and the neglect of certain higher order terms in the conductivity (see following text) is retained in the magnetic field case. This is based on the experience gained in treating the electron and phonon self-energy and the full EPI vertex part. Thus, except for oscillatory terms, the calculations in H. Appendix IV, V is expected to apply to the magnetic field case.

[36] It should be noted that the higher order diagrams collectively correspond to a scattering-in term (the "B" term of Ref. 2). This can be simply seen from an inspection of Fig. 5. An electron in a state k' contributes to the occupation of state k via collisions with phonons.

[37] The regularity of the integrand in the entire cut $\tilde{\omega}$ plane is not obtained if the ω_r dependence in $f^{(-)}(\mathcal{E}'-\hbar\omega_r)$ is retained. The ω_r dependence was eliminated with the use of $e^{\beta\omega_r}=1$. Ambiguities, such as these, in the analytical continuation from a set of isolated points in the complex plane are discussed in Ref. 30.

and a rearrangement of terms, one has the following:

$$\mathfrak{F}_{yy}(\omega+i0)=-\frac{1}{2\pi i}\sum_{\substack{n,n'\\k_y,k_z}}\int_{-\infty}^{\infty}\frac{d\mathcal{E}\,[f^{(-)}(\mathcal{E})-f^{(-)}(\mathcal{E}-\hbar\omega)]\,|\langle l'|v_{q,y}|l\rangle|^2}{[\mathcal{E}+\hbar\omega-\epsilon_{k_z}{}^{n}-G_{nk_z}(\mathcal{E}+\hbar\omega+i0)][\mathcal{E}-\epsilon_{k_z}{}^{n'}-G_{n'k_z}(\mathcal{E}-i0)]}$$

$$+\frac{1}{2\pi i}\sum_{\substack{n,n'\\k_y,k_z}}\int_{-\infty}^{\infty}d\mathcal{E}\,|\langle l'|v_{q,y}|l\rangle|^2\left\{\frac{f^{(-)}(\mathcal{E})}{[\mathcal{E}+\hbar\omega-\epsilon_{k_z}{}^{n}-G_{nk_z}(\mathcal{E}+\hbar\omega+i0)][\mathcal{E}-\epsilon_{k_z}{}^{n'}-G_{n'k_z}(\mathcal{E}+i0)]}\right.$$

$$\left.-\frac{f^{(-)}(\mathcal{E}+\hbar\omega)}{[\mathcal{E}+\hbar\omega-\epsilon_{k_z}{}^{n}-G_{nk_z}(\mathcal{E}+\hbar\omega-i0)][\mathcal{E}-\epsilon_{k_z}{}^{n'}-G_{n'k_z}(\mathcal{E}-i0)]}\right\}. \tag{3.5}$$

Before any simplifications of the propagators in (3.5) can be attempted, some basic preliminaries must be considered. The eventual simplifications are analogous to those which lead to the delta-function approximation in the treatment of the self-energy parts, i.e., the replacement of the propagators by suitable delta and principal-value functions.

As discussed earlier in this section, the denominators of the propagator pairs can become simultaneously small in the neighborhood of $\epsilon_l=\mathcal{E}$ and $(n-n')\hbar\omega_c\sim\hbar\omega$. The "overlapping" of the resonances of the propagator pairs must be considered explicitly. Also, as discussed in the preceding section the approximate treatment of the propagators depend on the slow "k" (n,n',k_z) variation of quantities in the integrand. Therefore, as in Sec. II, the oscillatory parts of the n, n' sums must be considered separately in order to affect the essential simplifications.

The rapidity of the oscillations depends upon the values of n, n' which contribute most significantly to the sums. It will be shown, shortly, that the significant values are, $(n+n'+1)\leq E_F/\hbar\omega_c$ and $(n-n')\lesssim v_F q_x/\omega_c$. Therefore, it is convenient to introduce a change in summation variables $N\equiv(n+n')/2$ and $r\equiv n-n'$. The sums over n,n' are replaced by

$$\sum_{n',n=0}^{\infty}\rightarrow\sum_{r=-\infty}^{\infty}\sum_{N=0}^{\infty}, \tag{3.6}$$

to a very good approximation. [The terms added to the n,n' sums by the replacement (3.6) are those for which $|r|/N>1$; by virtue of the above remarked limitation on $|r|\equiv|n-n'|$ these terms are quite negligible.] Because of the established weak dependence of $G_{n'k_z}$ on n',k_z one has to order $(n-n')\hbar\omega_c/[(N+\frac{1}{2})\hbar\omega_c+\hbar^2k_z{}^2/2m]\sim(n-n')/(E_F/\hbar\omega_c)$ (which is at worst of the order $q_x/k_F\ll1$, i.e., for a skin depth $\delta=10^{-6}$ cm, $q_x/k_F\sim1/100$),

$$G_{n'k_z}(\mathcal{E})=G_{N-r/2,k_z}(\mathcal{E})\simeq G_{Nk_z}(\mathcal{E}),\qquad G_{nk_z}(\mathcal{E}+\hbar\omega)=G_{N+r/2,k_z}(\mathcal{E})\simeq G_{Nk_z}(\mathcal{E}+\hbar\omega). \tag{3.7}$$

It is only essential to separate out the oscillatory part of the N sum as these constitute the more rapid variation. The Poisson sum rule is used, as in (2.16), and the oscillatory part, the $l\neq0$ terms, is calculated in Appendix II. With the use of the Poisson sum rule, $N+\frac{1}{2}$ is changed to a continuous variable η and the sum over N into an integral over η (from zero to infinity). Further, the variable η is changed to $\hbar k_1{}^2/2m\omega_c$ and the definitions $k^2=k_1{}^2+k_z{}^2$ and $\epsilon_k=\hbar^2k^2/2m\omega_c$ are introduced.

Now the propagator pairs in (3.5) are expanded in partial fractions and use is made of the above change in variables on the right-hand side of the equations to give[38]

$$([\mathcal{E}+\hbar\omega-\epsilon_{k_z}{}^{n}-G_{Nk_z}(\mathcal{E}+\hbar\omega+i0)][\mathcal{E}-\epsilon_{k_z}{}^{n'}-G_{Nk_z}(\mathcal{E}-i0)])^{-1}$$
$$=(\hbar\omega-r\hbar\omega_c+M_k(\mathcal{E})-M_k(\mathcal{E}+\hbar\omega)+i[\Gamma_k(\mathcal{E})+\Gamma_k(\mathcal{E}+\hbar\omega)])^{-1}$$
$$\times\{[\mathcal{E}-\epsilon_k+\tfrac{1}{2}r\hbar\omega_c-G_k(\mathcal{E}-i0)]^{-1}-[\mathcal{E}+\hbar\omega-\epsilon_k+\tfrac{1}{2}r\hbar\omega_c-G_k(\mathcal{E}+\hbar\omega+i0)]^{-1}\}, \tag{3.8}$$

$$([\mathcal{E}+\hbar\omega-\epsilon_{k_z}{}^{n}-G_{Nk_z}(\mathcal{E}+\hbar\omega\pm i0)][\mathcal{E}-\epsilon_{k_z}{}^{n'}-G_{Nk_z}(\mathcal{E}\pm i0)])^{-1}$$
$$=(\hbar\omega-r\hbar\omega_c+M_k(\mathcal{E})-M_k(\mathcal{E}+\hbar\omega)\pm i[\Gamma_k(\mathcal{E}+\hbar\omega)-\Gamma_k(\mathcal{E})])^{-1}$$
$$\times\{[\mathcal{E}-\epsilon_k+\tfrac{1}{2}r\hbar\omega_c-G_k(\mathcal{E}\pm i0)]^{-1}-[\mathcal{E}+\hbar\omega-\epsilon_k-\tfrac{1}{2}r\hbar\omega_c-G_k(\mathcal{E}+\hbar\omega\pm i0)]^{-1}\}, \tag{3.9}$$

where $\Gamma_{\eta-\frac{1}{2},k_z}(\mathcal{E})=\Gamma_k(\mathcal{E})$ from (2.26) and H. 2.26. The main purpose of the partial fraction expansion in (3.8) and (3.9) is to exhibit the effect of the "overlap" in resonance. Since the terms $\hbar\omega$, $M_k(\mathcal{E})$, and $\Gamma_k(\mathcal{E})$ are of comparable order of magnitude and the values of r which will contribute most significantly to the sum are of order ω/ω_c, the term in front of the curly bracket in (3.8) and (3.9) has a slow-variation with respect to k. The terms within the curly bracket in (3.8) and (3.9) each contain a singly resonant denominator as did the terms in the self-energy,

[38] One has $\epsilon_{k_z}{}^{n}=\epsilon_k+r\hbar\omega_c/2$; $\epsilon_{k_z}{}^{n'}=\epsilon_k-r\hbar\omega_c/2$.

(2.16). Now for the $l=0$ term these singly resonant denominators can be expanded in a Taylor series

$$[\mathcal{E}-\epsilon_k+\tfrac{1}{2}r\hbar\omega_c-G_k(\mathcal{E}\pm i0)]^{-1}=(\mathcal{E}-\epsilon_k\pm i0)^{-1}-[\tfrac{1}{2}r\hbar\omega_c-M_k(\mathcal{E})\pm i\Gamma_k(\mathcal{E})](\partial/\partial\epsilon_k)(\mathcal{E}-\epsilon_k\pm i0)^{-1} \quad (3.10)$$

$$[\mathcal{E}+\hbar\omega-\epsilon_k-\tfrac{1}{2}r\hbar\omega_c-G_k(\mathcal{E}+\hbar\omega\pm i0)]^{-1}$$
$$=(\mathcal{E}-\epsilon_k\pm i0)^{-1}-[\hbar\omega-\tfrac{1}{2}r\hbar\omega_c-M_k(\mathcal{E}+\hbar\omega)\pm i\Gamma_k(\mathcal{E}+\hbar\omega)](\partial/\partial\epsilon_k)(\mathcal{E}-\epsilon_k\pm i0)^{-1}. \quad (3.11)$$

The small expansion parameters of the series in (3.10) and (3.11) are $r\hbar\omega_c/E_F$, $M_k(\mathcal{E})/E_F$, and $\Gamma_k(\mathcal{E})/E_F$. This can be seen by considering the role played by the operator $\partial/\partial\epsilon_k$ in a subsequent k integration. The rest of the integrand in a k integration contains functions, designated by f, which have a weak k dependence. The weak k dependence means that $\partial f/\partial\epsilon_k\sim f/E_F$. In a spherical system of coordinates in k space, ϵ_k can be regarded as one of the variables of integration; then integrating by parts the operator $\partial/\partial\epsilon_k$ can be seen to be equivalent to multiplication by $1/E_F$. It is now clear why the $l\neq 0$ terms must be exlcuded before using the expansions of the propagators in (3.10) and (3.11). The ϵ_k integration by parts on the term $f=\exp\{2\pi il\hbar k_\perp^2/2m\omega_c\}$ will produce a factor of the order of magnitude $\partial\ln f/\partial\epsilon_k\sim 2\pi il/\hbar\omega_c$, the expansion parameter in (2.10) and (3.11) then would be of order unity or greater.

With the introduction of (3.10) and (3.11)[39] into the expressions (3.8) and (3.9), one has

$$\{[\mathcal{E}+\hbar\omega-\epsilon_{k_z}{}^n-G_{Nk_z}(\mathcal{E}+\hbar\omega\pm i0)][\mathcal{E}-\epsilon_{k_z}{}^{n'}-G_{Nk_z}(\mathcal{E}\pm i0)]\}^{-1}=\frac{\partial}{\partial\epsilon_k}\frac{1}{\mathcal{E}-\epsilon_k\pm i0}=-P'\left(\frac{1}{\mathcal{E}-\epsilon_k}\right)\pm i\pi\delta'(\mathcal{E}-\epsilon_k), \quad (3.12)$$

$$\{[\mathcal{E}+\hbar\omega-\epsilon_{k_z}{}^n-G_{Nk_z}(\mathcal{E}+\hbar\omega+i0)][\mathcal{E}-\epsilon_{k_z}{}^{n'}-G_{Nk_z}(\mathcal{E}-i0)]\}^{-1}$$
$$=\frac{2\pi i\delta(\mathcal{E}-\epsilon_k)}{\hbar\omega-r\hbar\omega_c+M_k(\mathcal{E})-M_k(\mathcal{E}+\hbar\omega)+i[\Gamma_k(\mathcal{E})+\Gamma_k(\mathcal{E}+\hbar\omega)]}-P'\left(\frac{1}{\mathcal{E}-\epsilon_k}\right). \quad (3.13)$$

The term proportional to $\delta'(\mathcal{E}-\epsilon_k)$ has been omitted from the right-hand side of (3.13) as it represents a higher order correction to the first term.

Employing the approximation embodied in (3.12) and (3.13) one has for the nonoscillatory part of the velocity correlation function

$$\mathfrak{F}_{yy}(\omega+i0)=i\sum_{r,k_z,k_y}\int_0^\infty\frac{hk_\perp dk_\perp}{m\omega_c}\int_{-\infty}^\infty\frac{d\mathcal{E}\,[f^{(-)}(\mathcal{E})-f^{(-)}(\mathcal{E}+\hbar\omega)]\omega_c{}^2(\hbar^2k_\perp{}^2/m^2\omega_c{}^2)\,|J_r'(hk_\perp q_x/m\omega_c)|^2\delta(\mathcal{E}-\epsilon_k)}{-i[\hbar\omega-r\hbar\omega_c+M_k(\mathcal{E})-M_k(\mathcal{E}+\hbar\omega)]+\Gamma_k(\mathcal{E})+\Gamma_k(\mathcal{E}+\hbar\omega)}$$
$$+\tfrac{1}{2}\sum_{r,k_z,k_y}\int_0^\infty\frac{\hbar k_\perp dk_\perp}{m\omega_c}\int_{-\infty}^\infty d\mathcal{E}\,[f^{(-)}(\mathcal{E})+f^{(-)}(\mathcal{E}+\hbar\omega)]\omega_c{}^2\frac{\hbar k_\perp{}^2}{m^2\omega_c{}^2}\left|J_r'\left(\frac{hk_\perp q_x}{m\omega_c}\right)\right|^2\delta'(\mathcal{E}-\epsilon_k). \quad (3.14)$$

The $P'(1/(\mathcal{E}-\epsilon_k))$ terms in (3.12) and (3.13) cancel when inserted into (3.5). The approximation, (1.20), for the velocity matrix element has been used in (3.14) and $J_r'(z)$ is the derivative of a Bessel function with respect to its argument. Strictly speaking, the approximation (1.20) for the velocity matrix element is valid for $n+n'+1\equiv\hbar k_\perp{}^2/m\omega_c\gg\hbar(q_x/2)^2/m\omega_c$, i.e., $(q_x/2k_\perp)^2\ll 1$. In the first term of (3.14) the $f^{(-)}(\mathcal{E})-f^{(-)}(\mathcal{E}+\hbar\omega)$ factor limits the $\mathcal{E}$ integration to $\mu-\hbar\omega\leq\mathcal{E}\leq\mu$ so that, to within an error of $\hbar\omega/\mu$, the delta function can be replaced by $\delta(\mu-\epsilon_k)$. The condition imposed on $k_\perp,k_z$ is $\hbar^2k_\perp{}^2/2m+\hbar^2k_z{}^2/2m=\mu$ and the presence of the $k_\perp{}^3$ factor in the integrand weighs the contributions of $k_\perp,k_z$ towards[40] $k_\perp\sim k_F$. In the second term in (3.14), $\mathcal{E}$ ranges from the bottom of the conduction band to the Fermi surface $[f^{(-)}(\mathcal{E})+f^{(-)}(\mathcal{E}+\hbar\omega)\cong 2f^{(-)}(\mathcal{E})$, to within an error of $\hbar\omega/\mu]$. The derivative of the delta function in the integrand, if used in a $\mathcal{E}$ integration yields, $f^{(-)\prime}(\epsilon_k)\approx\delta(\mu-\epsilon_k)$, so that the arguments for the validity of the approximation is also maintained for the second term in (3.14).

Inserting the expression for $\mathfrak{F}_{yy}(\omega+i0)$ in (3.14) into the expression for $\sigma_{yy}(\mathbf{q},\omega)$ in (1.10) one has for the contribution of the second term of (3.14):

$$\frac{e^2}{i\omega\Omega}\sum_{r,k_z,k_y}\int_0^\infty\left(\frac{hk_\perp}{m}\right)^3\frac{dk_\perp}{\omega_c}\int_{-\infty}^\infty d\mathcal{E}\,f^{(-)}(\mathcal{E})\left|J_r'\left(\frac{hk_\perp q_x}{m\omega_c}\right)\right|^2\delta'(\mathcal{E}-\epsilon_k). \quad (3.15)$$

[39] The higher order corrections to the delta-function approximation, used in (2.19), can now be stated. Employing (3.10) and (3.11) in the square bracket of (2.16) one has

$$2\pi i\delta(x-\epsilon_{k'})-2\pi iM_{k'}(x)\delta'(x-\epsilon_{k'})-2i\Gamma_{k'}(x)P'(x-\epsilon_{k'})^{-1},$$

where $\mathbf{k}'=\mathbf{k}-\mathbf{Q}$, $\eta\equiv\hbar k_\perp{}'^2/2m\omega_c$ and a vector $\mathbf{k}_\perp$ is defined such that $\hbar^2k_\perp{}^2/2m\equiv(n+\frac{1}{2})\hbar\omega_c$.

[40] One can now see that the above restriction $(q_x/2k_\perp)^2\ll 1$ is very mild. For $\delta=1/q_x=10^{-6}$ cm and $k_\perp=k_F/10$, $(q_x/2k_\perp)^2=1/400$; $k_\perp\cong k_F/10$ corresponds to $k_z=0.995k_F$.

Using

$$J_r'(z)=\tfrac{1}{2}(J_{r-1}(z)-J_{r+1}(z)),\quad \sum_{r=-\infty}^{\infty} J_{r-1}^2(z)=\sum_{r=-\infty}^{\infty} J_{r+1}^2(z)=1,\quad \sum_{r=-\infty}^{\infty} J_{r-2}(z)J_r(z)=0$$

(pp. 17 and 31 of Ref. 23) and[41]

$$\sum_{k_y}=\frac{L_xL_y}{2\pi}\frac{\omega_c m}{\hbar},$$

the contribution of (3.15) becomes

$$\frac{L_xL_y}{2\pi}\frac{e^2}{2i\omega\Omega}\sum_{k_y}\int_0^\infty\left(\frac{\hbar k_\perp}{m}\right)^2 k_\perp dk_\perp\int_{-\infty}^{\infty} d\mathcal{E}\, f^{(-)}(\mathcal{E})\delta'(\mathcal{E}-\epsilon_k). \tag{3.16}$$

The sum over k_z is converted into an integral and using $\hbar^2k_\perp/m\delta'(\mathcal{E}-\epsilon_k)=-(\partial/\partial k_\perp)\delta(\mathcal{E}-\epsilon_k)$ and integrating $k_\perp$ by parts one has

$$\frac{\Omega}{(2\pi)^3}\frac{e^2}{im\omega\Omega}\int_0^\infty k_\perp dk_\perp\int_{-\infty}^{\infty} dk_z\int_0^{2\pi} d\varphi\, f^{(-)}(\epsilon_k)=\frac{e^2}{im\omega\Omega}\sum_k f^{(-)}(\epsilon_k)=\frac{ne^2}{im\omega}. \tag{3.17}$$

The final result in (3.17) is seen to cancel the first term in the conductivity in (1.10). One now obtains for the conductivity

$$\sigma_{yy}(\mathbf{q},\omega)=\frac{2e^2}{\Omega}\frac{\Omega}{(2\pi)^2}\frac{\omega_c m}{\hbar}\sum_{k_z}\int_0^\infty\frac{\hbar k_\perp dk_\perp}{m\omega_c}\int_{\mu-\hbar\omega_c}^{\mu}\frac{d\mathcal{E}}{\hbar\omega}\frac{\hbar^2k_\perp^2}{m^2\omega_c^2}\delta(\mu-\epsilon_k)$$
$$\times\sum_{r=-\infty}^{\infty}\frac{[J_r'(\hbar k_\perp q_x/m\omega_c)]^2\hbar\omega_c}{-i[\hbar\omega-r\hbar\omega_c+M_k(\mathcal{E})-M_k(\mathcal{E}+\hbar\omega)]+\Gamma_k(\mathcal{E})+\Gamma_k(\mathcal{E}+\hbar\omega)}. \tag{3.18}$$

A factor of 2 has been inserted in the front of (3.18) to account for electron spin. The sum over k_z is converted to an integral and spherical coordinates in k space are introduced. The result is

$$\sigma_{yy}(\mathbf{q},\omega)=\frac{3}{4}\frac{ne^2}{v_F}\int_{\mu-\hbar\omega}^{\mu}\frac{d\mathcal{E}}{\hbar\omega}\sum_{r=-\infty}^{\infty}\frac{\hbar\omega_c S_r(q_x)}{-i[\hbar\omega-r\hbar\omega_c+M_{k_F}(\mathcal{E})-M_{k_F}(\mathcal{E}+\hbar\omega)]+\Gamma_{k_F}(\mathcal{E})+\Gamma_{k_F}(\mathcal{E}+\hbar\omega)}, \tag{3.19}$$

where the function S_r is defined

$$S_r(q_x)\equiv\frac{2v_F}{\omega_c}\int_0^\pi\sin^3\theta\left[J_r'\left(\frac{v_Fq_x}{\omega_c}\sin\theta\right)\right]^2 d\theta. \tag{3.20}$$

The functions $S_r(q_x)$ is approximately evaluated for $r<v_Fq_x/\omega_c$ by using the asymptotic form for $J_r(z)\sim(2/\pi z)^{1/2}\times\cos(z-r\pi/2-\pi/4)$. To lowest order in ω_c/v_Fq_x one has

$$S_r(q_x)\simeq 1/q_x \tag{3.21}$$

for $r>v_Fq_x/\omega_c$, the function $S_r(q_x)$ is small due to the smallness of the Bessel function $J_r(z)$ for $r>z$. The sum over r in (3.19) is hence restricted to the range $|r|\lesssim v_Fq_x/\omega_c$ with $S_r(q_x)$ given by (3.21). To within an error[42] of ω_c/v_Fq_x the sum over r can be extended to its original range in (3.19). The r sum can now be evaluated directly [cf. Eq. (4.5.14) of Ref. 33] and the final expression for the bulk conductivity is

$$\sigma_{yy}(\mathbf{q},\omega)=\frac{3}{4}\frac{ne^2}{mv_Fq_x}\int_{\mu-\hbar\omega}^{\mu}\frac{d\mathcal{E}}{\hbar\omega}\pi\coth\left[\pi\left\{-i\frac{(\hbar\omega+M(\mathcal{E})-M(\mathcal{E}+\hbar\omega))}{\hbar\omega_c}+\frac{\Gamma(\mathcal{E})+\Gamma(\mathcal{E}+\hbar\omega)}{\hbar\omega_c}\right\}\right], \tag{3.22}$$

where $M_{k_F}(\mathcal{E})\equiv M(\mathcal{E})$ and $\Gamma_{k_F}(\mathcal{E})\equiv\Gamma(\mathcal{E})$.

---

[41] F. Seitz, *The Modern Theory of Solids* (McGraw-Hill Book Company, Inc., New York, 1900), 1st ed., p. 585.
[42] M. H. Cohen, M. J. Harrison, and W. A. Harrison, Phys. Rev. **117**, 937 (1960).

IV. SURFACE IMPEDANCE

The pertinent function to compute is the surface impedance, as the power absorbed by the metal from the electromagnetic field is proportional to its real part. In this section, the relationship between the expression for the bulk conductivity, (3.22), and the surface impedance of the metal will be exhibited, and the results of a numerical computation of the surface impedance will be shown for a range of the physical parameters of interest.

As is well known, a proper account of the scattering of the electrons from the surface of the metal must be taken,[2] in order to calculate the surface impedance.

For the geometry outlined in Sec. III with the surface of metal taken as the plane $x=0$, the x axis being considered positive into the metal, and the z axis in the surface of the metal, one has for the surface impedance,

$$Z=\frac{4\pi i\omega}{c^2}\frac{E(+0)}{E'(+0)}. \tag{4.1}$$

In (4.1), $E(+0)=E_y(x)|_{x\to+0}$, $E'(+0)=\partial E_y(x)/\partial x|_{x\to+0}$ and the time variation of the electromagnetic field is $\exp(-i\omega t)$. The E field is a solution of Maxwell's equation, which in the present case can be written

$$\frac{\partial^2 E_y(x)}{\partial x^2}=-\frac{4\pi i\omega}{c^2}j_y(x). \tag{4.2}$$

It might be added at this point that in the transverse geometry being considered in this paper (i.e., the E field perpendicular to H), a Hall field $E_x(x)$ exists. However (cf. footnote 43), the Hall field $E_x(x)$ does almost no work on the electrons which contribute most to resonance (those electrons with $v_{k_z}\sim 0$ in the skin depth); in particular, if the condition $\omega\tau\ll(R_c/\delta)^2$ holds, as will be assumed here, $E_x(x)$ can be neglected.

The yy component of the conductivity tensor $\sigma(x,x')$ is, thus, sufficient to calculate the electron current density, $j_y(x)$ in (4.2). Thus, one has, in general,

$$j_y(x)=\int_0^\infty \tilde{\sigma}_{yy}(x,x')E_y(x')dx', \tag{4.3}$$

with $E_y(x)$ defined to be zero for $x<0$. However, the Fourier transform of $\tilde{\sigma}_{yy}(x,x')$ is not, in general, equal to the Fourier transform[44] of the bulk conductivity, $\sigma_{yy}(\mathbf{q},\omega)$, calculated in Sec. III, when the presence of the boundary of the sample is considered. In lieu of a proper quantal treatment of boundary effects, the following recipe will be followed. One introduces a quasiclassical transport equation [cf. Eq. (4.4) below] which

(a) reduces to the conventional Boltzmann equation in the absence of EPI, and

(b) which gives the same results for the bulk conductivity as obtained in Sec. III.

Such an equation may be obtained from the quantal transport Eq. H. (3.32) with the addition of the magnetic-force term $(\mathbf{v}_k/c)\times\mathbf{H}\cdot\mathrm{grad}_k f$ of the standard Boltzmann equation.[45] The scattering-in term of H. (3.32) is neglected as it yields a relative contribution of the order δ/R_c (cf. Appendix II). The transport equation in question then takes the form

$$\left[-i\left(\omega+\frac{M_k(\mathcal{E})-M_k(\mathcal{E}+\hbar\omega)}{\hbar}\right)+\frac{\Gamma_k(\mathcal{E})+\Gamma_k(\mathcal{E}+\hbar\omega)}{\hbar}\right]f(x,\varphi;\mathcal{E})$$
$$+v_{kx}\frac{\partial f}{\partial x}(x,\varphi;\mathcal{E})+\omega_c\frac{\partial f}{\partial\varphi}(x,\varphi;\mathcal{E})=v_{ky}E_y(x), \tag{4.4}$$

where φ is the azimuthal angle in k space and where[46] $f(x,\varphi;\mathcal{E})$ is the Fourier transform of the "distribution function" $\chi(q,\varphi;\mathcal{E})$ of H. (3.32), i.e.,

$$\chi(q,\varphi;\mathcal{E})=\frac{1}{2\pi}\int_0^\infty dx\, f(x,\varphi;\mathcal{E})e^{+iqx}. \tag{4.5}$$

The Fourier transform (F.T.) of $j_y(x)$ is, from H. (3.31),

$$J_y(q)=\frac{2e^2}{\Omega}\sum_k v_{ky}\int_{-\infty}^\infty \delta(\mathcal{E}-\epsilon_k)\times\left[\frac{f^{(-)}(\mathcal{E})-f^{(-)}(\mathcal{E}+\hbar\omega)}{\hbar\omega}\right]\chi(q,\varphi;\mathcal{E})d\mathcal{E}. \tag{4.6}$$

The transport Eq. (4.4) is solved, using the method of Jones and Sondheimer,[47] with the assumption of diffuse electron scattering at the metal surface. The F.T. of the electron current density $J_y(q)$ obtained from (4.6) is inserted into the F.T. of (4.2) and the result is an integral equation for the F.T. of $E_y(x)$. The integral equa-

---

[43] M. Ya. Azbel, and I. M. Lifshitz, *Progress of Low Temperature Physics*, edited by C. J. Görter (North-Holland Publishing Company, Amsterdam, 1960), Vol. III, Chap. VII, Sec. 1.2.

[44] $\sigma_{yy}(q,\omega)$ is here referred to as the Fourier transform of the bulk conductivity to distinguish it from the conductivity in real space.

[45] J. M. Ziman, *Theory of Solids* (Cambridge University Press, New York, 1964), p. 253.

[46] The relation between $f(x,\varphi;\mathcal{E})$ and the full Boltzmann distribution function f_k, is

$$f_k=f_k^{(-)}+ef(x,\varphi;\mathcal{E})e^{-i\omega t}(-\partial f_k^{(-)}/\partial\epsilon_k).$$

The function $\chi(q,\varphi;\mathcal{E})$ differs from the function $\chi_k(z,\omega)$ of H. by the inclusion of E_y on the right-hand side of (4.4) in contrast to H. (3.32).

[47] M. C. Jones and E. H. Sondheimer, Proc. Roy. Soc. (London) **A278**, 256 (1964).

tion is treated approximately by a numerical iteration scheme[48] similar to that used on p. 740 of Ref. 2.

In the final result, the functional dependence of the surface impedance on the bulk conductivity is the same as one finds in the literature.[49] Moreover, the expression for the bulk conductivity is the same as that calculated quantum mechanically in Sec. III. The surface impedance is

$$Z\equiv R+iX=2R_0e^{-i\pi/3}[\sigma'(\omega)]^{-1/3}, \tag{4.7}$$

where $R_0=8/9(\omega^2\pi mv_F\sqrt{3}/ne^2c^4)^{1/3}$ and

$$\sigma'(\omega)=\int_{\mu-\hbar\omega}^{\mu}\frac{d\mathcal{E}}{\hbar\omega}\coth\left[\pi\left\{-i\frac{(\hbar\omega+M(\mathcal{E})-M(\mathcal{E}+\hbar\omega))}{\hbar\omega_c}+\frac{\Gamma(\mathcal{E})+\Gamma(\mathcal{E}+\hbar\omega)}{\hbar\omega_c}\right\}\right]. \tag{4.8}$$

The expressions for $M(\mathcal{E})$ and $\Gamma(\mathcal{E})$ are given in (2.28) and (2.30) with $[2m(n+\frac{1}{2})\omega_c/\hbar+k_z^2]^{1/2}=k_F$. It can be readily seen that in the limit of low frequency, $\omega/\omega_D\ll1$, one obtains for (4.8),

$$\sigma'(\omega)=\coth\left\{\pi\left[-i\frac{\omega}{\omega_c}(1-M'(\mu))+\frac{2\Gamma(\mu)}{\hbar\omega_c}\right]\right\}, \tag{4.9}$$

which is similar to the result contained in Eq. (4.19) of Ref. 9(2). The virtual effects of EPI at low frequency are to modify the cyclotron mass, i.e., ω_c is replaced by

$$\omega_c^*\equiv eH/m^*c, \tag{4.10}$$

where $m^*\equiv m(1-M'(\mu))$. The value for $M'(\mu)$ computed from (2.30) is

$$M'(\mu)=-3F/8(2)^{1/3}, \tag{4.11}$$

where $F\equiv C^2/Mc_s^2E_F$. The value of $-M'(\mu)$ can be taken as the EPI coupling constant.

The attenuation effects of EPI due to real collisions with phonons are negligible at low frequency. The energy separation of the electron-hole pair, created by the electromagnetic field at low frequency, is insufficient to allow the pair a significant sampling of phonon modes with which to interact (dissipatively). For the sake of comparison to Ref. 9(2), let us note that the term $\hbar/(\Gamma(\mathcal{E})+\Gamma(\mathcal{E}+\hbar\omega))$ in (4.8) corresponds to an effective relaxation time $\tau_{\rm EPI}$, which is infinite at low frequency, as $\Gamma(\mu)=0$. One can phenomenologically add a term $1/\omega_c\tau_I$ to $2\Gamma(\mu)/\hbar\omega_c$ in (4.9), where τ_I is the relaxation time due to electron scattering with impurities. It is only when the effective $\tau_{\rm EPI}$ is much less than τ_I that one can assume ideal resistance conditions. It will be shown that for sufficiently pure metals, such a situation prevails at higher frequencies.

[48] The iteration does not seem to involve an expansion in a physical parameter, e.g., δ/R_c. However, a recent completely rigorous solution of the integral equation by J. M. Luttinger and L. Hartmann (private communication) has substantiated the iterative approximation in Ref. 2.

[49] S. Rodriguez, Phys. Rev. 112, 1616 (1958).

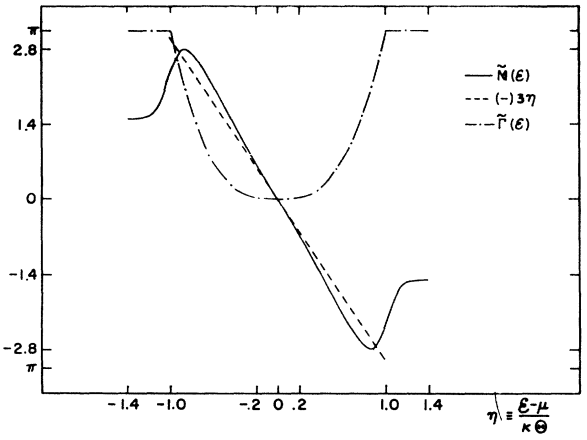

FIG. 7. The real and imaginary part of the dimensionless self-energy, $\tilde{M}(\eta)$ and $\tilde{\Gamma}(\eta)$.

The τ in Eq. (4.19) of Ref. 9(2) is essentially τ_I and thus the only effects of EPI at low frequency is to modify the cyclotron mass.

As the frequency is increased, the function

$$[M(\mathcal{E})-M(\mathcal{E}+\hbar\omega)]/\hbar\omega$$

deviates from $M'(\mu)$. The condition for resonance is now approximately shifted from

$$\omega/\omega_c^*=n, \tag{4.12}$$

where n is an integer, to

$$\omega+\frac{M(\mathcal{E})-M(\mathcal{E}+\hbar\omega)}{\hbar}=n\omega_c. \tag{4.13}$$

The exact resonance condition at higher frequencies can only be determined after the $\mathcal{E}$ integration in (4.8) is performed. The $\mathcal{E}$ integration is computed numerically and curves of the derivative of the reduced surface resistance, $R'\equiv R/R_0$, with respect to a reduced field $H^*\equiv eH/m^*c\omega_D$, plotted against $1/H'$ ($H'\equiv eH/m^*c\omega$) will be shown below for a range of ω/ω_D. First, however, some insight into the final results may be gained by a discussion of the energy dependence of the self-energy parts. In Fig. 7 the dimensionless function $\tilde{M}(\eta)\equiv M(\mathcal{E})/F/8(2)^{1/3}\kappa\Theta$ and the line[50] $(-)3\eta$ are plotted, where $\eta\equiv(\epsilon-\mu)/\kappa\Theta$. The term $(M(\mathcal{E})-M(\mathcal{E}+\hbar\omega))/\hbar\omega$ is the slope of a chord between the two points on the $\tilde{M}(\eta)$ curve, evaluated at η and $\eta+\omega/\omega_D$ ($\eta<0$, since $\mu-\hbar\omega\leq\epsilon\leq\mu$). The deviation of this slope from the value $(-)3$ as a function of ω is a measure of the modification of the resonance condition, (4.12). The maximum deviation of $\tilde{M}(\eta)$ from $(-)3\eta$, 14.4%, occurs at $\eta=\pm\sqrt{2}/2$. The maximum of $|\tilde{M}(\eta)|$ is 2.802 and occurs at the points $\eta=\pm0.886$. Also significant is the point of inflection which occurs at $\eta=\pm0.473$. Thus, at about

[50] This line has the same slope as $M(\eta)$ at the Fermi surface ($\eta=0$).

half of the Debye frequency range, the rate of the deviation of the slope of $\tilde{M}(\eta)$ from $(-)3\eta$ changes sign from positive to negative.

Also shown in Fig. 7 is the function $\tilde{\Gamma}(\eta)=\pi|\eta|^3$ for $|\eta|\leq 1$ and $\tilde{\Gamma}(\eta)=\pi$ for $|\eta|>1$. The relaxation rate due to real collisions with phonons increases as the separation between the electron-hole pair, created by the electromagnetic field, increases.

To estimate the effect of $(\Gamma(\mathcal{E})+\Gamma(\mathcal{E}+\hbar\omega))/\hbar\omega_c$ on the magnitude of $\sigma'(\omega)$ one can assume that the condition (4.13) is maintained, at resonance, through the range of the $\mathcal{E}$ integration. One has, at resonance,

$$\sigma'(\omega)=\frac{4}{\sqrt{3}}\frac{\omega_c}{\omega}\left(\frac{\omega_D}{\omega}\right)^2\left(\frac{8(2)^{1/3}}{3F}\right), \qquad (4.14)$$

assuming that the right-hand side of (4.14) is much greater than unity. The maximum value of the conductivity at resonance decreases with the inverse cube of increasing frequency.

In Fig. 8 the dR'/dH^* versus $1/H'$ curves [H^*, H' defined above in text after (4.13)] for four different values of ω/ω_D are superimposed. The value of the EPI coupling constant, Eq. (4.11), needed to compute the field derivative-absorption curves is appropriate for the case of cesium and will be discussed below ($F=1.5$, $m^*/m=1.45$). The frequency dependence of $\Gamma(\mathcal{E})+\Gamma(\mathcal{E}+\hbar\omega)$ manifests itself in the scale change of the four curves [due to the decrease in the conductivity, at resonance, with increasing frequency, cf. (4.14)] and also in the increasing attenuation of the subharmonics at higher frequency. This latter behavior is completely analogous to the analysis of the expression for dR/dH given by Azbel' and Kaner.[51] The height of the maxima of dR/dH (in Ref. 51) increases with subharmonic number, i.e., $dR/dH\sim n^{4/3}$, until $2\pi/\omega_c\tau>1$; then since dR/dH varies as $\exp(-2\pi/\omega_c\tau)$, the maxima decrease exponentially with decreasing magnetic field. In the present case since the effective τ decreases with increasing frequency, $2\pi/\omega_c\tau$ becomes greater than unity, for higher frequencies, at a higher value of the magnetic field. Thus, the onset of the attenuation of subharmonics moves to lower subharmonics as the frequency increases.

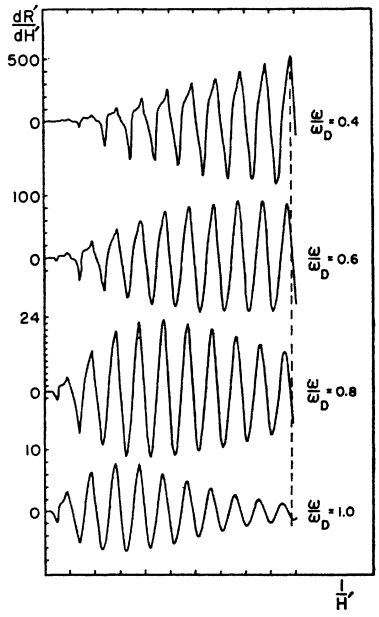

FIG. 8. Plots of the field-derivative absorption curves (dimensionless), dR'/dH^*, versus the reciprocal applied magnetic field (dimensionless), for four values of ω/ω_D.

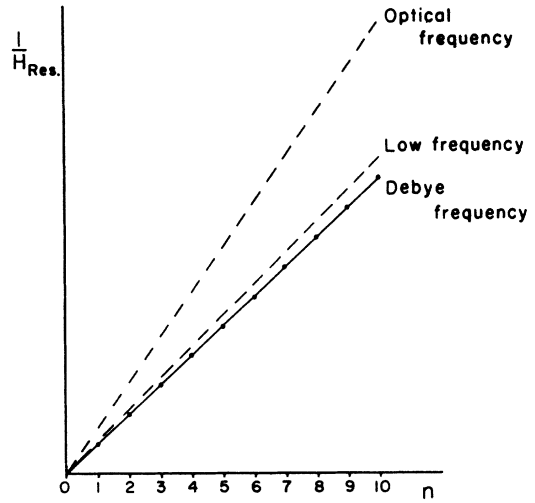

FIG. 9. A plot of the value of the reciprocal applied magnetic field (dimensionless) at resonance, $1/H_{res}$, versus subharmonic number n for $\omega=\omega_D$ (solid line). The dashed lines correspond to an effective cyclotron mass, at $\omega=\omega_D$, equal to the mass at low frequency, and at optical frequency, respectively.

The lowest value of ω/ω_D equal to 0.4 corresponds to an effective $\tau_{EPI}\sim 1.4\times 10^{-11}$ sec for cesium. For ultra pure materials one can expect a $\tau_I\sim 10^{-9}-10^{-10}$ sec. Thus, at lower ω/ω_D, the condition $\tau_{EPI}\ll\tau_I$ cannot be fulfilled.

The frequency-dependent shift of the resonance is illustrated by the dashed line in Fig. 8, drawn perpendicular to the $1/H'$ axis through the position of the tenth maximum of the upper curve (the maxima of the dR/dH curves are the positions of resonance[51]). The frequency dependence of the effective cyclotron mass is more cogently illustrated in Fig. 9. The effective cyclotron mass is usually obtained from experimental data by plotting the reciprocal of the value of H at resonance, H_{res}, versus subharmonic number n. The slope of the $1/H$ line $\Delta(1/H)$ determines the cyclotron mass m_c by the relation

$$m_c=e/c\omega\Delta(1/H). \qquad (4.15)$$

In Fig. 9, the values of $1/H'$ at the maxima of the $\omega=\omega_D$ curve (Fig. 8) are plotted versus subharmonic number n. A straight line is drawn between these points and is labeled "Debye frequency." For the sake of com-

[51] M. Ya. Azbel' and E. A. Kaner, Zh. Eksperim. i Teor. Fiz. 39, 80 (1960) [English transl.: Soviet Phys.—JETP 12, 58 (1961)].

parison two dashed lines are drawn whose slope yields $m_c=m^*$, the low-frequency mass and $m_c=m$, the bare band or optical mass, at the same frequency ($\omega=\omega_D$), respectively. The low-frequency line has slope unity since $H_{\rm res}$ is measured in units of $m^*c\omega_D/e$.

The cyclotron mass determined by the slope of the "Debye frequency" line is 6% larger than m^*. It would be expected that at high frequencies ($\omega\sim\omega_D$) the effective mass would be less than m^* and approach m as the frequency increased. The fact that the mass increases with frequency up to the Debye frequency (and then subsequently decreases for $\omega>\omega_D$) depends on the details of the functional form of $\tilde{M}(\eta)$ (cf. Fig. 7). In Fig. 7, it can be seen that the slope of $\tilde{M}(\eta)$ first increases with $\mathcal{E}$ (to a maximum of -3.85) and then decreases at higher $\mathcal{E}$. The point of inflection is at $\eta\equiv(\mathcal{E}-\mu)/\kappa\Theta=\pm0.473$. The latter fact explains the results (obtained with plots similar to Fig. 9) that the greatest rate of change of the cyclotron mass, from a 3% to a 5% increase over m^*, occurs between $\omega/\omega_D=0.6$ and $\omega/\omega_D=0.8$.

An estimate for the EPI coupling constant is obtained from the high-temperature resistivity. The relation between F and the relaxation time (in units of 10^{-14} sec), derived from Eq. (9.5.1) in Ref. 16, is

$$0.265F=1/\tau.$$

The value obtained, $F=1.5$ is equivalent to $C/E_F=1$ if one assumes the relation[52] $c_s^2=\frac{1}{3}(m/M)v_F^2$, derived for jellium (neglecting Coulomb interactions).

It should be stated that the high-temperature resistivity incorporates contributions from EPI umklapp processes. Since the form of the EPI assumed in the present paper[16] only includes normal processes with longitudinal phonons, the value for the coupling constant could be overestimated by the resistivity data. However, a study of Ziman[53] showed a good fit to the resistivity of Na over a large temperature range could be obtained by a constant EPI coupling function adjusted to the high-temperature limit of the resistivity. The EPI coupling function is cut off at a value of the phonon wave vector corresponding to a lower Debye temperature.

If similar considerations hold for Cs, then the EPI coupling constant considered in the present paper is *underestimated* as compared to Ziman's result for Na. In any case, the main result of the present paper is to present a model calculation of the effects, to be expected, on high-frequency cyclotron resonance by EPI. To compare the present calculations with eventual experimental data a detailed calculation of the self-energy parts, including a more realistic EPI and phonon spectrum, would be needed.

[52] C. Kittel, *Quantum Theory of Solids*, John Wiley & Sons, Inc., New York, 1963), p. 147.

[53] J. M. Ziman, Proc. Roy. Soc. (London **A226**, 436 (1954). In particular, attention is drawn to Fig. 5 on p. 451.

In this connection, it is of interest to note that, in the case of superconductors, the necessary information concerning EPI and phonon spectrum may be inferred from tunneling data. Specifically, starting from H. (2.19) and H. (2.20) one obtains, after some manipulations:

$$\langle\Gamma_k(\mathcal{E})\rangle=\pi\int_0^{|\mu-\mathcal{E}|}\alpha^2(\xi)F(\xi)d\xi, \tag{4.16}$$

for $\mathcal{E}\sim\mu$, and

$$\langle M_k(\mathcal{E})\rangle-\langle M_k(\mathcal{E}+\hbar\omega)\rangle=\int_0^{\infty}d\xi\,\alpha^2(\xi)F(\xi)$$
$$\times\left\{\ln\left|\frac{\mathcal{E}-\mu-\xi}{\mathcal{E}-\mu+\xi}\right|-\ln\left|\frac{\mathcal{E}+\hbar\omega-\mu-\xi}{\mathcal{E}+\hbar\omega-\mu+\xi}\right|\right\}, \tag{4.17}$$

with

$$\alpha^2(\xi)F(\xi)\equiv\langle\sum_{k'}|V_{k'k}|^2\delta(\hbar\omega_{kk'}-\xi)\delta(\mu-\epsilon_{k'})\rangle, \tag{4.18}$$

where the sum over k' also includes a sum over phonon modes. The angular brackets denote an average over the Fermi surface, $\epsilon_k=\mu$. All the essential information concerning the EPI and the phonon spectrum are contained in $\alpha^2(\xi)F(\xi)$. For the simple spherical model used in the present paper one has

$$\alpha^2(\xi)F(\xi)=\frac{3}{8(2)^{1/3}}F\frac{\xi^2}{(\hbar\omega_D)^2}, \quad \xi\leq\hbar\omega_D$$
$$=0, \quad \xi>\hbar\omega_D. \tag{4.19}$$

The notation $\alpha^2(\xi)F(\xi)$ has been chosen to conform to that used in the paper by McMillan and Rowell.[54] The function $\alpha^2(\xi)F(\xi)$ is obtained (in Ref. 54) for Pb by a numerical inversion technique using the data of tunneling (between superconductors) experiments. The $\alpha^2(\xi)F(\xi)$, obtained by this technique can be used in Eqs. (4.16) and (4.17) to compute a more exact expression for the self-energy parts. Qualitatively, the $\alpha^2(\xi)F(\xi)$ for Pb as shown in Fig. 1 of Ref. 54 may be considered as the sum of two contributions of the form (4.19). The parameters for the transverse and longitudinal contributions are $F=3.2$, $\hbar\omega_D=4.4$ meV and $F=4$, $\hbar\omega_D=8.3$ meV, respectively ($\hbar\omega_D$ for Cs is 3.6 meV). Thus, aside from the complications due to the fact that the Fermi surface of Pb extends beyond the first Brillouin zone (B.Z.), one could expect measurable resonance line shifts at lower frequencies in Pb due to the stronger EPI coupling constant.

It would, indeed, be interesting to use the $\alpha^2(\xi)F(\xi)$ obtained from a metal in the superconducting state to explain the results of an experiment performed on the metal in the normal state.

[54] W. L. McMillan and J. M. Rowell, Phys. Rev. Letters **14**, 108 (1965).

APPENDIX I: THE OSCILLATORY PARTS OF THE ELECTRON SELF-ENERGY AND THE CONDUCTIVITY

In Secs. II and III the nonoscillatory part of the self-energy and conductivity, respectively, was calculated. The essential feature characterizing the calculations was the slow "k" variation of the integrand. With the slow variation it was argued that the expansion parameters in the Taylor series in (3.10) and (3.11) are $r\hbar\omega_c/E_F$, $\hbar\omega/E_F$, $M_k(\mathcal{E})/E_F$, and $\Gamma_k(\mathcal{E})/E_F$. These parameters are all of order c_s/v_F for the conditions stated in (2.15) and for $r\gtrsim\omega/\omega_c$.

The expansions (3.10) and (3.11) are invalid for the oscillatory part, i.e., the $l\neq 0$ terms in (2.16). The discussson in the text preceding (3.12) points out that if the series (3.10) and (3.11) are used with the oscillatory terms, the expansion parameters are of order unity for the conditions assumed in the present paper, (2.15).

In this Appendix the oscillatory part of the self-energy and conductivity is calculated. The essential feature of the calculation is the largeness of the parameter $E_F/\hbar\omega_c(=10^4-10^3$ for $\omega_c=10^{12}-10^{13}$ sec$^{-1})$.

(A) The $l\neq 0$ terms of the self-energy from (2.16) are

$$G_{nk_z}(\zeta_l)_{\rm osc}=\frac{1}{2\pi i}\sum_{l=-\infty}^{\infty}{}'(-)^l\sum_{\mathbf{Q},\pm}\int_0^\infty\frac{\hbar k_\perp'}{m\omega_c}dk_\perp'$$
$$\times\int_{-\infty}^{\infty}\frac{dx|V_Q|^2(1+\sin 2\theta)f^{(\mp)}(x)\exp\{2\pi li(\hbar k_\perp'^2/2m\omega_c)\}}{\pi\{[(n+\frac{1}{2})+(\hbar k_\perp'^2/2m\omega_c)](\hbar Q_\perp^2/m\omega_c)-[n+\frac{1}{2}-(\hbar k_\perp'^2/2m\omega_c)]^2-(\hbar Q_\perp^2/2m\omega_c)^2\}^{1/2}}$$
$$\times(\zeta_l-x\pm\hbar\omega_Q)^{-1}\{[x-(\hbar^2k'^2/2m)-G_{k'}(x-i0)]^{-1}-[x-(\hbar^2k'^2/2m)-G_{k'}(x+i0)]^{-1}\},\quad\text{(AI.1)}$$

with the prime on the l sum designating the deletion of $l=0$; and the following definitions are used:

$$\hbar k_\perp'^2/2m\omega_c\equiv\eta,\quad\text{(AI.2a)}$$

$$k'^2=k_\perp'^2+(k_z-Q_z)^2,\quad\text{(AI.2b)}$$

$$\theta=\int_{\alpha_0}^{\alpha}\left\{n+\frac{1}{2}+\frac{\hbar k_\perp'^2}{2m\omega_c}-\frac{(n+\frac{1}{2}-\hbar^2k_\perp'^2/2m\omega_0)^2}{\alpha'^2}-\frac{\alpha'^2}{4}\right\}^{1/2}d\alpha',\quad\text{(AI.2c)}$$

where $\alpha=\hbar Q_\perp^2/m\omega_c$ and α_0 is the lower root of the radicand. It is convenient to also introduce the definitions

$$\hbar k_\perp^2/2m\omega_c\equiv n+\tfrac{1}{2},\quad\text{(AI.3a)}$$

$$k^2\equiv k_\perp^2+k_z^2.\quad\text{(AI.3b)}$$

Although $k_\perp$ is discrete in (AI.3a), it becomes a continuous variable, via the Poisson sum rule, when the self-energy is used in the expression for the conductivity.

The $\mathbf{Q}$ sum is converted to an integral and cylindrical coordinates in $\mathbf{Q}$ space are introduced. The limits on the $Q_\perp$ integration are the upper and lower roots of the radicand in the curly bracket in (AI.1),

$$|k_\perp-k_\perp'|\leq Q_\perp\leq k_\perp+k_\perp'.\quad\text{(AI.4)}$$

To this must be added the restriction $\mathrm{Max}Q=Q_m$, the Debye wave vector. In Fig. 10 the shaded region represents the equatorial cross section of the admissible volume in the Debye sphere for the $\mathbf{Q}$ integration. From Fig. 10 one can see that the upper limit of the $Q_\perp$ integration is, more specifically, $\min\{[Q_m^2-Q_z^2]^{1/2}, k_\perp+k_\perp'\}$. The maximum value for Q_z is: $Q_z^{\max}=[Q_m^2-(k_\perp-k_\perp')^2]^{1/2}$.

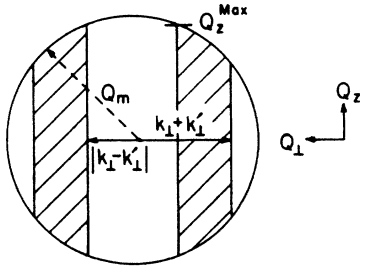

FIG. 10. The admissible volume in the Debye sphere for the $\mathbf{Q}$ integration.

To simplify the expressions in (AI.1), the angle φ is introduced,

$$\cos\varphi \equiv (k_\perp^2+k_\perp'^2-Q_\perp^2)/2k_\perp'k_\perp. \tag{AI.5}$$

In terms of φ, one has

$$\frac{Q_\perp dQ_\perp}{\left\{2\left(\frac{\hbar k_\perp^2}{2m\omega_c}+\frac{\hbar k_\perp'^2}{2m\omega_c}\right)\frac{\hbar Q_\perp^2}{2m\omega_c}-\left(\frac{\hbar k_\perp^2}{2m\omega_c}-\frac{\hbar k_\perp'^2}{2m\omega_c}\right)^2-\left(\frac{\hbar Q_\perp^2}{2m\omega_c}\right)^2\right\}^{1/2}}=\frac{m\omega_c}{\hbar}d\varphi, \tag{AI.6}$$

$$\theta=\frac{1}{2}\left(\frac{\hbar k_\perp^2}{2m\omega_c}+\frac{\hbar k_\perp'^2}{2m\omega_c}\right)\varphi+\frac{\hbar k_\perp' k_\perp}{2m\omega_c}\sin\varphi-\left|\frac{\hbar k_\perp'^2}{2m\omega_c}-\frac{\hbar k_\perp^2}{2m\omega_c}\right|\tan^{-1}\left\{\frac{(k_\perp'+k_\perp)}{|k_\perp-k_\perp'|}\tan\frac{\varphi}{2}\right\}, \tag{AI.7}$$

and the limits of the φ integration are: $0\leq\varphi\leq\varphi_0\equiv$

$$\min\left\{\cos^{-1}\left[\frac{k_\perp^2+k_\perp'^2-Q_m^2+(k_z-k_z')^2}{2k_\perp k_\perp'}\right],\pi\right\} \quad \text{where} \quad k_z'\equiv k_z-Q_z.$$

The self-energy in (AI.1) is rewritten as (the $\sin 2\theta$ term will be considered below)

$$G_k(\zeta_l)_{\rm osc}=\frac{1}{2\pi i}\sum_{l=-\infty}^{\infty}{}'(-)^l\frac{\Omega}{4\pi^2}\int_{-\infty}^{\infty}f^{(\mp)}(x)dx\int_0^\infty k_\perp' dk_\perp'\int_{k_z-Q_z^{\rm Max}}^{k_z+Q_z^{\rm Max}}dk_z'$$
$$\times\int_0^{\varphi_0}\frac{d\varphi\,|V_Q|^2 e^{\pi i l(\hbar k_\perp'^2/m\omega_c)}}{\zeta_l-x\pm\hbar\omega_Q}\left[\frac{1}{x-\epsilon_{k'}-G_{k'}(x-i0)}-\frac{1}{x-\epsilon_{k'}-G_{k'}(x+i0)}\right], \tag{AI.8}$$

where now

$$Q^2=k_\perp^2+k_\perp'^2-2k_\perp k_\perp'\cos\varphi+(k_z-k_z')^2. \tag{AI.8a}$$

Spherical coordinates k', θ' are now introduced. The two limits on the θ' integration are the two solutions of

$$k'^2-2ck'\cos(\theta'-\gamma)+c^2=Q_m^2 \tag{AI.9}$$

as a function of k', where $c^2=k_\perp^2+k_z^2$, $\gamma=\tan^{-1}(k_\perp/k_z)$. The calculation is now restricted to the pertinent value of $c\sim k_F$. The solutions for the limits of the θ' integration are illustrated in Fig. 11. The θ' integration is performed by the method of saddle-point integration (anticipating that the significant value for k' is $k'\sim k_F$). The θ' integral is

$$\int_\alpha^\beta F(Q(\theta'))\exp\left\{-\pi i l\frac{\hbar k'^2}{m\omega_c}\cos^2\theta'\right\}d(\cos\theta'), \tag{AI.10}$$

where $F(Q(\theta'))=|V_Q|^2[\zeta_l-x\pm\hbar\omega_Q]^{-1}$ and is regarded as slowly varying with θ' as compared to the exponential factor. The integral in (AI.10) is rewritten, using $\mu=\cos\theta'$

$$\int_{\cos\alpha}^{\cos\beta}F(Q(\mu))\exp\left\{-\pi i l\frac{\hbar k'^2}{m\omega_c}\mu^2\right\}d\mu. \tag{AI.11}$$

The saddle point in the μ-complex plane is $\mu=0$ and the contour is illustrated in Fig. 12. The contribution from the

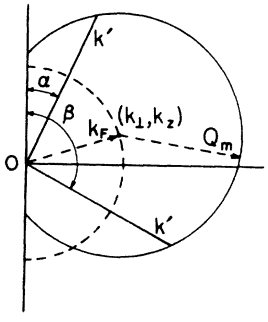

FIG. 11. The limits (α,β) on the θ' integration are obtained by the intersection of a circle with radius k' centered at the origin with the circle (solid line) of radius Q_m, centered at $(k_\perp,k_z)$.

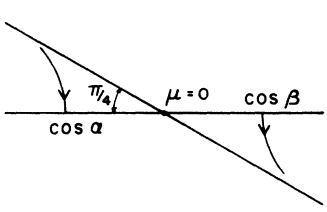

FIG. 12. The paths of steepest descent in the μ-complex plane (for $l>0$). The paths through $\cos\alpha$, $\cos\beta$ are rectangular hyperbolas.

saddle point to the integral in (AI.11) is

$$\left[\frac{\hbar\omega_c}{2|l|(\hbar^2k'^2/2m)}\right]e^{\mp i\pi/4}, \tag{AI.12}$$

the $-$ $(+)$ sign corresponds to positive (negative) values of l. The contributions to (AI.11) from the end points are of the order $\hbar\omega_c(\hbar^2k'^2/2m)^{-1}$ and are neglected (the integrand has no singularities at $\mu=\cos\alpha$, $\cos\beta$).

In order for the saddle point, $\theta'=\pi/2$, to lie within the angular range of the θ' integration for $k'\sim k_F$, the values of k_z must be restricted. From Fig. 11 it is seen that for $k'\sim k_F$, one must have

$$|k_z|/k_F\leq\sin(2\sin^{-1}(2^{-2/3}))=0.978.$$

The physical significance of this fact is apparent. Due to the upper limit on the phonon wave vector, the states on the Fermi surface which can scatter, via phonons, to the saddle point (the equatorial plane, $k_\perp'=k_F$) are restricted.

For $k'\geq k_F+Q_m$, the angular range of the θ' integration diminishes to zero. The self-energy is now equal to

$$G_k(\zeta_l)_{\text{osc}}=\frac{1}{2\pi i}\sum_{l=-\infty}^{\infty}{}'(-)^l\int_{-\infty}^{\infty}f^{(\mp)}(x)dx\int_0^{\infty}d\epsilon_{k'}\left[\frac{2m\epsilon_{k'}}{\hbar^2}\right]^{1/2}\left[\frac{\hbar\omega_c}{2\epsilon_{k'}|l|}\right]^{1/2}$$
$$\times\exp\left\{2\pi i\frac{l\epsilon_{k'}}{\hbar\omega_c}-\frac{l}{|l|}i\frac{\pi}{4}\right\}\left[\frac{1}{x-\epsilon_{k'}-G_{k'}(x-i0)}-\frac{1}{x-\epsilon_{k'}-G_{k'}(x+i0)}\right]\chi_k(\epsilon_{k'}), \tag{AI.13}$$

where

$$\chi_k(\epsilon_{k'})\equiv\frac{\Omega}{4\pi^2}\frac{C^2}{NMc_s}\frac{m}{\hbar}\int_{Q_{c-}}^{Q^0}\frac{Q^2dQ}{[(Q_{c+}{}^2-Q^2)(Q^2-Q_{c-}{}^2)]^{1/2}(\zeta_l-x\pm\hbar\omega_Q)}, \tag{AI.14}$$

and $Q_{c\pm}=(k'\pm k_\perp)^2+k_z{}^2$, $Q^0=\text{Min}\{Q_m,Q_{c+}\}$ [the φ integration was transformed to a Q integration using (AI.8a)]. The $\epsilon_{k'}$ integration is now evaluated by the method of residues.[10] The function $\chi_k(\epsilon_{k'})$ will be assumed to have no branch cuts in the finite complex $\epsilon_{k'}$ plane, as the limits of the Q integration in (AI.14) are defined so that the radicand is always nonzero.

For $l>0$ the contour of integration in the $\epsilon_{k'}$ plane is shown in Fig. 13. Also shown are the simple poles at $\epsilon_{k'}=x-M_{k'}(x)\pm i\Gamma_{k'}(x)$. As it will be seen that $x\sim E_F$, the k' dependence of M and Γ are ignored in a first iterative solution for the poles. The upper limit on the $\epsilon_{k'}$ integration in (AI.13) should really be $\hbar^2/2m(k_F+Q_m)^2$. However, such a restriction on the magnitude of $\epsilon_{k'}$ results in oscillatory terms depending on the sharp cutoff Q_m in the Debye model. These oscillatory terms depending on Q_m are regarded as physically spurious and are neglected. The $\epsilon_{k'}$ integration for $l>0$ is now evaluated to yield

$$\frac{1}{2\pi i}\int_0^{\infty}d\epsilon_{k'}\left[\frac{2m}{\hbar^2}\frac{\hbar\omega}{2l}\right]^{1/2}e^{2\pi il\epsilon_{k'}/\hbar\omega_c-i\pi/4}\left[\frac{1}{x-\epsilon_{k'}-G_{k'}(x-i0)}-\frac{1}{x-\epsilon_{k'}-G_{k'}(x+i0)}\right]$$
$$=-\left[\frac{2m\hbar\omega_c}{\hbar^2 2l}\right]^{1/2}\exp\left\{\frac{2\pi il}{\hbar\omega_c}(x-M(x)+i\Gamma(x))-i\frac{\pi}{4}\right\}\chi_k(x-M(x)+i\Gamma(x))$$
$$+\frac{e^{-i\pi/4}}{2\pi i}\left[\frac{2m\hbar\omega_c}{\hbar^2 2l}\right]^{1/2}i\int_0^{\infty}dy\,e^{-2\pi ly/\hbar\omega_c}\left[\frac{1}{x-M(x)+i\Gamma(x)-iy}-\frac{1}{x-M(x)-i\Gamma(x)-iy}\right]\chi_k(iy). \tag{AI.15}$$

The second term on the right-hand side of (AI.15) is the contribution from the part of the contour along the

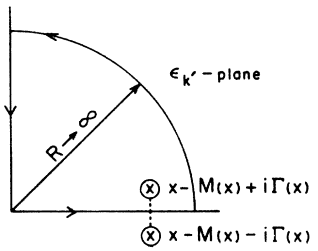

FIG. 13. The contour of integration in the $\epsilon_{k'}$ plane for $l>0$.

imaginary axis, $\epsilon_{k'}=iy$. This contribution is readily seen to be

$$\approx\frac{e^{-i\pi/4}}{2\pi i}\left[\frac{\hbar\omega_c}{2lE_F}\right]^{1/2}\frac{\hbar\omega_c}{2\pi l}\frac{2\Gamma(x)}{(x-M(x))^2+\Gamma(x)^2}\left[\frac{2mE_F}{\hbar^2}\right]^{1/2}\chi_k(0)\,, \tag{AI.16}$$

which is completely negligible, as it is a factor $\hbar\omega_c/E_F\times\kappa\Theta/E_F$ smaller than the contribution from the pole. For the last factor in (AI.16)

$$\left(\frac{2mE_F}{\hbar^2}\right)^{1/2}\chi_k(0)=\lim_{\epsilon\to 0}k_F\frac{\Omega}{4\pi^2}\frac{C^2}{NMc_s}\frac{m}{\hbar}\int_{Q_{c-}}^{Q_{c+}}\frac{Q^2dQ}{[(Q_{c+}^2-Q^2)(Q^2-Q_{c-}^2)]^{1/2}(\zeta_l-z\pm\hbar\omega_Q)}$$

where now $Q_{c\pm}=(k_\perp\pm\epsilon)^2+k_z^2$. The result is

$$\left(\frac{2mE_F}{\hbar^2}\right)^{1/2}\chi_k(0)=\frac{3}{16}\frac{C^2}{Mc_s^2E_F}\frac{\hbar\omega_{k_F}}{\zeta_l-x\pm\hbar\omega_{k_F}}\,,$$

which can be seen to be of order unity when $\zeta_l\to z\pm i0$ and $z\sim E_F$.

For $l<0$ the contour is closed in the lower $\epsilon_{k'}$ plane with similar results. The self-energy is now expressed

$$G_k(\zeta_l)_{\rm osc}=-\sum_{\substack{l=1\\ \pm}}^{\infty}(-)^l\int_{-\infty}^{\infty}f^{(\mp)}(x)dx\left[\frac{\hbar\omega_c}{2lE_F}\right]^{1/2}e^{-2\pi l\Gamma(x)/\hbar\omega_c}2\left(\cos\left\{\frac{2\pi l}{\hbar\omega_c}[x-M(x)]-\frac{\pi}{4}\right\}\right)k_F\chi_k(x)\,, \tag{AI.17}$$

where $\chi_k(x-M(x)\pm i\Gamma(x))\approx\chi_k(x)$.

One now takes the analytical continuation $\zeta_l\to z\pm i0$ and the imaginary part of (AI.17) is considered,

$$\Gamma_k(z)_{\rm osc}=-\pi\sum_{\substack{l=1\\ \pm}}^{\infty}(-)^l\left[\frac{\hbar\omega_c}{2lE_F}\right]^{1/2}k_F\frac{\Omega}{4\pi^2}\frac{C^2}{NMc_s}\frac{2m}{\hbar}$$

$$\times\int_{Q_{c-}}^{Q_m}\frac{Q^2dQ\,f^{(\mp)}(z\pm\hbar\omega_Q)\exp(-(2\pi l/\hbar\omega_c)\Gamma(z\pm\hbar\omega_Q))}{[(Q_{c+}^2-Q^2)(Q^2-Q_{c-}^2)]^{1/2}}\cos\left\{\frac{2\pi l}{\hbar\omega_c}(z\pm\hbar\omega_Q-M(z\pm\hbar\omega_Q))-\frac{\pi}{4}\right\}\,, \tag{AI.18}$$

where $Q_{c\pm}=((2mz/\hbar^2)^{1/2}\pm k_\perp)^2+k_z^2$ and the approximation, as in (AI.17), of neglecting a typical value of $\hbar\omega_Q$ in $Q_{c\pm}$ has been used. The $\pm\hbar\omega_Q$ is only retained in the functions which vary rapidly with their arguments, i.e., $\Gamma(z)$, $M(z)$, $f^{(\mp)}(z)$, and $\cos(2\pi lz/\hbar\omega_c)$.

An order of magnitude calculation for the integral in (AI.18) for

$$(2mz/\hbar^2)^{1/2}\simeq k_F\,,\quad k_\perp\sim k_F\,,\quad (Q_{c-}\sim 0)\,,\quad [(Q_{c+}^2-Q^2)(Q^2-Q_{c-}^2)]^{1/2}\approx\sqrt{2}k_FQ_m$$

yields

$$\Gamma_k(z)_{\rm osc}\cong-\sum_{l=1}^{\infty}(-)^l\left[\frac{\hbar\omega_c}{2lE_F}\right]^{1/2}\frac{\Omega}{4\pi^2}k_F\frac{C^2}{NMc_s}\frac{2me^{-2\pi l\Gamma(z)/\hbar\omega_c}}{\hbar\sqrt{2}k_FQ_m}\cos\left\{\frac{2\pi l}{\hbar\omega_c}(z-M(z))-\frac{\pi}{4}\right\}\sum_{\pm}\pi\int_{Q_{c-}}^{Q_m}Q^2dQ\,f^{(\mp)}(z\pm\hbar\omega_Q)$$

$$\cong\Gamma(z)_{\rm nonosc}\sum_{l=1}^{\infty}(-)^l\left[\frac{\hbar\omega_c}{2lE_F}\right]^{1/2}e^{-2\pi l\Gamma(z)/\hbar\omega_c}\cos\left\{\frac{2\pi l}{\hbar\omega_c}(z-M(z))-\frac{\pi}{4}\right\}\,. \tag{AI.19}$$

Thus,

$$\frac{\Gamma_k(z)_{\rm osc}}{\Gamma_k(z)_{\rm nonosc}}\approx\left[\frac{\hbar\omega_c}{2lE_F}\right]^{1/2}\exp\left(-\frac{2\pi l\Gamma(z)}{\hbar\omega_c}\right).$$

Equation (AI.18) is actually a rather complicated integral equation for $\Gamma_k(z)_{\rm osc}$. In fact, one must include the equation for $M_k(z)_{\rm osc}$ and obtain coupled integral equations! However, in light of the estimate made in (AI.19), the $\Gamma_k(z)$ and $M_k(z)$ can be replaced, on the right-hand side of (AI.18), by the leading nonoscillatory part. Even so, further progress with (AI.18) would necessitate computer calculation as in the case for the conductivity.

An interesting feature of (AI.18) is the limit Q_{c-} on the Q integration. The upper limit is determined by $f^{(\mp)}(z\pm\hbar\omega_Q)$ for $(z-\mu)\leq\kappa\Theta$. For $\mu<z<\mu+\kappa\Theta$, the condition

$$z-\mu\geq\hbar c_sQ_{c-}\cong\hbar c_s[(k_F-k_\perp)^2+k_z^2]^{1/2} \tag{AI.20}$$

must hold or $\Gamma_k(z)_{\rm osc}=0$, to within the order of $[\hbar\omega_c/E_F]^{1/2}$. In (AI.20), the approximation $[2mz/\hbar^2]^{1/2}\approx k_F$ in Q_{e^-} was made.

Because of the saddle-point condition the electron is scattered from a state characterized by $k_\perp$, k_z to the equatorial plane of the Fermi surface. The energy of the phonon, with the necessary wave vector for the transition, must be supplied; hence, condition (AI.20). One can also see that the slow k variation holds for $\Gamma_k(z)_{\rm osc}$.

An order of magnitude estimate of the $\sin 2\theta$ term, omitted in the above calculations, will now be considered. It will be assumed that $k_\perp'\sim k_F$. For $k_\perp\sim 0$ one has to order $k_\perp/k_\perp'$,

$$\theta\cong\frac{\hbar k_\perp^2}{2m\omega_c}\varphi+\frac{\hbar k_\perp' k_\perp}{2m\omega_c}\sin\varphi. \tag{AI.21}$$

The $\sin 2\theta$ term is thus small and can be disregarded. For $k_\perp\sim k_F$, one has to within an error of $|k_\perp'-k_\perp|/|k_\perp'+k_\perp|$ for the φ-dependent part of θ and for $\varphi\neq 0$

$$\theta\cong\frac{1}{2}\left(\frac{\hbar k_\perp^2}{2m\omega_c}+\frac{\hbar k_\perp'^2}{2m\omega_c}\right)\varphi+\frac{\hbar k_\perp' k_\perp}{2m\omega_c}\sin\varphi \tag{AI.22}$$

with comparable results for $\varphi\cong 0$.

The φ dependence of Q in (AI.8) can be considered as slowly varying as compared to $\sin 2\theta$. The Debye cutoff Q_m is disregarded for this order of magnitude calculation. The upper limit on φ is, thus, equal to π. The φ integral is proportional to a Weber function (cf. p. 308 of Ref. 22), $-\mathbf{E}_\nu(z)$, where

$$-\nu=\left(\frac{\hbar k_\perp}{2m\omega_c}+\frac{\hbar k_\perp'^2}{2m\omega_c}\right)\quad\text{and}\quad z=\hbar k_\perp' k_\perp/m\omega_c.$$

For large ν, z and $z\approx\nu$,

$$-\mathbf{E}_{-\nu}(z)\approx\Gamma(\tfrac{1}{3})[\cos(\nu\pi)-\tfrac{1}{2}]/3\pi(\tfrac{1}{6}z)^{1/3}. \tag{AI.23}$$

Thus, the φ integration gives an additional factor of $(E_F/\hbar\omega_c)^{-1/3}$ and the phase factor in (AI.23) does not alter the saddle point of the θ' integration. For $\nu>z(k_\perp<k_\perp'\sim k_F)$ the additional factor due to the $\sin 2\theta$ term is $\sim[E_F/\hbar\omega_c]^{-1/2}$. The $\sin 2\theta$ term will therefore be neglected.

(B) The oscillatory part of the conductivity is

$$\begin{aligned}\sigma_{yy}(q,\omega)_{\rm osc}=&\frac{e^2}{2\pi i\Omega}\sum_{\substack{r,l=-\infty\\ k_y,k_z}}^{\infty\,\prime}(-)^l\int_{-\infty}^{\infty}d\mathcal{E}\frac{f^{(-)}(\mathcal{E})-f^{(-)}(\mathcal{E}+\hbar\omega)}{\hbar\omega}\\
&\times\int_0^\infty\frac{\left(\frac{\hbar k_\perp}{m}\right)^3\frac{dk_\perp}{\omega_c^2}\exp\left(\frac{\pi i l\hbar k_\perp^2}{m\omega_c}\right)\left|J_r'\left(\frac{\hbar k_\perp q_x}{m\omega_c}\right)\right|^2\hbar\omega_c}{-i[\hbar\omega-r\hbar\omega_c+M_k(\mathcal{E})-M_k(\mathcal{E}+\hbar\omega)]+\Gamma_k(\mathcal{E})+\Gamma_k(\mathcal{E}+\hbar\omega)}\\
&\times\{[\mathcal{E}-\epsilon_k-\tfrac{1}{2}r\hbar\omega_c-G_k(\mathcal{E}-i0)]^{-1}-[\mathcal{E}+\hbar\omega-\epsilon_k+\tfrac{1}{2}r\hbar\omega_c-G_k(\mathcal{E}+\hbar\omega+i0)]^{-1}\}\\
&-\frac{e^2}{2\pi i\Omega}\sum_{\substack{r,l=-\infty\\ k_y,k_z}}^{\infty\,\prime}\int_{-\infty}^{\infty}\frac{d\mathcal{E}}{\hbar\omega}\int_0^\infty\left(\frac{\hbar k_\perp}{m}\right)^3\frac{dk_\perp}{\omega_c^2}\exp\left(\frac{\pi i l\hbar k_\perp^2}{m\omega_c}\right)\\
&\times\Bigg[\frac{f^{(-)}(\mathcal{E})\hbar\omega_c}{-i[\hbar\omega-r\hbar\omega_c+M_k(\mathcal{E})-M_k(\mathcal{E}+\hbar\omega)]+\Gamma_k(\mathcal{E}+\hbar\omega)-\Gamma_k(\mathcal{E})}\\
&\times\{[\mathcal{E}-\epsilon_k+\tfrac{1}{2}r\hbar\omega_c-G_k(\mathcal{E}+i0)]^{-1}-[\mathcal{E}+\hbar\omega-\epsilon_k-\tfrac{1}{2}r\hbar\omega_c-G_k(\mathcal{E}+\hbar\omega+i0)]^{-1}\}\\
&-\frac{f^{(-)}(\mathcal{E}+\hbar\omega)\hbar\omega_c}{-i[\hbar\omega-r\hbar\omega_c+M_k(\mathcal{E})-M_k(\mathcal{E}+\hbar\omega)]-\Gamma_k(\mathcal{E}+\hbar\omega)+\Gamma_k(\mathcal{E})}\\
&\times\{[\mathcal{E}-\epsilon_k+\tfrac{1}{2}r\hbar\omega_c-G_k(\mathcal{E}-i0)]^{-1}-[\mathcal{E}+\hbar\omega-\epsilon_k-\tfrac{1}{2}r\hbar\omega_c-G_k(\mathcal{E}+\hbar\omega-i0)]^{-1}\}\Bigg],\end{aligned} \tag{AI.24}$$

where the prime on the summation sign pertains only to the l sum and signifies the deletion of the $l=0$ term.

After a change to spherical coordinates in k space, one has for the integration over the polar angle θ,

$$\exp\left(\frac{\pi i l\hbar k^2}{2m\omega_c}\right)\frac{1}{2\pi}\int_0^{\pi}\sin^2\theta\exp\left(-\frac{\pi i l\hbar k^2}{2m\omega_0}\cos 2\theta\right)d\theta$$

$$=\tfrac{1}{4}\exp\left(\frac{\pi i l\hbar k^2}{2m\omega_c}\right)\left[J_0\left(\frac{\pi|l|\hbar k^2}{2m\omega_c}\right)+i\frac{l}{|l|}J_1\left(\frac{\pi|l|\hbar k^2}{2m\omega_c}\right)\right]\approx\frac{1}{2\pi}\left[\frac{\hbar\omega_c}{2|l|\epsilon_k}\right]^{1/2}\exp\left[\frac{2\pi i l\epsilon_k}{\hbar\omega_c}-i\frac{l}{|l|}\frac{\pi}{4}\right], \quad \text{(AI.25)}$$

where the phase factor in the asymptotic expression for $J_r'(\hbar k_\perp q_x/m\omega_c)$ has been dropped as compared to $\exp(i\pi l\hbar k_\perp^2/m\omega_c)$.

The k integration is changed to an ϵ_k integration. The integration is performed by the method of residues with the same contour as used for the $\epsilon_{k'}$ integration in part A of this Appendix. In this case, however, the ϵ_k plane is cut along the negative real axis due to the presence of the function $\epsilon_k^{1/2}$ in the integrand.

The contribution to the conductivity by the first integral on the right-hand side of (AI.24), denoted by $\sigma_{yy}^{(1)}(q,\omega)_{\rm osc}$, is

$$\sigma_{yy}^{(1)}(q,\omega)_{\rm osc}=-\frac{3ne^2}{4mv_Fq_x}\sum_{l=1}^{\infty}(-)^l\left[\frac{\hbar\omega_c}{2\pi^2 lE_F}\right]^{1/2}\int_{\mu-\hbar\omega}^{\mu}\frac{d\mathcal{E}}{\hbar\omega_c}\exp\left[\frac{\pi i l}{\hbar\omega_c}(\hbar\omega-M(\mathcal{E}+\hbar\omega)+M(\mathcal{E}))-\frac{\pi l}{\hbar\omega_c}(\Gamma(\mathcal{E}+\hbar\omega)+\Gamma(\mathcal{E}))\right]$$

$$\times 2\left(\cos\left\{\frac{\pi l}{\hbar\omega_c}[(2\mathcal{E}+\hbar\omega-M(\mathcal{E})-M(\mathcal{E}+\hbar\omega))+i(\Gamma(\mathcal{E}+\hbar\omega)-\Gamma(\mathcal{E}))]-\frac{\pi}{4}\right\}\right)$$

$$\times\sum_{r=-\infty}^{\infty}\frac{(-)^{rl}\hbar\omega_c}{-i[\hbar\omega-r\hbar\omega_c+M(\mathcal{E})-M(\mathcal{E}+\hbar\omega)]+\Gamma(\mathcal{E})+\Gamma(\mathcal{E}+\hbar\omega)}. \quad \text{(AI.26)}$$

It can be seen that the ratio of $\sigma^{(1)}(q,\omega)_{\rm osc}$ to $\sigma(q,\omega)_{\rm nonosc}$ is at least as small as $(\hbar\omega_c/E_F)^{1/2}$. The approximation

$$[\mathcal{E}-\tfrac{1}{2}r\hbar\omega_c-M(\mathcal{E})-i\Gamma(\mathcal{E})]^{1/2}\approx[\mathcal{E}+\hbar\omega+\tfrac{1}{2}r\hbar\omega_c-M(\mathcal{E}+\hbar\omega)+i\Gamma(\mathcal{E}+\hbar\omega)]^{1/2}\approx E_F^{1/2}, \quad \text{(AI.27)}$$

has been used in (AI.26). The contribution to the conductivity of the second integral in (AI.24), denoted by $\sigma_{yy}^{(2)}(q,\omega)_{\rm osc}$ is

$$\sigma_{yy}^{(2)}(q,\omega)_{\rm osc}=\frac{3ne^2}{4mv_F}\sum_{l=1}^{\infty}(-)^l\left[\frac{\hbar\omega_c}{2\pi^2 lE_F}\right]^{1/2}$$

$$\times\int_0^{\mu}\frac{d\mathcal{E}}{\hbar\omega}\left[\frac{\mathcal{E}}{E_F}\right]^{1/2}\exp\left[\frac{\pi i l}{\hbar\omega_c}(2\mathcal{E}-M(\mathcal{E})-M(\mathcal{E}+\hbar\omega)+\hbar\omega)-\frac{\pi l}{\hbar\omega_c}(\Gamma(\mathcal{E}+\hbar\omega)+\Gamma(\mathcal{E}))-i\frac{\pi}{4}\right]$$

$$\times 2i\left(\sin\left\{\frac{\pi l}{\hbar\omega_c}[\hbar\omega-M(\mathcal{E}+\hbar\omega)+M(\mathcal{E})+i(\Gamma(\mathcal{E}+\hbar\omega)-\Gamma(\mathcal{E}))]\right\}\right)$$

$$\times\sum_{r=-\infty}^{\infty}\frac{(-)^{rl}\hbar\omega_c}{-i[\hbar\omega-r\hbar\omega_c+M(\mathcal{E})-M(\mathcal{E}+\hbar\omega)]+\Gamma(\mathcal{E}+\hbar\omega)-\Gamma(\mathcal{E})}$$

$$-\int_0^{\mu-\hbar\omega}\frac{d\mathcal{E}}{\hbar\omega}\left[\frac{\mathcal{E}}{E_F}\right]^{1/2}\exp\left[-\frac{\pi i l}{\hbar\omega_c}(2\mathcal{E}-M(\mathcal{E})-M(\mathcal{E}+\hbar\omega)+\hbar\omega)-\frac{\pi l}{\hbar\omega_c}(\Gamma(\mathcal{E}+\hbar\omega)+\Gamma(\mathcal{E}))+i\frac{\pi}{4}\right]$$

$$\times 2i\left(\sin\left\{\frac{\pi l}{\hbar\omega_c}[\hbar\omega+M(\mathcal{E})-M(\mathcal{E}+\hbar\omega)-i(\Gamma(\mathcal{E}+\hbar\omega)-\Gamma(\mathcal{E}))]\right\}\right)$$

$$\times\sum_{r=-\infty}^{\infty}\frac{(-)^{rl}\hbar\omega_c}{-i[\hbar\omega-r\hbar\omega_c+M(\mathcal{E})-M(\mathcal{E}+\hbar\omega)]-(\Gamma(\mathcal{E}+\hbar\omega)-\Gamma(\mathcal{E}))}. \quad \text{(AI.28)}$$

In contrast to the $\mathcal{E}$ integration in (AI.26), the range of $\mathcal{E}$ in (AI.28) is not limited to $\mu-\hbar\omega\leq\mathcal{E}\leq\mu$. In (AI.28) the bottom of the conduction band is taken at $\mathcal{E}=0$. For $\mathcal{E}<\mu-2\hbar\omega$,

$$M_k(\mathcal{E})-M_k(\mathcal{E}+\hbar\omega)\approx\Gamma_k(\mathcal{E})-\Gamma_k(\mathcal{E}+\hbar\omega)\approx 0,$$

so that the k dependence of $M(\mathcal{E})$, $\Gamma(\mathcal{E})$, etc., will be evaluated at $k\sim k_F$. The square-root factors [as in (AI.27) are approximated by $\mathcal{E}^{1/2}$ in (AI.28), which is valid for most of the $\mathcal{E}$ range.

When l is an even integer one has, as in Sec. III,

$$\sum_{r=-\infty}^{\infty}\frac{\hbar\omega_c}{-i[\hbar\omega-r\hbar\omega_c+M(\mathcal{E})-M(\mathcal{E}+\hbar\omega)]\pm(\Gamma(\mathcal{E}+\hbar\omega)-\Gamma(\mathcal{E}))}$$
$$=\frac{i\pi\cos\left[\frac{\pi}{\hbar\omega_c}[\hbar\omega+M(\mathcal{E})-M(\mathcal{E}+\hbar\omega)\pm i(\Gamma(\mathcal{E}+\hbar\omega)+\Gamma(\mathcal{E}))]\right]}{\sin\left[\frac{\pi}{\hbar\omega_c}[\hbar\omega+M(\mathcal{E})-M(\mathcal{E}+\hbar\omega)\pm i(\Gamma(\mathcal{E}+\hbar\omega)-\Gamma(\mathcal{E}))]\right]}.$$

For the case when l is an odd integer the sum over r is

$$\sum_{r=-\infty}^{\infty}\frac{(-)^r\hbar\omega_c}{-i[\hbar\omega-r\hbar\omega_c+M(\mathcal{E})-M(\mathcal{E}+\hbar\omega)]\pm(\Gamma(\mathcal{E}+\hbar\omega)-\Gamma(\mathcal{E}))}$$
$$=i\pi\left[\sin\left[\frac{\pi}{\hbar\omega_c}[\hbar\omega+M(\mathcal{E})-M(\mathcal{E}+\hbar\omega)\pm i(\Gamma(\mathcal{E}+\hbar\omega)-\Gamma(\mathcal{E}))]\right]\right]^{-1}.$$

One can see that in either case the terms in (AI.28) are nonresonant, i.e., the ratio of the sine functions in the numerator and denominator are of order l, for small l, at resonance.

The difference between the terms $\sigma^{(1)}(q,\omega)_{\text{osc}}$ can be traced to the fact that the terms in the curly bracket in the second integral in (AI.24) have poles in the same half of the ϵ_k plane in contrast to the terms in the curly bracket in the first integral. The terms in the first integral have poles on opposite sides of the real axis in the ϵ_k plane and therefore the contributions from the poles to the integral can be seen to add.

APPENDIX II: HIGHER CORRECTIONS TO THE CONDUCTIVITY

In this Appendix, the contribution to $\mathfrak{F}_{yy}(\omega_r)$, (1.11) of the higher order ladder diagrams will be considered. In particular, the ladder diagram, shown in Fig. 14, will be calculated. As the calculation is quite lengthy, the main details will be discussed.

Using the rules for evaluating skeleton diagrams, outlined in Sec. II and H. p. 418, the correction to $\mathfrak{F}_{yy}(\omega_r)$ from the diagram in Fig. 14, denoted by $\mathfrak{F}_{yy}^{(1)}(\omega_r)$, is

$$\mathfrak{F}_{yy}^{(1)}(\omega_r)=-\frac{1}{\beta^2}\sum_{\substack{\bar{n},\bar{n}',n,n'\\ k_y,k_z,\mathbf{Q},\pm\\ \zeta_l,\zeta_{l'}}}[\langle\bar{l}|v_{q,y}|\bar{l}'\rangle\langle l'|v_{-q,y}|l\rangle V_{l\bar{l}}(\mathbf{Q})V_{l'\bar{l}'}{}^*(\mathbf{Q})]$$
$$\times[[\hbar\omega_Q\pm(\zeta_l-\zeta_{l'})][\zeta_{l'}-\epsilon_{k_z-Q_z}{}^{\bar{n}}-G_{\bar{n}k_z-Q_z}(\zeta_{l'})]]^{-1}[\zeta_{l'}+\hbar\omega_r-\epsilon_{k_z-Q_z}{}^{\bar{n}'}-G_{\bar{n}',k_z-Q_z}(\zeta_{l'}+\hbar\omega_r)]^{-1}$$
$$\times[[\zeta_l-\epsilon_{k_z}{}^{n}-G_{nk_z}(\zeta_l)][\zeta_l+\hbar\omega_r-\epsilon_{k_z}{}^{n'}-G_{n'k_z}(\zeta_l+\hbar\omega_r)]]^{-1},\quad\text{(AII.1)}$$

where

$$\bar{l}=\{\bar{n},k_y-Q_y,k_z-Q_z\},\qquad \bar{l}'=\{\bar{n}',k_y-Q_y,k_z-Q_z\},$$
$$l=\{n,k_y,k_z\},\qquad l'=\{n',k_y,k_z\}.$$

The sums over ζ_l, $\zeta_{l'}$ are converted into integrals over suitable contours in the ζ,ζ' planes as in (3.4), (3.5). The change in summation variables, $\bar{N}\equiv\bar{n}+\bar{n}'/2$, $\bar{r}\equiv\bar{n}-\bar{n}'$, $N\equiv n+n'/2$, $r\equiv n-n'$ are introduced as in (3.6). The partial fraction expansions (3.8), (3.9) are used with the approximation (3.7). The Poisson sum rule is employed in conjunction with the sums over $\bar{N}$, N and only the nonoscillatory parts are retained, i.e., $\bar{N}$, N are changed to $\hbar\bar{k}_\perp{}^2/2m\omega_c$, $\hbar k_\perp{}^2/2m\omega_c$ and the $\bar{N}$, N sums are replaced by integrations over $\bar{k}_\perp$, $k_\perp$. Only the resonance type terms

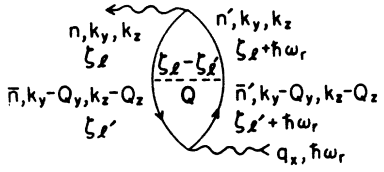

FIG. 14. The "one-rung" ladder diagram for the velocity-correlation function.

as in (3.8) are to be discussed and the Taylor series expansions of (3.10) and (3.11) are used to yield expressions as in (3.13). The result of all these steps and the use of (1.8), (1.16), (1.19), and (1.20) for the velocity and EPI matrix elements in (AII.1) is

$$\mathfrak{F}_{yy}{}^{(1)}(\omega+i0)=-\sum_{r,\bar{r}=-\infty}^{\infty}\sum_{\mathbf{Q},\pm}\int_{-\infty}^{\infty}dxdx'\int_0^{\infty}\frac{\dfrac{hk_\perp dk_\perp}{m\omega_c}\dfrac{h\bar{k}_\perp dk_\perp}{m\omega_c}[f^{(-)}(x)-f^{(-)}(x+\hbar\omega)]\delta(x-\epsilon_k)\delta(x'-\epsilon_{k'})}{[\hbar\omega-r\hbar\omega_c+M_k(x)-M_k(x+\hbar\omega)]+i[\Gamma_k(x)+\Gamma_k(x+\hbar\omega)]}$$

$$\times\frac{e^{-i(\hbar q_x Q_y/m\omega_c)}\dfrac{\hbar^2\bar{k}_\perp k_\perp}{m^2}J_{\bar{r}}'\left(\dfrac{h\bar{k}_\perp q_x}{m\omega_c}\right)J_r'\left(\dfrac{hk_\perp q_x}{m\omega_c}\right)|V_Q|^2e^{i(\bar{r}-r)\varphi}\chi_+(Q_\perp)\chi_-(Q_\perp)}{\hbar\omega-\bar{r}\hbar\omega_c+M_{k'}(x')-M_{k'}(x'+\hbar\omega)+i[\Gamma_{k'}(x')+\Gamma_{k'}(x'+\hbar\omega)]}$$

$$\times\left\{(f^{(\mp)}(x')-f^{(\mp)}(x'+\hbar\omega))P\left(\frac{1}{x-x'\pm\hbar\omega_Q}\right)+2\pi i\delta(x-x'\pm\hbar\omega_Q)\left[\frac{f^{(\mp)}(x')+f^{(\mp)}(x'+\hbar\omega)}{2}+N_Q\right]\right\}, \quad \text{(AII.2)}$$

where $Q_x+iQ_y=Q_\perp e^{i\varphi}$, $k^2=k_\perp{}^2+k_z{}^2$, $k'^2=\bar{k}_\perp{}^2+(k_z-Q_z)^2$, and

$$\chi_\pm(Q_\perp)=\left[\frac{2}{\pi}\right]^{1/2}\left[\cos\left\{\int_{\alpha_0}^{\alpha}\left[\left[\frac{h\bar{k}_\perp{}^2}{2m\omega_c}+\frac{hk_\perp{}^2}{2m\omega_c}\pm\frac{\bar{r}+r}{2}\right]\alpha'^2-\left(\frac{h\bar{k}_\perp{}^2}{2m\omega_c}-\frac{hk_\perp{}^2}{2m\omega_c}\pm\frac{\bar{r}-r}{2}\right)^2-\left(\frac{\alpha'^2}{2}\right)^2\right]^{1/2}\frac{d\alpha'}{\alpha'}-\frac{\pi}{4}\right\}\right]$$

$$\div\left[\left(\frac{h\bar{k}_\perp{}^2}{2m\omega_c}+\frac{hk_\perp{}^2}{2m\omega_c}\pm\frac{\bar{r}+r}{2}\right)\alpha^2-\left(\frac{h\bar{k}_\perp{}^2}{2m\omega_c}-\frac{hk_\perp{}^2}{2m\omega_c}\pm\frac{\bar{r}-r}{2}\right)^2-\left(\frac{\alpha^2}{2}\right)^2\right]^{1/4}, \quad \text{(AII.3)}$$

where $\alpha^2=\hbar Q_\perp{}^2/m\omega_c$ and $\alpha_0=\hbar(k_\perp-\bar{k}_\perp)^2/m\omega_c$. The radical in (AII.3) is now expanded in powers of $\bar{r}+r$, $\bar{r}-r$ and to order q_x/k_F only the first term in the expansion is kept for the denominator. Introducing the angle $\bar{\varphi}$,[55]

$$Q_\perp{}^2\equiv\bar{k}_\perp{}^2+k_\perp{}^2-2\bar{k}_\perp k_\perp\cos\bar{\varphi}, \quad \text{(AII.4)}$$

one has for the phase factor of $\chi_\pm(Q_\perp)$,

$$\cos(\theta-\pi/4\pm\tfrac{1}{2}[r,\bar{r}]\bar{\varphi}), \quad \text{(AII.5)}$$

where θ is defined in (AI.7) (with $k_\perp'$ replaced by $\bar{k}_\perp$) and $[r,\bar{r}]=r$ for $\bar{k}_\perp>k_\perp$, $[r,\bar{r}]=\bar{r}$ for $k_\perp>\bar{k}_\perp$. The simple additional factor $\pm[r,\bar{r}]\bar{\varphi}/2$ has been obtained with use of the approximation

$$\tan^{-1}\left\{\frac{\bar{k}_\perp+k_\perp}{|k_\perp-\bar{k}_\perp|}\tan\frac{\bar{\varphi}}{2}\right\}\simeq\frac{\bar{\varphi}}{2}. \quad \text{(AII.6)}$$

One now has for the term in (AII.2),

$$\chi_+(Q_\perp)\chi_-(Q_\perp)=\frac{2m\omega_c}{h\pi}\frac{\cos([r,\bar{r}]\bar{\varphi})+\sin2\theta}{[(Q_\perp{}^2-(k_\perp-\bar{k}_\perp)^2)((k_\perp+\bar{k}_\perp)^2-Q_\perp{}^2)]^{1/2}}. \quad \text{(AII.7)}$$

The additional phase factor in (AII.2) from the EPI matrix elements is $e^{i(\bar{r}-r)\varphi}$. The factor $e^{-i\hbar q_y Q_x/m\omega_c}$ arises from the velocity matrix elements.

The $\mathbf{Q}$ sum in (AII.2) is converted into an integral and cylindrical coordinates Q_z, $Q_\perp$, φ are utilized. The integral over the azimuthal angle φ is simply performed, to yield

$$\frac{1}{2\pi}\int_0^{2\pi}d\varphi\exp\left[-i\frac{hq_xQ_\perp}{m\omega_c}\sin\varphi+i(\bar{r}-r)\varphi\right]=J_{\bar{r}-r}\left(\frac{hq_xQ_\perp}{m\omega_c}\right). \quad \text{(AII.8)}$$

The effective range of the difference for the r's associated with the propagator pairs can now be seen, from (AII.8), to be of the order $(\hbar q_x/m\omega_c)Q_m\sim q_xv_F/\omega_c$. It will suffice, to use the asymptotic form for (AII.8), assuming $\bar{r}-r<\hbar q_xQ_y/m\omega_c$,

$$J_{\bar{r}-r}\left(\frac{hq_xQ_\perp}{m\omega_c}\right)\sim\left(\frac{2m\omega_c}{\pi hq_xQ_\perp}\right)^{1/2}\cos\left(\frac{hq_xQ_\perp}{m\omega_c}-\tfrac{1}{2}(\bar{r}-r)\pi-\frac{\pi}{4}\right). \quad \text{(AII.9)}$$

[55] The angle $\bar{\varphi}$ can be understood to be the angle between the vectors $\mathbf{k}_\perp$, $\bar{\mathbf{k}}_\perp$. It is in this sense that the approximation, $\epsilon_{k'}\cong\epsilon_{k-Q}$, following (AII.14) is made.

The $Q_\perp$ integration will now be considered,

$$\int_{Q_{\perp c}}^{Q_m} Q_\perp dQ_\perp f(Q)\left(\frac{2m\omega_c}{\pi\hbar q_x Q_\perp}\right)^{1/2}\left[\cos\left(\frac{\hbar q_x Q_\perp}{m\omega_c}-\tfrac{1}{2}(\bar r-r)\pi-\frac{\pi}{4}\right)\right]\chi_+(Q_\perp)\chi_-(Q_\perp), \tag{AII.10}$$

where $Q_{\perp c}=|k_\perp-\bar k_\perp|$ and $f(Q)=|V_Q|^2P(1/x-x'\pm\hbar\omega_Q)$ or $f(Q)=|V_Q|^2\delta(x-x'\pm\hbar\omega_Q)$ depending on the term in (AII.2) being considered. Now the terms in the sums over r, $\bar r$ which contribute significantly are such that r, $\bar r<q_xv_F/\omega_c$. The phase factor $\cos([r,\bar r]\bar\varphi)$ in (AII.7) can, therefore, be neglected in comparison to $\cos(\hbar q_xQ_\perp/m\omega_c)$. The $\sin2\theta$ term in (AII.7) need not be considered, as this factor dominates $\cos(\hbar q_xQ_\perp/m\omega_c)$ and leads to smaller corrections of the order $\sim(\hbar\omega_c/E_F)^{1/2}$ as discussed in Appendix I. The $Q_\perp$ integration is performed by the method of stationary phase[56] and changing the integration variable in (AII.10) to $S=Q_\perp/Q_m$, the result is

$$\frac{2m\omega_c}{\hbar\pi}\left(\frac{2m\omega_c}{\pi\hbar q_xQ_m}\right)^{1/2}\int_{S_c}^{1}(\sqrt{S})dS\frac{f([Q_m^2S^2+Q_z^2]^{1/2})[S-S_c]^{-1/2}\cos\left(\dfrac{\hbar q_xQ_m}{m\omega_c}S-\tfrac{1}{2}(\bar r-r)\pi-\dfrac{\pi}{4}\right)}{[S+S_c]^{1/2}[(k_\perp+\bar k_\perp)^2/Q_m^2-S^2]^{1/2}}$$

$$=\frac{2m\omega_c}{\hbar\pi}\left(\frac{m\omega_c}{\pi\hbar q_xQ_m}\right)^{1/2}\left\{\left(\frac{\pi m\omega_c}{\hbar q_xQ_m}\right)^{1/2}f([Q_{\perp c}^2+Q_z^2]^{1/2})\frac{Q_m}{2[k_\perp\bar k_\perp]^{1/2}}\cos\left(\frac{\hbar q_xQ_{\perp c}}{m\omega_c}-\frac{\pi}{2}(\bar r-r)\right)+O\left(\left(\frac{m\omega_c}{\hbar q_xQ_m}\right)^{3/2}\right)\right\}, \tag{AII.11}$$

where $S_c=Q_{\perp c}/Q_m$. It is tacitly assumed that the relevant values of $k_\perp+\bar k_\perp$ are greater than Q_m.

The asymptotic form for the Bessel functions, $J_{\bar r}'$, J_r', in (AII.2) is introduced with the same justifications discussed in Sec. III. The product of the asymptotic forms for $J_{\bar r}'$, J_r' and the final result of (AII.11) is

$$\frac{1}{q_x}\left(\frac{2m\omega_c}{\hbar\pi}\right)^2\frac{1}{2k_\perp\bar k_\perp}\left(\frac{m\omega_c}{\hbar q_x}\right)\frac{f([Q_{\perp c}^2+Q_z^2]^{1/2})}{2}$$

$$\times\left\{\cos\left(\frac{\hbar q_x}{m\omega_c}(\bar k_\perp-k_\perp)-\frac{\bar r-r}{2}\pi\right)-\sin\left(\frac{\hbar q_x}{m\omega_c}(\bar k_\perp+k_\perp)-\frac{\bar r-r}{2}\pi\right)\right\}\cos\left(\frac{\hbar q_xQ_{\perp c}}{m\omega_c}-\frac{\pi}{2}(\bar r-r)\right). \tag{AII.12}$$

Let $Q_{\perp c}=\bar k_\perp-k_\perp$ for definiteness. The product of the phase factors in (AII.12) becomes

$$\frac{1}{2}\left(1+(-)^{\bar r-r}\cos\left(\frac{2\hbar q_xQ_{\perp c}}{m\omega_c}\right)-(-)^r\sin\left(\frac{2\hbar q_xk_\perp}{m\omega_c}\right)-(-)^{\bar r}\sin\left(\frac{2\hbar q_xk_\perp}{m\omega_c}\right)\right). \tag{AII.13}$$

Only the first term in (AII.13) will be retained; the other terms lead to additional corrections of order $\sim(\omega_c/q_xv_F)^{1/2}$.

The correction to the conductivity, denoted by $\sigma_{yy}'(q,\omega)$, provided by (AII.2) can now be written

$$\sigma_{yy}'(q,\omega)=-\frac{m\omega_c}{2\pi^2\hbar q_x^2}\frac{e^2}{i(2\pi)^2}\frac{\Omega}{(2\pi)^2}\int_{-\infty}^{\infty}dk_z\int_0^\infty\frac{\hbar k_\perp}{m}dk_\perp\int_0^\infty\bar k_\perp d\bar k_\perp\int_{-\infty}^{\infty}dx\,dx'\frac{[f^{(-)}(x)-f^{(-)}(x+\hbar\omega)]}{\hbar\omega}\delta(x-\epsilon_k)\delta(x'-\epsilon_{k'})$$

$$\times\sum_{r,\bar r=-\infty}^{\infty}\frac{\hbar\omega}{\hbar\omega-r\hbar\omega_c+M_k(x)-M_k(x+\hbar\omega)+i[\Gamma_k(x)+\Gamma_k(x+\hbar\omega)]}$$

$$\times\{\hbar\omega-\bar r\hbar\omega_c+M_{k'}(x')-M_{k'}(x'+\hbar\omega)+i[\Gamma_{k'}(x')+\Gamma_{k'}(x'+\hbar\omega)]\}^{-1}$$

$$\times\int_{-Q_m}^{Q_m}dQ_z|V_Q|^2\sum_{\pm}\left\{(f^{(\mp)}(x')-f^{(\mp)}(x'+\hbar\omega))P\left(\frac{1}{x-x'\pm\hbar\omega_Q}\right)+\pi i\delta(x-x'\pm\hbar\omega_Q)(f^{(\mp)}(x')+f^{(\mp)}(x'+\hbar\omega))\right\}, \tag{AII.14}$$

where $Q^2=(\bar k_\perp-k_\perp)^2+Q_z^2$. The N_Q term has been dropped [cf. (2.15)]. The integration over $k_\perp$, $\bar k_\perp$, is transformed to one over $k_\perp$, $Q_\perp$, where $Q_\perp\equiv\bar k_\perp-k_\perp$. Now[55] $\epsilon_{k'}\simeq\epsilon_{k-Q}$ and $Q^2=Q_\perp^2+Q_z^2$. Inspection of the two terms in the curly bracket in (AII.14) leads to the conclusion that the range of x' in (AII.14) is the same as x, i.e., $\mu-\hbar\omega\leq x'\leq\mu$. In order to obtain an order of magnitude estimate of (AII.14) and in order to emphasize the simultaneous resonance of the r, $\bar r$ sums, the x' variable is replaced by x in the self-energy terms, $M_{k'}$, $\Gamma_{k'}$. Due to the delta functions $\delta(x-\epsilon_k)$, $\delta(x'-\epsilon_{k'})$ the k, k' of the self-energy terms are understood to be equal to k_F.

[56] A. Erdelyi, *Asymptotic Expansions* (Dover Publications, New York, 1956), p. 48 (with $\lambda=\frac{1}{2}$).

The integrations over $Q_\perp$, Q_z are converted into a sum over $\mathbf{Q}$ and in conjunction with the x' integration one has [cf. H. (2.18)]

$$\sum_{\mathbf{Q},\pm}\int_{-\infty}^{\infty}dx'\,|V_Q|^2[f^{(\mp)}(x')-f^{(\mp)}(x'+\hbar\omega)]P\left(\frac{1}{x-x'+\hbar\omega_Q}\right)\delta(x'-\epsilon_{k-Q})=M_k(x)-M_k(x+\hbar\omega), \quad \text{(AII.15)}$$

$$\sum_{\mathbf{Q},\pm}\pi i\int_{-\infty}^{\infty}dx'\,|V_Q|^2[f^{(\mp)}(x')+f^{(\mp)}(x'+\hbar\omega)]\delta(x-x'\pm\hbar\omega_Q)\delta(x'-\epsilon_{k-Q})=i[\Gamma_k(x)+\Gamma_k(x+\hbar\omega)]. \quad \text{(AII.16)}$$

Using (AII.15), (AII.16), and transforming to spherical coordinates in k space, one has for (AII.14)

$$\sigma_{yy}'(q,\omega)=\frac{m\omega_c e^2}{2\pi^2 hq_x{}^2}\frac{1}{2\pi^2}\int_0^\infty\frac{hk^2}{m}dk\,\delta(\mu-\epsilon_k)\int_{\mu-\hbar\omega}^{\mu}\frac{dx}{\hbar\omega}\sum_r\frac{\hbar\omega_c}{-i[\hbar\omega-r\hbar\omega_c+M(x)-M(x+\hbar\omega)]+\Gamma(x)+\Gamma(x+\hbar\omega)}$$
$$\times\sum_{\bar r}\frac{M(x)-M(x+\hbar\omega)+i[\Gamma(x)+\Gamma(x+\hbar\omega)]}{\hbar\omega-\bar r\hbar\omega_c+M(x)-M(x+\hbar\omega)+i[\Gamma(x)+\Gamma(x+\hbar\omega)]}. \quad \text{(AII.17)}$$

The k integration in (AII.17) yields a factor $k_F/\hbar$. After multiplying and dividing by $k_F{}^2$, one has finally

$$\sigma_{yy}'(q,\omega)=\frac{3ne^2}{4mv_Fq_x}\left(\frac{\omega_c}{\pi^2q_xv_F}\right)\int_{\mu-\hbar\omega}^{\mu}\frac{dx}{\hbar\omega}\sum_r\frac{\hbar\omega_c}{-i[\hbar\omega-r\hbar\omega_c+M(x)-M(x+\hbar\omega)]+\Gamma(x)+\Gamma(x+\hbar\omega)}$$
$$\times\sum_{\bar r}\frac{M(x)-M(x+\hbar\omega)+i[\Gamma(x)+\Gamma(x+\hbar\omega)]}{\hbar\omega-\bar r\hbar\omega_c+M(x)-M(x+\hbar\omega)+i[\Gamma(x)+\Gamma(x+\hbar\omega)]}. \quad \text{(AII.18)}$$

The $\bar r$ sum in (AII.18) is seen to be of order unity and thus

$$\frac{\sigma_{yy}'(q,\omega)}{\sigma_{yy}(q,\omega)}\cong\frac{\omega_c}{\pi^2q_xv_F}=\frac{\delta}{\pi^2R_c}\ll1.$$

The calculation in this Appendix constitutes a quantum-mechanical justification for the neglect of scattering-in terms under cyclotron resonance conditions.

A factor δ/R_c can be expected with each additional phonon rung of the higher order ladder diagrams.

APPENDIX III: PHONON RENORMALIZATION AND THE EPI VERTEX PART

In this Appendix the principal contributions to the phonon self-energy and the EPI vertex part will be evaluated in the magnetic field case. In particular, it is shown: (1) (in part A) that the phonon self-energy is identical to the value obtained in the zero-magnetic-field case, except for small oscillatory terms (like those calculated in Appendix I); and (2) (in part B) that the ratio of the lowest order correction to the EPI vertex part to the elementary vertex is of order c_s/v_F.

(A) The diagram that will be evaluated for the phonon self-energy part is shown in Fig. 15. The diagonality of the phonon self-energy (in the Q variables) is demonstrated in Appendix IV. The contribution of the diagram in Fig. 15, using the rules outlined in Sec. II and H. p. 418, is

$$P_Q(\xi_m)=-\frac{1}{\beta}\sum_{\substack{n,n',k_y,k_z\\ \zeta_l}}[|V_Q|^2]\div\left[\pi\left[(n+n'+1)\frac{\hbar Q_\perp{}^2}{m\omega_c}-(n-n')^2-\left(\frac{\hbar Q_\perp{}^2}{2m\omega_c}\right)^2\right]^{1/2}\right.$$
$$\left.\times[\zeta_l-\epsilon_{k_z}{}^n-G_{nk_z}(\zeta_l)][\zeta_l+\xi_m-\epsilon_{k_z+Q_z}{}^{n'}-G_{nk_z+Q_z}(\zeta_l+\xi_m)]\right]. \quad \text{(AIII.1)}$$

The ζ_l sum is transformed into an integral in the ζ plane by the same procedure as used for the conductivity in

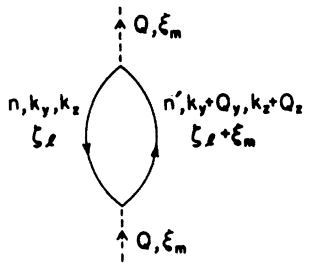

FIG. 15. Skeleton diagram representing the principal contribution to the phonon self-energy.

Sec. III and the continuation $\xi_m \to \xi+i0$ is made. The result is

$$P_Q(\xi+i0)=-\frac{1}{2\pi i}\sum_{n,n',k_y,k_z}\frac{|V_Q|^2}{\pi[(n+n'+1)(\hbar Q_\perp^2/m\omega_c)-(n-n')^2-(\hbar Q_\perp^2/2m\omega_c)^2]^{1/2}}\int_{-\infty}^{\infty}f^{(-)}(x)dx$$
$$\times\Bigg[\frac{1}{x+\xi-\epsilon_{k_z+Q_z}{}^{n'}-G_{n',k_z+Q_z}(x+\xi+i0)}\Bigg\{\frac{1}{x-\epsilon_{k_z}{}^{n}-G_{nk_z}(x-i0)}-\frac{1}{x-\epsilon_{k_z}{}^{n}-G_{nk_z}(x+i0)}\Bigg\}$$
$$+\frac{1}{x-\xi-\epsilon_{k_z}{}^{n}-G_{nk_z}(x-\xi-i0)}\Bigg\{\frac{1}{x-\epsilon_{k_z+Q_z}{}^{n'}-G_{n',k_z+Q_z}(x-i0)}-\frac{1}{x-\epsilon_{k_z+Q_z}{}^{n'}-G_{n',k_z+Q_z}(x+i0)}\Bigg\}\Bigg]. \quad \text{(AIII.2)}$$

The nonoscillatory part of $P_Q(\xi+i0)$ is considered and to this end the sum over n,n' is changed to integrals over $k_\perp,k_\perp'$ and $n+\frac{1}{2}$, $n'+\frac{1}{2}$ is replaced by $\hbar k_\perp^2/2m\omega_c$, $\hbar k_\perp'^2/2m\omega_c$. Further, the delta-function approximation for the square brackets in (AIII.2) is introduced as for the electron self-energy part calculated in Sec. II and the Taylor series (3.10) is used for the remaining propagators. The problem of "overlapping" resonances of the propagator denominators does not occur if the value of Q is selected to be that of a typical phonon, i.e., $Q\sim Q_m$. In this case $\hbar v_F Q \gg \Gamma_k(x)$ and the self-energy effects are negligible (cf. Sec. III and H. Appendix III).

Performing the x integration, and converting the k_z sum into an integral, one has

$$P_Q(\xi+i0)=-\frac{\Omega}{(2\pi)^2}\int_{-\infty}^{\infty}dk_z\int_0^{\infty}k_\perp dk_\perp\int_0^{\infty}\frac{2k_\perp'dk_\perp'|V_Q|^2}{\pi[2(k_\perp^2+k_\perp'^2)Q_\perp^2-(k_\perp^2-k_\perp'^2)^2-Q_\perp^4]^{1/2}}\Bigg\{\frac{f^{(-)}(\epsilon_k)}{\epsilon_k+\xi-\epsilon'+i0)}+\frac{f^{(-)}(\epsilon')}{\epsilon'-\xi-\epsilon_k-i0}\Bigg\}, \quad \text{(AIII.3)}$$

where $\epsilon'\equiv\hbar^2k_\perp'^2/2m+\hbar^2(k_z+Q_z)^2/2m$. The $k_\perp'$ integration in (AIII.3) is restricted to yield non-negative values of the radicand; this is most conveniently accomplished by introducing the angle variable φ

$$k_\perp'^2\equiv k_\perp^2+Q_\perp^2+2k_\perp Q_\perp\cos\varphi, \quad \text{(AIII.4)}$$

where the limits on φ are: $0\leq\varphi\leq\pi$. Introducing the vectors $\mathbf{k}_\perp$, $\mathbf{k}_\perp'$, (AIII.4) is equivalent to $\mathbf{k}_\perp'=\mathbf{k}_\perp+\mathbf{Q}_\perp$ and the angle φ is now simply seen to be the azimuthal angle of the vector $\mathbf{k}=\mathbf{k}_\perp+\mathbf{k}_z$ measured from the fixed direction $\mathbf{Q}_\perp$. In terms of φ, one has

$$2k_\perp'dk_\perp'[2(k_\perp^2+k_\perp'^2)Q_\perp^2-(k_\perp^2-k_\perp'^2)^2-Q_\perp^4]^{-1/2}=-d\varphi. \quad \text{(AIII.5)}$$

The minus sign in (AIII.5) is interpreted simply from a vector diagram of $\mathbf{k}_\perp$, $\mathbf{k}_\perp'$, $\mathbf{Q}_\perp$, i.e., $\varphi=\pi$ when k' takes on its lowest value, $|k_\perp-Q_\perp|$. The integration over $k_\perp'$ sweeps out half the range of the azimuthal angle φ of $\mathbf{k}$. One now has for (AIII.3),

$$-\frac{\Omega}{2(2\pi)^2}\int_{-\infty}^{\infty}dk_z\int_0^{\infty}k_\perp dk_\perp\int_0^{2\pi}\frac{d\varphi}{\pi}|V_Q|^2\Bigg(\frac{f^{(-)}(\epsilon_k)-f^{(-)}(\epsilon_{k+Q})}{\epsilon_k+\xi-\epsilon_{k+Q}+i0}\Bigg)=-\sum_{\mathbf{k}}|V_Q|^2\Bigg(\frac{f^{(-)}(\epsilon_k)-f^{(-)}(\epsilon_{k+Q})}{\epsilon_k+\xi-\epsilon_{k+Q}+i0}\Bigg), \quad \text{(AIII.6)}$$

where the substitution $\epsilon'=\hbar(\mathbf{k}_\perp+\mathbf{Q}_\perp)^2/2m+\hbar^2(k_z+Q_z)^2/2m\equiv\hbar^2(\mathbf{k}+\mathbf{Q})^2/2m$ has been used. The final expression in (AIII.6) is equivalent to the one in H. (AIII.13) for $|V_{k+Q,k}|^2\to|V_Q|^2$. Thus, the results for the nonoscillatory part of the phonon self-energy are identical to those calculated in H. Appendix III and these results are reviewed in Sec. II.

(B) The EPI vertex part will now be considered. To this end one can calculate the lowest order correction, denoted by $\mathcal{V}_{t',t}{}^{(1)}(\zeta_l+\xi_m,\zeta_l)$, to the elementary EPI vertex, $V_{t',t}(\mathbf{Q})$, shown in Fig. 16.

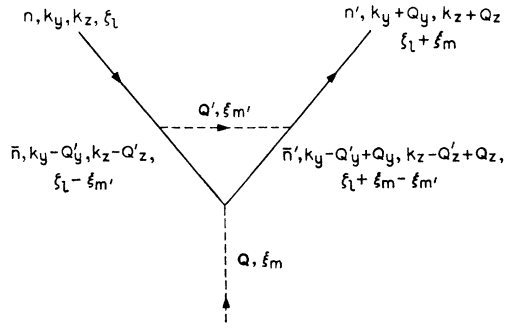

FIG. 16. The lowest order correction to the EPI vertex part.

According to the rules outlined in Sec. II and H. p. 418, one has for the skeleton diagram in Fig. 16

$$\mathcal{V}_{\iota',\iota}^{(1)}(\zeta_l+\xi_m,\zeta_l)=\frac{1}{\beta}\sum_{\substack{\mathbf{Q},\bar{n},\bar{n}'\\ \zeta_{l'},\pm}}[V_{\iota',\bar{\iota}'}(\mathbf{Q}')V_{\iota,\bar{\iota}}{}^{*}(\mathbf{Q}')V_{\bar{\iota}',\bar{\iota}'}(\mathbf{Q})]$$
$$\div[[\hbar\omega_{Q'}\pm(\zeta_l-\zeta_{l'})][\zeta_{l'}-\epsilon_{\bar{\iota}}-G_{\bar{\iota}}(\zeta_{l'})][\zeta_{l'}+\xi_m-\epsilon_{\bar{\iota}'}-G_{\bar{\iota}'}(\zeta_{l'}+\xi_m)]], \quad \text{(AIII.7)}$$

where $\zeta_{l'}=\zeta_l-\xi_{m'}$ and from (1.8) and (1.20),

$$V_{\iota',\bar{\iota}'}(\mathbf{Q}')V_{\iota,\bar{\iota}}{}^{*}(\mathbf{Q}')V_{\bar{\iota}',\bar{\iota}}(\mathbf{Q})=|V_{Q'}|^2\exp\left(\frac{i\hbar Q_x'Q_y}{m\omega_c}\right)e^{i(\bar{n}'-n'-(\bar{n}-n))\varphi'}\mathcal{G}_{\bar{n}'n'}\left(\frac{\hbar Q_\perp'^2}{2m\omega_c}\right)\mathcal{G}_{\bar{n}n}\left(\frac{\hbar Q_\perp'^2}{2m\omega_c}\right)$$
$$\times V_Q\exp\left[\frac{i\hbar}{m\omega_c}\left(Q_x(k_y-Q_y')+\frac{Q_xQ_y}{2}\right)\right]e^{i(\bar{n}-n')\varphi}\mathcal{G}_{\bar{n}\bar{n}'}\left(\frac{\hbar Q_\perp^2}{2m\omega_c}\right). \quad \text{(AIII.8)}$$

In (AIII.8), the angles φ', φ are the azimuthal angles of $\mathbf{Q}'$, $\mathbf{Q}$, respectively. The $\mathbf{Q}'$ sum is converted into an integral over the cylindrical coordinates $Q_\perp'$, Q_z', φ'. The integration over φ' is readily performed; using the fact that

$$Q_x'Q_y-Q_xQ_y'=Q_\perp'Q_\perp\sin(\varphi-\varphi'), \quad \text{(AIII.9)}$$

one has

$$\frac{e^{i(\bar{n}-\bar{n}')\varphi}}{2\pi}\int_0^{2\pi}d\varphi'\exp\left(\frac{i\hbar}{m\omega_c}Q_\perp'Q_\perp\sin(\varphi-\varphi')+i(\bar{n}'-n'-(\bar{n}-n))\varphi'\right)=e^{i(n-n')\varphi}J_{\bar{n}'-n'-(\bar{n}-n)}\left(\frac{\hbar Q_\perp'Q_\perp}{m\omega_c}\right). \quad \text{(AIII.10)}$$

The same procedure is used now as for the phonon self-energy in part A of this Appendix. The $\zeta_{l'}$ sum is converted into a integral in the ζ' plane and the $\bar{n}$, $\bar{n}'$ sums are changed to an integral over $\bar{k}_\perp$, $\bar{k}_\perp'$ with the use of the Poisson sum rule; further, the oscillatory terms are dropped. The problem of "overlapping" resonances of the propagator denominators [as in Sect. AIII.A] does not occur if the value of Q is selected to be that of a typical phonon i.e., $Q\sim Q_m$. After factoring out some phase factors and using (AIII.8) and (AIII.10), one has for (AIII.7),

$$\frac{\mathcal{V}^{(1)}(\zeta+\xi,\zeta)}{V_Q\exp\left[\frac{i\hbar}{m\omega_c}(Q_xk_y+\frac{1}{2}Q_xQ_y)\right]e^{i(n-n')\varphi}}=\frac{\Omega}{4\pi^2}\sum_{\pm}\int dQ_z'Q_\perp'dQ_\perp'\int_0^\infty\frac{\hbar k_\perp dk_\perp}{m\omega_c}\frac{\hbar k_\perp'dk_\perp'}{m\omega_c}|V_{Q'}|^2J_\nu\left(\frac{\hbar Q_\perp'Q_\perp}{m\omega_c}\right)$$
$$\times\frac{\chi(\bar{k}_\perp',k_\perp';Q_\perp')\chi(\bar{k}_\perp,k_\perp;Q_\perp')\chi(\bar{k}_\perp,k_\perp';Q_\perp)}{\bar{\epsilon}+\xi-\bar{\epsilon}'}\left[\frac{f^{(\mp)}(\bar{\epsilon})}{\zeta-\bar{\epsilon}\pm\hbar\omega_{Q'}}-\frac{f^{(\mp)}(\bar{\epsilon}')}{\zeta+\xi-\bar{\epsilon}'\pm\hbar\omega_{Q'}}\right], \quad \text{(AIII.11)}$$

where $\nu=\hbar(\bar{k}_\perp'^2-k_\perp'^2-(\bar{k}_\perp^2-k_\perp^2))/2m\omega_c$,

$$\bar{\epsilon}\equiv\frac{\hbar^2k_\perp^2}{2m}+\frac{\hbar^2}{2m}(k_z-Q_z')^2, \qquad \bar{\epsilon}'\equiv\frac{\hbar^2k_\perp'^2}{2m}+\frac{\hbar^2}{2m}(k_z-Q_z'+Q_z)^2;$$

with

$$\hbar k_\perp'^2/2m\omega_c\equiv n'+\tfrac{1}{2}, \qquad \hbar k_\perp^2/2m\omega_c\equiv n+\tfrac{1}{2}.$$

The χ's are the $\mathcal{G}$'s, in obvious notation, with the above substitutions for the n's.

Because of the complicated phase factors in the χ's [cf. (1.19)], an order of magnitude calculation for the right-hand side of (AIII.11) will be attempted. From (AIII.10) it can be seen that the significant values of $\bar{k}_\perp'$, $\bar{k}_\perp$ are restricted to $|\nu| \lesssim \hbar Q_\perp' Q_\perp / m\omega_c$. It will suffice to assume $|\nu| < \hbar Q_\perp' Q_\perp / m\omega_c$ and, therefore, the Bessel function in (AIII.11) is represented by the asymptotic expression

$$J_\nu\left(\frac{\hbar Q_\perp' Q_\perp}{m\omega_c}\right) \sim \left(\frac{\pi \hbar Q_\perp' Q_\perp}{2m\omega_c}\right)^{-1/2} \cos\left(\frac{\hbar Q_\perp' Q_\perp}{m\omega_c} - \tfrac{1}{2}\nu\pi - \frac{\pi}{4}\right); \tag{AIII.12}$$

also in line with the assumption $|\nu| < \hbar Q_\perp' Q_\perp / m\omega_c$,

$$\chi(\bar{k}_\perp', k_\perp'; Q_\perp')\chi(\bar{k}_\perp, k_\perp; Q_\perp') \sim \chi^2(\bar{k}_\perp', k_\perp'; Q_\perp') \tag{AIII.13}$$

is introduced. The right-hand side of (AIII.13) corresponds to two terms representing the difference and sum of the phase factors of $\chi(\bar{k}_\perp', k_\perp'; Q_\perp')$. The two terms give equal order of magnitude contributions when multiplied by the phase factor on the right-hand side of (AIII.12). For brevity, the difference in phase-factor term is considered. The terms depending only on Q' in (AIII.11), i.e., $|V_{Q'}|^2$ and $\hbar\omega_{Q'}$, are evaluated at the typical value of Q', namely $Q' \sim Q_m$.

The $Q_\perp'$ integration is now performed using the method of stationary phase[56] [as in (AII.11)]; one has

$$\frac{1}{\pi}\left(\frac{2m\omega_c}{\pi\hbar Q_\perp}\right)^{1/2} \int_{Q_{\perp c}'}^{Q_m} \frac{[Q_\perp']^{1/2} dQ_\perp' \cos\left(\frac{\hbar Q_\perp Q_\perp'}{m\omega_c} - \frac{\pi}{4}\right)[Q_\perp' - Q_{\perp c}']^{-1/2}}{\frac{\hbar}{2m\omega_c}[(\bar{k}_\perp' + k_\perp')^2 - Q_\perp'^2]^{1/2}[Q_\perp' + Q_{\perp c}']^{1/2}} = \frac{1}{2}\left(\frac{m\omega_c}{\hbar Q_\perp}\right)\left(\frac{2}{\pi}\right) \frac{\cos\left(\frac{\hbar Q_\perp}{m\omega_c}(\bar{k}_\perp' - k_\perp')\right)}{\frac{\hbar(\bar{k}_\perp' k_\perp')^{1/2}}{m\omega_c}}, \tag{AIII.14}$$

where $Q_{\perp c}' \equiv \bar{k}_\perp' - k_\perp'$ and it is assumed that $\bar{k}_\perp' + k_\perp' > Q_m$.

To proceed further, the simplification

$$\chi(k_\perp, k_\perp'; Q_\perp) \sim \left[\frac{2}{\pi}\right]^{1/2} \frac{\cos(\hbar Q_\perp k_\perp'/m\omega_c - \frac{1}{4}\pi)}{(\hbar Q_\perp k_\perp'/m\omega_c)^{1/2}} \tag{AIII.15}$$

is introduced; this simplification amounts to replacing the radicand in (1.19) by the first term [see the text following (1.19) for a discussion of the order of magnitude of each term in the radicand in the EPI case] with $k_\perp \sim k_\perp'$ and $\bar{k}_\perp \sim \bar{k}_\perp'$.

Two changes of variable are now introduced:

$$\bar{k}_z \equiv k_z - Q_z', \tag{AIII.16}$$

for the Q_z' integration and

$$\bar{k}_\perp'^2 = \bar{k}_\perp'^2 + Q_\perp^2 + 2Q_\perp \bar{k}_\perp \cos\bar{\varphi}, \tag{AIII.17}$$

for the $\bar{k}_\perp'$ integration. As in part A of this Appendix [cf. the discussion following (AIII.4)], the angle $\bar{\varphi}$ can be taken as the azimuthal angle of $\mathbf{k}(\bar{k}^2 \equiv \bar{k}_\perp^2 + \bar{k}_z^2)$, measured with respect to $\mathbf{Q}_\perp$. The result of the substitutions (AIII.16) and (AIII.17) and with the use of (AIII.15), one has finally

$$\frac{\mathcal{V}_{t',t}^{(1)}(\zeta+\xi, \zeta)}{V_Q \exp[(i\hbar/m\omega_c)(Q_x k_y + \frac{1}{2}Q_x Q_y)] e^{i(n-n')\varphi} \chi(k_\perp, k_\perp'; Q_\perp)}$$

$$\simeq \sum_{\bar{k},\pm} \frac{|V_{Q_m}|^2}{\epsilon_{\bar{k}} + \xi - \epsilon_{\bar{k}+Q}} \left[\frac{f^{(\mp)}(\epsilon_{\bar{k}})}{\zeta - \epsilon_{\bar{k}} \pm \hbar\omega_{Q_m}} - \frac{f^{(\mp)}(\epsilon_{\bar{k}+Q})}{\zeta + \xi - \epsilon_{\bar{k}+Q} \pm \hbar\omega_{Q_m}}\right]. \tag{AIII.18}$$

The right-hand side of (AIII.18) is equivalent to (H.AIV.7) and in particular it is shown in H. Appendix IV to be of the order c_s/v_F for $Q \sim k_F$ and $\zeta \sim E_F$ [cf. (H.AIV.13)].

APPENDIX IV: GENERAL DIAGONALITY PROOFS

In this Appendix, the diagonality of the phonon propagator in the momentum representation, i.e.,

$$D_{Q'Q}(\xi_m) = \delta_{Q'Q} D_Q(\xi_m) \tag{AIV.1}$$

will be established.[57] For this purpose, it is expedient to write the Hamiltonian in the form

$$H=\int\psi^\dagger(\mathbf{r})\left[\frac{1}{2m}\left(\mathbf{p}-\frac{e\mathbf{A}(\mathbf{r})}{c}\right)^2\right]\psi(\mathbf{r})d^3r+\sum_Q\hbar\omega_Q{}^{(0)}b_Q{}^\dagger b_Q+\sum_Q\int\psi^\dagger(\mathbf{r})V_Q{}^{(0)}e^{i\mathbf{Q}\cdot\mathbf{r}}\psi(\mathbf{r})d^3r[b_Q+b_Q{}^\dagger],\quad\text{(AIV.2)}$$

where, as usual, $\mathbf{p}\equiv\hbar/i\,\mathrm{grad}_\mathbf{r}$, where $A(\mathbf{r})=(0,Hx,0)$ (as in the text), and where $\psi^\dagger(\mathbf{r})$ and $\psi(\mathbf{r})$ are the electron creation and annihilation operators in the position representation; they obey the standard anticommutation rules:

$$\psi(\mathbf{r})\psi(\mathbf{r}')+\psi(\mathbf{r}')\psi(\mathbf{r})=0,\quad\text{(AIV.3a)}$$

$$\psi(\mathbf{r})\psi^\dagger(\mathbf{r}')+\psi^\dagger(\mathbf{r}')\psi(\mathbf{r})=\delta(\mathbf{r}-\mathbf{r}'),\quad\text{(AIV.3b)}$$

and are related to the previously introduced $a_t{}^\dagger$ and a_t by the equation

$$\psi(\mathbf{r})=\sum_t\langle\mathbf{r}|t\rangle a_t\equiv\sum_{n,k_y,k_z}\langle\mathbf{r}|nk_yk_z\rangle a_t\quad\text{(AIV.4)}$$

and its adjoint.[58]

The procedure to be used is based on subjecting expressions of the type[59]

$$\langle b_Q(\tau)b_{Q'}{}^\dagger(0)\rangle\equiv(1/Z_G)\,\mathrm{Tr}\{e^{-\beta(H-\mu N)}e^{H\tau}b_Qe^{-H\tau}b_{Q'}{}^\dagger\}\quad\text{(AIV.5)}$$

to two successive canonical transformations; the first of these corresponds to a uniform displacement of all the electronic coordinates, whereas the second is a gauge transformation chosen so as to bring the Hamiltonian back to its original form.

The "displacement" transformation is carried out by introducing into (AIV.5) the replacements

$$\psi(\mathbf{r})\rightarrow\psi'(\mathbf{r})\equiv\psi(\mathbf{r}+\boldsymbol{\varrho}),\quad\text{(AIV.6a)}$$

$$\psi^\dagger(\mathbf{r})\rightarrow\psi^{\dagger\prime}(\mathbf{r})\equiv\psi^\dagger(\mathbf{r}+\boldsymbol{\varrho}),\quad\text{(AIV.6b)}$$

$$b_Q\rightarrow b_Q'\equiv b_Qe^{i\mathbf{Q}\cdot\boldsymbol{\rho}},\quad\text{(AIV.6c)}$$

$$b_Q{}^\dagger\rightarrow b_Q{}'^\dagger\equiv b_Q{}^\dagger e^{-i\mathbf{Q}\cdot\boldsymbol{\rho}},\quad\text{(AIV.6d)}$$

(where $\boldsymbol{\varrho}$ is an arbitrary vector).

Since these replacements (obviously) preserve the basic commutation and anticommutation relationships for the boson and fermion field operators, it follows from general quantum-mechanical principles that the primed quantities are related to their unprimed counterparts via a unitary transformation[60]; i.e., there exists a unitary operator U such that

$$\psi'(\mathbf{r})=U\psi(\mathbf{r})U^{-1}\quad\text{(AIV.7)}$$

(and similarly for the other primed field operators). Since (AIV.5) is a trace, it then follows that it is invariant with respect to the replacements (AIV.6). Thus,

$$\langle b_Q(\tau)b_{Q'}{}^\dagger(0)\rangle=(1/Z_G)\,\mathrm{Tr}\{e^{-\beta(H'-\mu N)}e^{H'\tau}b_Q{}'e^{-H'\tau}b_{Q'}{}'^\dagger\}=e^{i(\mathbf{Q}-\mathbf{Q}')\cdot\boldsymbol{\rho}}(1/Z_G)\,\mathrm{Tr}\{e^{-\beta(H'-\mu N)}e^{H'\tau}b_Qe^{-H'\tau}b_{Q'}{}^\dagger\},\quad\text{(AIV.8)}$$

where H' is the Hamiltonian which is obtained from H by introducing the replacements (AIV.6) into (AIV.2).

---

[57] Once (AIV.1) is established, the corresponding diagonality of the phonon self-energy part follows immediately from the matrix generalization of [H. (2.2b)], which is text Eq. (2.2).

[58] The single-particle states, $\langle\mathbf{r}|t\rangle=\langle\mathbf{r}|nk_yk_z\rangle$ are the usual Landau eigenstates in the position representation. They are the space-Fourier transforms of the objects given in the text Eq. (1.6). It may incidentally be noted that, if (AIV.4) and its adjoint be substituted in the third member of (AIV.2), one obtains $V_{t't}{}^{(0)}=V_Q{}^{(0)}\langle n'k_y'k_z'|e^{i\mathbf{Q}\cdot\mathbf{r}}|nk_yk_z\rangle$, which is completely equivalent to (1.5).

[59] The phonon propagator $D_{Q'Q}(\xi_m)$ may be defined as

$$D_{Q'Q}(\xi_m)=\int_0^\beta e^{-u\xi_m}\langle T(b_{Q'}{}^\dagger(u)+b_{-Q'}(u))(b_Q(0)+b_{-Q}{}^\dagger(0))\rangle du.$$

The equivalence of this definition and that provided by a diagrammatic prescription [in particular, the matrix generalization of H.(2.2b)] may be established by an approach similar to that used in H. Appendix II for the velocity-correlation function.

[60] Specifically, the unitary transformation is given by

$$U=\exp\left(-\frac{i}{\hbar}\boldsymbol{\varrho}\cdot\int\psi^\dagger(r)\mathbf{p}\psi(r)d^3r\right).$$

where $\mathbf{p}=\hbar/i\,\mathrm{grad}_\mathbf{r}$.

It is easily verified that, when H' is written in terms of the unprimed field operators, it has the same form as (AIV.2), except that the vector potential $\mathbf{A}$ is replaced by

$$\mathbf{A}'=(0,H(x-\xi),0) \tag{AIV.9}$$

(where ξ is the x component of ϱ).

Let us now introduce the second canonical transformation; it is given by the prescription

$$\psi(\mathbf{r})\rightarrow\psi''(\mathbf{r})\equiv e^{-ieH\xi y/\hbar c}\psi(\mathbf{r}), \tag{AIV.10a}$$

$$\psi^\dagger(\mathbf{r})\rightarrow\psi''(\mathbf{r})\equiv e^{ieH\xi y/\hbar c}\psi^\dagger(\mathbf{r}), \tag{AIV.10b}$$

with the b_Q''s going into themselves.[61] Introducing (AIV.10) into (AIV.8) yields

$$\langle b_Q(\tau)b_{Q'}{}^\dagger(0)\rangle=e^{i(\mathbf{Q}-\mathbf{Q}')\cdot\rho}(1/Z_G)\ \mathrm{Tr}\{e^{-\beta(H''-\mu N)}e^{H''\tau}b_Qe^{-H''\tau}b_{Q'}{}^\dagger\}, \tag{AIV.11}$$

where H'' is the Hamiltonian obtained from H' by replacing $\psi(\mathbf{r})$ and $\psi^\dagger(\mathbf{r})$ by their double-primed counterparts. Using (AIV.10a) and (AIV.10b), one then expresses H'' in terms of $\psi(\mathbf{r})$ and $\psi^\dagger(\mathbf{r})$.

It is easily seen that the effect of the transformation is solely a change of gauge of the vector potential: specifically,

$$\mathbf{A}'(\mathbf{r})\rightarrow\mathbf{A}''(\mathbf{r})=\mathbf{A}'(\mathbf{r})+\mathrm{grad}_\mathbf{r}H\xi y=(0,Hx,0)=\mathbf{A}(\mathbf{r}) \tag{AIV.12}$$

so that

$$H''=H. \tag{AIV.13}$$

Inserting (AIV.13) into (AIV.11), one has

$$\langle b_Q(\tau)b_{Q'}{}^\dagger(0)\rangle=e^{i(\mathbf{Q}-\mathbf{Q}')\cdot\rho}\langle b_Q(\tau)b_{Q'}{}^\dagger(0)\rangle. \tag{AIV.14}$$

In view of the arbitrariness of ϱ, it necessarily follows that

$$\langle b_Q(\tau)b_{Q'}{}^\dagger(0)\rangle=\delta_{Q,Q}\langle b_Q(\tau)b_Q(0)\rangle. \tag{AIV.15}$$

Introducing this result[62] into the equation for $D_{Q'Q}(\xi_m)$ given in footnote 59 yields (AIV.1) QED.

It should here be pointed out that, strictly speaking, an analysis equivalent to the above should also be applied to the velocity-correlation function to establish its diagonality in the wave-vector variable, $\mathbf{q}$; just as in the case of the phonon propagator, such diagonality is not *a priori* obvious, in view of the lack of translational symmetry in the presence of the dc magnetic field. Such an analysis is readily carried out, essentially in the same way as for the phonon propagator. In particular, from the expression

$$\mathbf{v}(\mathbf{q})=\int\psi^\dagger(\mathbf{r})\frac{1}{2m}\left\{e^{i\mathbf{q}\cdot\mathbf{r}}\left(\frac{h}{i}\mathrm{grad}_\mathbf{r}-\frac{e\mathbf{A}(\mathbf{r})}{c}\right)+\left(\frac{h}{i}\mathrm{grad}_\mathbf{r}-\frac{e\mathbf{A}(\mathbf{r})}{c}\right)e^{i\mathbf{q}\cdot\mathbf{r}}\right\}\psi(\mathbf{r})d^3r \tag{AIV.16}$$

[which is fully equivalent to the text relationship (1.13) and (1.14)], one sees that the first canonical transformation [given by (AIV.6)] results in the multiplication of (AIV.16) by the phase factor $e^{-i\mathbf{q}\cdot\rho}$, and in the replacement of $\mathbf{A}(\mathbf{r})$ by $\mathbf{A}'(\mathbf{r})$, as given by (AIV.9); the second (gauge) transformation, as in the above treatment of the phonon propagator, restores the vector potential to its original form. It is then readily seen that the sole effect of applying the two transformations to the velocity-correlation function is to multiply it by a factor $e^{i(\mathbf{q}'-\mathbf{q})\cdot\rho}$. The requirement of reconciling this result with the invariance of the correlation function towards unitary transformations leads necessarily to the conclusion that the velocity-correlation function is diagonal in q.

It is finally of interest to study the effect of the two transformations on the electron propagator. In the position representation, this quantity is[63]

$$\langle\mathbf{r}_1|S(\zeta_l)|\mathbf{r}_2\rangle=-\int_0^\beta e^{-\zeta_l u}\langle T\psi(\mathbf{r}_1,u)\psi^\dagger(\mathbf{r}_2,0)\rangle du \tag{AIV.17}$$

so that it suffices to study the object

$$\langle\psi(\mathbf{r}_1,u)\psi^\dagger(\mathbf{r}_2,0)\rangle=(1/Z_G)\ \mathrm{Tr}\{e^{-\beta(H-\mu N)}e^{Hu}\psi(\mathbf{r}_1)e^{-Hu}\psi^\dagger(\mathbf{r}_2)\}. \tag{AIV.18}$$

The first (displacement) transformation, given by (AIV.6), yields

$$\langle\psi(\mathbf{r}_1,u)\psi^\dagger(\mathbf{r}_2,0)\rangle=(1/Z_G)\ \mathrm{Tr}\{e^{-\beta(H'-\mu N)}e^{H'u}\psi(\mathbf{r}_1+\varrho)e^{-H'u}\psi^\dagger(\mathbf{r}_2+\varrho)\}, \tag{AIV.19}$$

---

[61] As before, the canonicity of the transformation follows from the fact that the anticommutation relationships of the fermion operators are preserved.

[62] The proof that expressions of the type $\langle b_{-Q'}(u)b_Q(0)\rangle$ vanish unless $Q=Q'$ essentially duplicates the proof of (AIV.15).

[63] J. M. Luttinger, Phys. Rev. **121**, 942 (1961).

which, upon being subjected to the second (gauge) transformation (AIV.10), becomes

$$\langle\psi(\mathbf{r}_1,u)\psi^\dagger(\mathbf{r}_2,0)\rangle=(1/Z_G)e^{ieH\xi(y_2-y_1)/\hbar c}\,\mathrm{Tr}\{e^{-\beta(H-\mu N)}e^{Hu}\psi(\mathbf{r}_1+\boldsymbol{\varrho})e^{-Hu}\psi^\dagger(\mathbf{r}_2+\boldsymbol{\varrho})\}$$
$$=e^{ieH\xi(y_2-y_1)/\hbar c}\langle\psi(\mathbf{r}_1+\boldsymbol{\varrho},u)\psi^\dagger(\mathbf{r}_2+\boldsymbol{\varrho},0)\rangle.$$

Hence, with the utilization of (AIV.17), one has

$$\langle\mathbf{r}_1|S(\zeta_l)|\mathbf{r}_2\rangle=e^{ieH(y_2-y_1)\xi/\hbar c}\langle\mathbf{r}_1+\boldsymbol{\varrho}|S(\zeta_l)|\mathbf{r}_2+\boldsymbol{\varrho}\rangle. \tag{AIV.20}$$

Now, let us choose $\boldsymbol{\varrho}=-(\mathbf{r}_1+\mathbf{r}_2)/2$; (AIV.20) then takes the form

$$\langle\mathbf{r}_1|S(\zeta_l)|\mathbf{r}_2\rangle=e^{ieH(x_1+x_2)(y_1-y_2)/2\hbar c}\mathcal{S}(\zeta_l,\mathbf{r}_2-\mathbf{r}_1), \tag{AIV.21}$$

where

$$\mathcal{S}(\zeta_l,\mathbf{r})\equiv\langle-\mathbf{r}/2|S(\zeta_l)|\mathbf{r}/2\rangle=-\int_0^\beta e^{-\zeta_l u}\langle T\psi(-\mathbf{r}/2,u)\psi^\dagger(\mathbf{r}/2,0)\rangle du \tag{AIV.22}$$

is a function only of the "difference coordinate," $\mathbf{r}=\mathbf{r}_2-\mathbf{r}_1$.

It is now desirable to utilize the essential cylindrical symmetry with respect to rotations about the z axis (magnetic-field direction) to prove that $\mathcal{S}(\zeta_l,\mathbf{r})$ is independent of the azimuthal angle of $\mathbf{r}$. For this purpose it is expedient to transform to the so-called "symmetric gauge,"

$$\mathbf{A}_s\equiv\tfrac{1}{2}\mathbf{H}\times\mathbf{r}. \tag{AIV.23}$$

The required transformation reads

$$\psi(\mathbf{r}_1)\rightarrow\psi'(\mathbf{r}_1)\equiv e^{ieHx_1y_1/2\hbar c}\psi(\mathbf{r}_1),\qquad \psi^\dagger(\mathbf{r}_2)\rightarrow\psi^{\dagger\prime}(\mathbf{r}_2)\equiv e^{-ieHx_2y_2/2\hbar c}\psi^\dagger(\mathbf{r}_2). \tag{AIV.24}$$

Introducing this transformation into (AIV.22), one notes that $\mathbf{r}$-dependent phase factors cancel, and one has simply

$$\mathcal{S}(\zeta_l,\mathbf{r})=\mathcal{S}^{(s)}(\zeta_l,\mathbf{r}), \tag{AIV.25}$$

where the superscript "(s)" denotes that in the right-hand side of (AIV.22), one uses the symmetric-gauge Hamiltonian (for which $\mathbf{A}=\mathbf{A}_s$).

Noting, now, that the quantity $(\mathbf{p}-e\mathbf{A}_s/c)^2$ is independent of the azimuth angle φ of $\mathbf{r}$ (its dependence on φ being limited to the occurrence of the differential operators, $\partial/\partial\varphi$ and $\partial^2/\partial\varphi^2$), one straightforwardly establishes that the Hamiltonian is left unchanged by "rotational" transformations of the type

$$\psi(\mathbf{r})\rightarrow\psi'(\mathbf{r})\equiv\psi(\mathbf{r}'),\qquad \psi^\dagger(\mathbf{r})\rightarrow\psi^{\dagger\prime}(\mathbf{r})\equiv\psi^\dagger(\mathbf{r}'),\qquad b_Q\rightarrow b_{Q'}\equiv b_{Q'},\qquad b_Q^\dagger\rightarrow b_Q^{\dagger\prime}\equiv b_{Q'}^\dagger,$$

where $\mathbf{r}'$ and $\mathbf{Q}'$ are obtained from $\mathbf{r}$ and $\mathbf{Q}$ by an arbitrary rotation about the z axis.[64] This operation yields

$$\mathcal{S}^{(s)}(\zeta_l,\mathbf{r})=\mathcal{S}^{(s)}(\zeta_l,\mathbf{r}'). \tag{AIV.26}$$

Inserting (AIV.26) into (AIV.25), one arrives at the conclusion that the dependence of $\mathcal{S}(\zeta_l,\mathbf{r})$ on the cylindrical coordinates of $\mathbf{r}$—namely, $r_\perp$, φ, z—is of the form

$$\mathcal{S}(\zeta_l,\mathbf{r})=\mathcal{S}(\zeta_l;r_\perp,z). \tag{AIV.27}$$

With the aid of (AIV.21) and (AIV.27), it will now be shown that the electron propagator is diagonal in the Landau representation, i.e., that

$$\langle n',k_y,k_z|S(\zeta_l)|n,k_y,k_z\rangle=\int\int\langle n'k_yk_z|\mathbf{r}_1\rangle\langle\mathbf{r}_1|S(\zeta_l)|\mathbf{r}_2\rangle\langle\mathbf{r}_2|nk_yk_z\rangle d^3r_1d^3r_2 \tag{AIV.28}$$

vanishes unless[65] $n=n'$. Introducing the transformations

$$\mathbf{r}=\mathbf{r}_2-\mathbf{r}_1,\qquad \mathbf{R}=\tfrac{1}{2}(\mathbf{r}_1+\mathbf{r}_2), \tag{AIV.29}$$

and making use of (AIV.21) and the explicit form of the coordinate representation of the single-particle wave functions, namely,

$$\langle\mathbf{r}_1|nk_yk_z\rangle=\frac{1}{\Omega^{1/3}L^{1/2}}e^{i[k_yy_1+k_zz_1]}\Phi_n\left(\frac{x_1-(\hbar c/eH)k_y}{L}\right) \tag{AIV.30}$$

---

[64] Strictly speaking, in order to utilize the intrinsic rotational symmetry of the Hamiltonian, it would be necessary to replace the usual rectangular box periodicity conditions on the wave vector $\mathbf{Q}$, by some cylindrically symmetrical prescription. However, in the opinion of the present authors, this difficulty is purely formal, and will hence be ignored.

[65] Diagonality in k_y,k_z follows automatically from the invariance of the Hamiltonian with respect to displacements in the yz plane.

[where the Φ_n is given by (1.7)] one has[66]

$$\langle n',k_y k_z|S(\zeta_l)|n,k_y,k_z\rangle=\int\int\langle n',k_y,k_z|\mathbf{R}-\tfrac{1}{2}\mathbf{r}\rangle e^{-ieHXy/\hbar c}\mathcal{S}(\zeta_l,\mathbf{r})\langle\mathbf{R}+\tfrac{1}{2}\mathbf{r}|n,k_y,k_z\rangle d^3Rd^3r$$

$$=\int d^3r\ \mathcal{S}(\zeta_l,\mathbf{r})e^{ikzz}\int_{-\infty}^{\infty}e^{-ieHXy/\hbar c}\Phi_{n'}\left(\frac{X-\frac{1}{2}x}{L}\right)\Phi_n\left(\frac{X+\frac{1}{2}x}{L}\right)\frac{dX}{L}. \qquad \text{(AIV.31)}$$

Now, an integral similar to the X integral in (AIV.31) occurs in the calculation of the EPI matrix element (1.5) and it is given explicitly[17] by

$$\int_{-\infty}^{+\infty}e^{-ieHXy/\hbar c}\Phi_{n'}\left(\frac{X-\frac{1}{2}x}{L}\right)\Phi_n\left(\frac{X+\frac{1}{2}x}{L}\right)\frac{dX}{L}=e^{i\varphi(n-n')}\mathcal{I}_{nn'}\left(\frac{r_\perp^2}{2L^2}\right), \qquad \text{(AIV.32)}$$

where φ is the azimuthal angle of $\mathbf{r}$, $r_\perp\equiv(x^2+y^2)^{1/2}$ and $\mathcal{I}_{nn'}$ is given by (1.9). An integration with respect to φ with account being taken of (AIV.27)] immediately yields the factor $\delta_{nn'}$, so that

$$\langle n',k_y,k_z|S(\zeta_l)|n,k_y,k_z\rangle=\delta_{nn'}\langle n,k_y,k_z|S(\zeta_l)|n,k_y,k_z\rangle, \qquad \text{(AIV.33)}$$

i.e., the electron propagator is diagonal in the Landau representation, QED.

---

[66] In obtaining the last equality of (AIV.31), the transformation $X=X'+\hbar ck_y/eH$ (followed by suppression of the prime superscript attached to X) was employed. A principal result is the cancellation of the factor, $e^{ik_y y}$, from the integrand.